Bioorganic Chemistry 95 (2020) 103523

Contents lists available at ScienceDirect

Bioorganic Chemistry

journal homepage: www.elsevier.com/locate/bioorg

Design, synthesis and SAR study of 3rd-generation taxoids bearing 3-CH_3, 3-CF_3O and 3-CHF_2O groups at the C2-benzoate position

Changwei Wang[a,b,c,1], Xin Wang[a,b,1], Yi Sun[a,b,1], Adam K. Taouil[a], Su Yan[a,b], Galina I. Botchkina[b,d], Iwao Ojima[a,b,*]

[a] Department of Chemistry, Stony Brook University, Stony Brook, NY 11794-3400, USA
[b] Institute of Chemical Biology and Drug Discovery, Stony Brook University, Stony Brook, NY 11794-3400, USA
[c] Drug Discovery Pipeline, Guangzhou Institute of Biomedicine and Health, Chinese Academy of Science, Guangzhou 510530, China
[d] Department of Pathology, Renaissance School of Medicine, Stony Brook University, Stony Brook, NY 11794-3400, USA

ARTICLE INFO

Keywords:
Taxane
3rd-generation taxoid
SAR study
Multidrug resistance
Cancer stem cells
Fluorine-containing
Trifluoromethoxy
Difluoromethoxy

ABSTRACT

It has been shown that inclusion of CF_3O and CHF_2O groups to drug candidates often improve their pharmacological properties, especially metabolic stability, membrane permeability and PK profile. Moreover, the unique non-spherical structure of the $OCHF_2$ group can provide interesting and beneficial characteristics. Accordingly, new 3rd-generation taxoids, bearing 3-OCF_3 or 3-OCF_2H (and 3-CH_3 for comparison) at the C2 benzoate moiety, were synthesized and their potencies against drug-sensitive and drug-resistant cancer cell lines examined. In this study, our previous SAR studies on 3rd-generation taxoids were expanded to disclose that CH_3, CF_3O and CHF_2O groups are well tolerated at this position and enhance potency, especially against MDR-cancer cell lines so that these taxoids can virtually overcome MDR. These new taxoids exhibit up to 7 times higher cytotoxicity (IC_{50}) than paclitaxel against drug-sensitive cancer cell lines (MCF7 and LCC6-WT) and 2–3 orders of magnitude higher potency than paclitaxel against drug-resistant ovarian, breast and colon cancer cell lines with MDR-phenotype (NCI/ADR, LCC6-MDR and LDL-1), as well as pancreatic cancer cell line, CFPAC-1. Since it has been shown that a bulky group at this position reduces potency, it is noteworthy that rather bulky CF_3O and CHF_2O groups are well tolerated. Molecular modeling analysis indicated the favorable van der Waals interactions of CF_3O and CHF_2O groups in the binding site. It is also worthy of note that new taxoids, bearing a CHF_2O group at the C2 benzoate position (**1-06** series), exhibited the highest potencies against MDR-cancer cell lines and cancer stem cell (CSC)-enriched cancer cell lines. These new 3rd-generation taxoids are promising candidates for highly potent chemotherapeutic agents, as well as payloads for tumor-targeting drug conjugates such as antibody-drug conjugates (ADCs).

1. Introduction

Paclitaxel and docetaxel are two of the most extensively used chemotherapeutic drugs in clinic for the treatment of various cancers, particularly for ovarian, lung, and breast cancers in the last quarter century (Fig. 1) [1,2]. Moreover, the exploration of their new clinical applications, particularly with new formulations and combination therapies, are actively underway [1]. Abraxane (nanoparticle albumin–bound paclitaxel) is more efficacious than paclitaxel for breast and non-small cell lung cancer with much muted undesirable side effects [3]. Furthermore, Abraxane is effective for the treatment of advanced pancreatic cancer in combination with gemcitabine [3–5]. Cabazitaxel, the third FDA-approved taxane (Fig. 1), exhibits good efficacy in hormone-refractory prostate cancer in combination with prednisone [6,7].

However, the first-generation taxane anticancer drugs, i.e., paclitaxel and docetaxel, show little efficacy in treating melanoma, pancreatic, gastric, brain and renal cancers [2,8]. These limitations are, at least in part, due to multi-drug resistance (MDR) caused by overexpression of ABC cassette efflux pumps, overexpression of β-III tubulin isoform, point mutations in the microtubule binding site and cancer

Abbreviations: MDR, multi-drug resistance; CSCs, cancer stem cells; RI, resistance index; SAR, structure-activity relationship; MOA, mechanism of action; MMPA, matched molecular pair analysis; $HCT116^{CSC}$, CSC-enriched colon cancer cell line; PPT2, a patient-derived prostate cancer stem cells; ADCs, antibody-drug conjugates; DPBS, Dulbecco's phosphate-buffered saline

* Corresponding author at: Department of Chemistry, Stony Brook University, Stony Brook, NY 11794, USA.
E-mail address: iwao.ojima@stonybrook.edu (I. Ojima).

[1] These three authors contributed equally.

https://doi.org/10.1016/j.bioorg.2019.103523
Received 15 October 2019; Received in revised form 18 December 2019; Accepted 18 December 2019
Available online 20 December 2019
0045-2068/

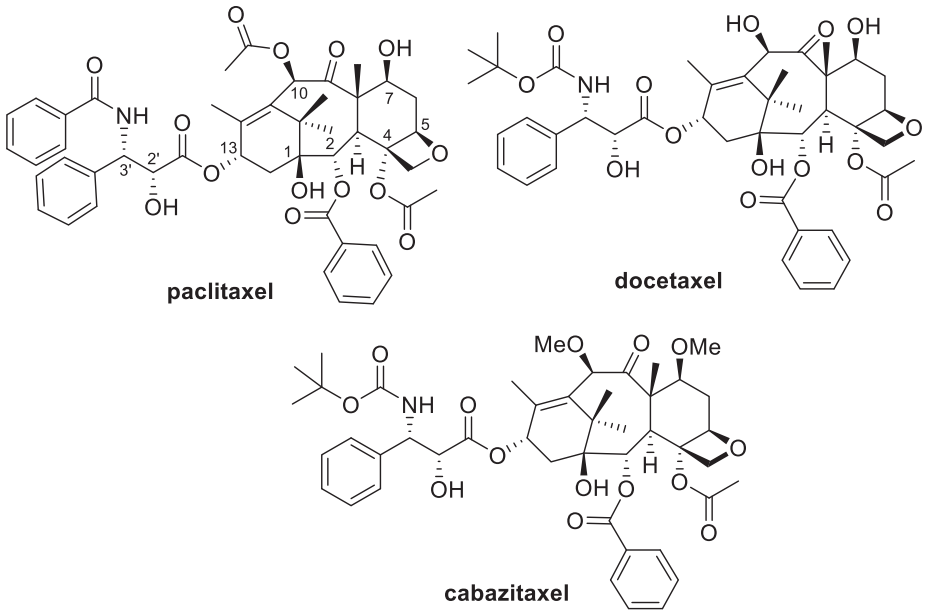

Fig. 1. Paclitaxel, docetaxel and cabazitaxel.

stem cells [8–10]. In order to address these issues, a number of new taxoids [11–17], new formulations [18–22] and new combination therapies [23–28] are currently in different stages of preclinical and clinical development [1,17]. Nevertheless, it is critical to keep developing next-generation taxoid anticancer agents with superior pharmacological properties and potency against various types of cancers, in particular drug-resistant and metastatic cancers, as well as cancer stem cells (CSCs), which are responsible for tumor recurrence and metastasis, causing major problems in cancer therapy [1,2]. Highly potent taxoids are also very important as payloads of tumor-targeting drug conjugates [2,21,29,30].

We have been developing 2nd-generation taxoids (modifications at C10, C3′ and C3′N) [14,16,31–34] and 3rd-generation taxoids (modifications at C2, C10, C3′ and C3′N) [31,32,35] which exhibit 2–3 orders of magnitude higher potency than paclitaxel and docetaxel against various drug-resistant cancer cell lines expressing the multidrug-resistance (MDR) phenotype (e.g., LCC6-MDR, breast; NCI-ADR, ovarian; DLD-1, colon; CFPAC-1, pancreas), as well as point mutations at the taxane-binding site in β-tubulin (e.g., 1A9PTX10, ovarian) [13]. A representative 2nd-generation taxoid, SB-T-1214 (**1c**), as well as its conjugate with decosahexaenoic acid, DHA-SB-T-1214 (**2c**) exhibited impressive efficacy *in vivo* against DLD-1 tumor xenografts in mice [36]. Also, a nanoemulsion formulation of **2c** demonstrated clear efficacy against PPT2 patient-derived prostate CSC-initiated tumor xenografts in a mice model and is currently in late stage preclinical development [37]. We have found that taxoid **1c** possesses high potency against CSCs from colon and prostate cancers by suppressing stemness gene expressions and restoring P21 and P53 expressions through “gene wake-up” [38].

Through our SAR studies, we found that C2-benzoate modifications with 3-substitutions with halogens (F, Cl), azide and methoxy groups enhanced the potency of 2nd-generation taxoids against MDR-cancer cell lines, leading to the development of 3rd-generation taxoids [31,35]. The 3-position of the C2-benzoate moiety in paclitaxel was identified as one of the metabolism site by cytochrome *C* P450 [39], and also as a potential van der Waals attractive interaction site with His 229 of β-tubulin, enhancing the binding affinity of paclitaxel [40,41] and taxoids [32,42].

Select 2nd- and 3rd-generation taxoids investigated in our SAR studies are shown in Table 1 together with the resistance index, *RI* (see Table 1 caption). In those previous SAR studies, we did not include Br, I, isopropyl, *tert*-butyl and CF_3 groups based on a computational analysis, which indicated that bulky substituents at the 3-position of C2-benzoate caused steric clash with the putative binding site (See Fig. S1 and Table S1 in the Supplementary Material). Also, we synthesized and evaluated only one 3-methyl analog, SB-T-121202 (**1a-02**). Accordingly, in the present SAR study, we investigated new 3rd-generation taxoids, bearing a methyl, trifluoromethoxy and difluoromethoxy group at the 3-position of the C2-benzoate moiety. As Table 1 shows, SB-T-121303 (**1b-03**), bearing a 3-methoxybenzoyl moiety at C2, was identified as the most potent 3rd-generation taxoid in the study.

In current drug discovery and development, it is quite common to explore fluorine-containing analogs of lead compounds. This is due to the fact that a large number of fluorine-containing compounds have been approved by the FDA for medical and agricultural use [43–48]. In fact, fluorine is ranked second as the most “favorite heteroatom” only after nitrogen in current drug discovery [48]. It has been shown that the replacement of a C—H or C—O bond with a C—F bond in medicinally active compounds induces or improves desirable pharmacological properties such as higher metabolic stability, increased binding affinity to target molecules, and enhanced membrane permeability [49,50].

It has been shown that the OCF_3 group in aromatic trifluoromethyl ethers (Ar-OCF3), e.g., trifluoroanisole, has a strong preference to be out of plane (i.e., $\beta = 90^\circ$ in Fig. 2A), while the methyl group in anisole is mostly in-plane with the phenyl moiety (i.e., $\beta = 18^\circ$ in Fig. 2A) [44,51–53]. Furthermore, the conformational preference of the $OCHF_2$ group in Ar-$OCHF_2$ has turned out to be in between the planar OCH_3 and the orthogonal OCF_3 [44,51] (Fig. 2B) [54]. Since the rotational barrier in Ar-$OCHF_2$ is considerably lower than that of Ar-OCF_3, the $OCHF_2$ group may serve as a bioisosteric replacement for the OCH_3 or OCF_3 moiety, depending on its conformation. Furthermore, the unique non-spherical feature of the $OCHF_2$ group can provide additionally interesting characteristics. The X-ray crystal structures of Ar-$OCHF_2$ indicate that either one or both of the C—F bonds can be in the anomeric position to take the *endo-exo* or *endo-endo* conformation. In the *endo-endo* conformation, the polarities of the C—F bond largely cancel out, while the polarity of the *endo-exo* conformation is three times higher than that of the *endo-endo* conformation [54]. Thus, Ar-$OCHF_2$ could be more (*endo-endo*) or less (*endo-exo*) lipophilic than their Ar-OCF_3 counterparts.

This unique ability of the $OCHF_2$ group to adopt different conformations in polar and nonpolar environments would provide unusual

Table 1

Cytotoxicity of select 2nd- and 3rd-generation taxoids (IC_{50} nM).[a]

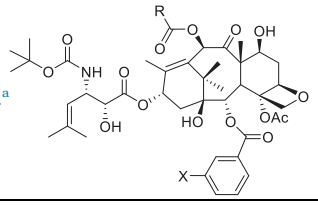

Taxoid	R	X	LCC6-WT[b]	LCC6-MDR[c]	*RI*[d]	MCF7[e]	NCI/ADR[f]	*RI*[d]
Paclitaxel			3.1	346	*112*	1.7	300	*176*
Docetaxel			1.0	120	*120*	1.0	235	*235*
SB-T-1213 (**1b**)	Et	H	–	–	–	0.18	4.0	*22*
SB-T-1214 (**1c**)	*c*-Pr	H	–	–	–	0.20	3.9	*20*
SB-T-1216 (**1d**)	Me_2N	H	–	–	–	0.13	4.9	*38*
SB-T-1217 (**1e**)	MeO	H	–	–	–	0.14	5.3	*38*
SB-T-121202 (**1a-02**)	Me	Me	1.5	5.8	*3.9*	0.8	5.0	*6.3*
SB-T-121203 (**1a-03**)	Me	MeO	0.6	2.7	*4.5*	0.8	2.3	*2.9*
SB-T-121303 (**1b-03**)	Et	MeO	1.0	0.9	*0.9*	0.36	0.33	*0.92*
SB-T-121403 (**1c-03**)	*c*-Pr	MeO	1.0	2.9	*2.9*	–	–	–
SB-T-121703 (**1e-03**)	MeO	MeO	0.6	1.6	*2.7*	0.4	1.4	*3.5*

[a] Concentration of compound which inhibits 50% (IC_{50}, nM) of the growth of human tumor cell line after 72 h drug exposure.
[b] LCC6-WT: human breast carcinoma cell line (Pgp−).
[c] LCC6-MDR: *mdr1* transduced cell line (Pgp+).
[d] Resistance index = (IC_{50} for drug resistant cell line)/(IC_{50} for drug-sensitive cell line).
[e] MCF7: human breast carcinoma cell line.
[f] NCI/ADR: multi-drug resistant human ovarian carcinoma cell line.

combination of attractive properties, such as good aqueous solubility and cellular permeability. Actually, the matched molecular pair analysis (MMPA) of the $OCHF_2$ group indicates that this group may be superior to the OCH_3 and OCF_3 groups for optimizing ADME properties, such as metabolic stability and passive transmembrane permeability [51]. Moreover, the fluorine atom can have multipolar interactions with the electrophilic carbon of nearby protein amide carbonyl groups in protein-ligand binding [44]. The importance of such molecular recognition is supported by structural and SAR studies [55–59]. The significance of the multipolar interaction of fluorine provides a rationale for the exploitation of the fluorine substitution in lead optimizations [44].

Accordingly, it would be worthwhile to examine the effects of the introduction of OCF_3 and $OCHF_2$ groups into the 3rd-generation taxoids on their potencies (i.e., cytotoxicity) in the present work, especially against drug-resitant cancer cell lines, since the benefits of incorporating these groups for pharmacological properties are already well anticipated as described above. Therefore, we synthesized novel 3rd-generation taxoids, bearing 3-OCF_3 and 3-$OCHF_2$ groups at the C2-benzoate moiety, as well as those taxoids bearing a methyl group at the same position for comparison.

Prior to the full SAR studies, we examined three 3rd-generation taxoids bearing the 3-CF_3O-benzoate moiety at C2 together with paclitaxel, **1c** and **1b-03** against the extremely paclitaxel-resistant breast cancer cell line, MCF-7/PTX. As Table 2 shows, SB-T-121205 (**1a-05**)

Table 2
Potency of select taxoids against MCF-7/PTX cell line [60].

Taxane	IC_{50} (nM)
Paclitaxel	2291 ± 125
1c	80.5 ± 7.6
1b-03	21.7 ± 2.3
SB-T-121205 (**1a-05**)	19.0 ± 2.0
SB-T-121405 (**1c-05**)	34.9 ± 3.0
SB-T-121605 (**1d-05**)	31.4 ± 2.8

exhibited the highest potency, which is 121 times better than that of paclitaxel, and **1b-03** was the close second. Detailed study on the mechanism of action (MOA) for **1a-05** disclosed that this taxoid effectively suppresses the PI3k/Akt pathway and epithelial-mesenchymal transition (EMT) by activating PTEN tumor suppressor expression [60]. This MOA is another new and significant feature associated with new-generation taxoids against highly drug-resistant cancer cells in addition to the recently revealed MOA in which new-generation taxoids exhibit high potency against CSCs by effectively suppressing the stemness gene expressions, promoting differentiation [38,61].

With highly anticipated benefits of introducing fluorinated methoxy groups to the 3rd-generation taxoids in ADME properties, as well as recently disclosed unique MOAs of new-generation taxoids, the discovery and development of potent and efficacious new 3rd-generation

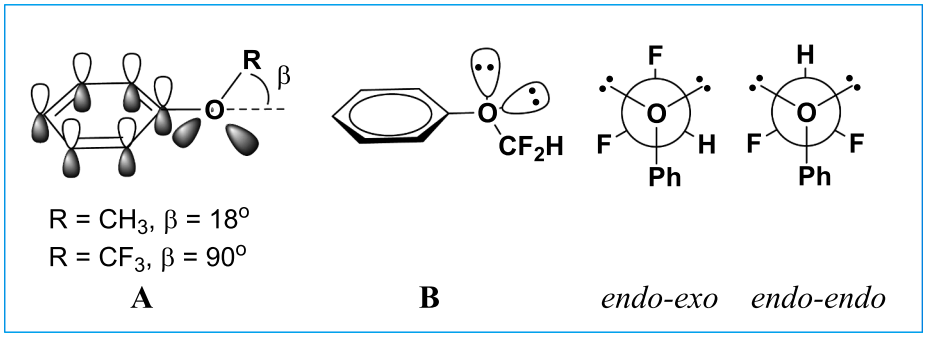

Fig. 2. Conformational characteristics of Ar-OCH_3, Ar-OCF_3 and Ar-$OCHF_2$.

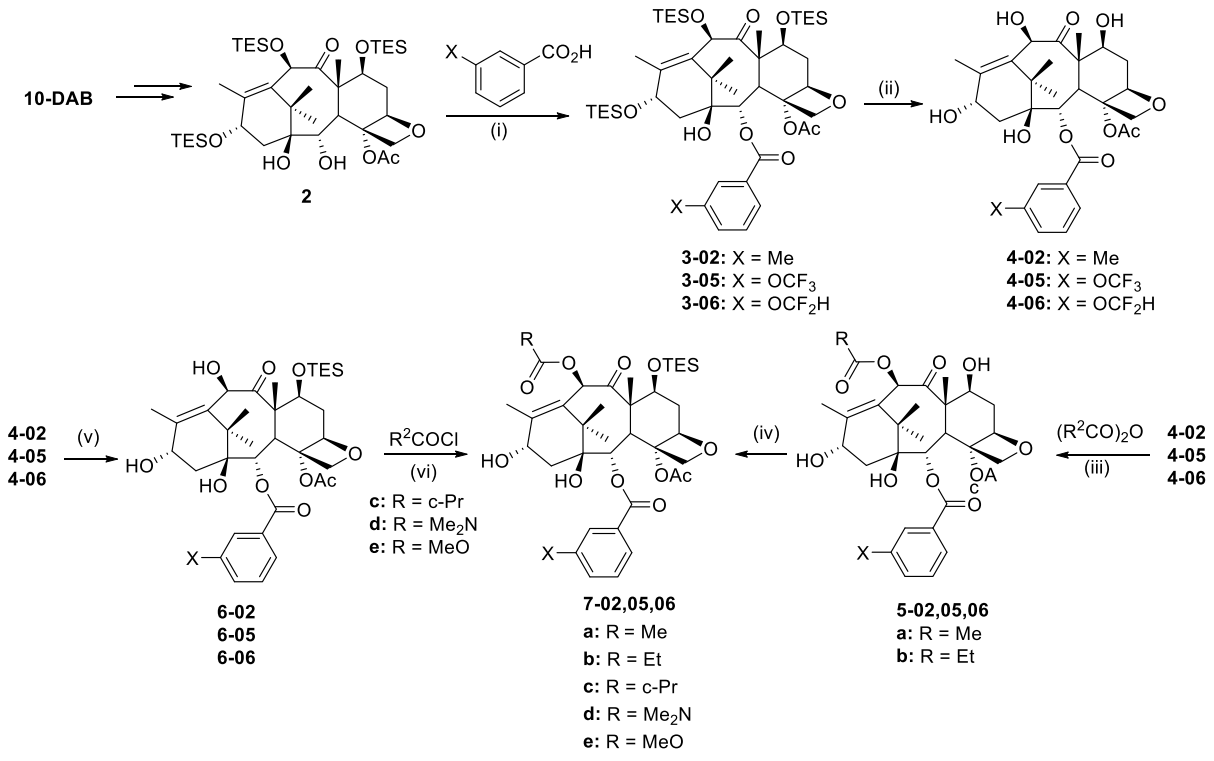

Reagents and conditions: (i) 3-CH_3-, 3-CF_3O- or 3-CHF_2O-benzoic acid (4-8 equiv.), DIC (8 equiv.), DMAP (8 equiv.), CH_2Cl_2, r.t., 2-5 days, 90-94%; (ii) HF/pyridine, pyridine/MeCN, 0 °C-r.t., overnight, 95-98%; (iii) acetic or propanoic anhydride (10 equiv.), $CeCl_3 \cdot 7H_2O$ (0.1 equiv.), THF, r.t., 4 h, 88-95%; (iv) TES-Cl (3 equiv.), imidazole (4 equiv.), DMF, 0 °C, 45 min, 85-88%; (v) TES-Cl (3 equiv.), imidazole (4 equiv.), DMF, 0 °C, 45 min, 85-90%; (vi) LiHMDS, THF, cyclopropanecarbonyl chloride, *N,N*-dimethylcarbamoyl chloride or methyl chloroformate, -40 °C -> r.t., 2-4 h, 73-91%.

Scheme 1. Synthesis of key intermediates, **7(a-e)-02,05,06**.

taxoids has obvious significance.

2. Results and discussion

2.1. Synthesis of new 3rd-generation taxoids bearing 3-CH_3, 3-OCF_3 or 3-OCF_2H group at the C2-benzoate moiety

The synthesis of new 3rd-generation taxoids followed the procedures that we developed and reported [30], starting from 10-deacetylbaccatin III (10-DAB) and using the β-lactam synthon method including the Ojima-Holton coupling, as illustrated in Schemes 1 and 2.

The synthesis of C2-modified baccatins **5-02,05,06** commenced with the exhaustive triethylsilyl (TES) protection of C7, C10, and C13-hydroxyl groups (Scheme 1). Due to the highly congested steric environment, the C1-hydroxyl cannot be protected with a TES group. This free hydroxyl group allowed the selective cleavage of the C2-benzoate by Red-Al in high yield. DIC coupling of 3-CH_3-, 3-OCF_3- or 3-OCF_2H-benzoic acid with tri-TES-baccatin **2** gave 2-modified-tri-TES-baccatins **3-02,05,06**. The subsequent HF/pyridine deprotection afforded 2-modified baccatins **4-02,05,06**, bearing a 3-CH_3, 3-OCF_3 or 3-OCF_2H group at the C2-benzoate moiety (Scheme 1).

Modification of the C10 position with various acyl groups was performed by two methods. The first method was the selective acylation of the 10-hydroxyl moiety by taking advantage of a site-selective Ce^{3+} complexation to block the 7-hydroxyl moiety, using acetic and propanoic anhydrides to give 2,10-modified baccatins, **5(a,b)-02,05,06**. Then, the subsequent TES protection of the 7-hydroxyl group afforded the key intermediates, **7(a,b)-02,05,06**. In the second method, the C7 hydroxyl group was first selectively protected with TES to give 2-modified 7-TES-baccatins, **5-02,05,06**, which were reacted with LiHMDS and various acyl chlorides to afford the corresponding key intermediates, **7(c,d,e)-02,05,06**, wherein the C10-acyl groups were cyclopropanecarbonyl, *N,N*-dimethylcarbamoyl and methoxycarbonyl.

The new 3rd-generation taxoids, **1(a-e)-02,05,06** (see Table 3), were synthesized by the Ojima-Holton coupling of the baccatin key intermediates, **7(a-e)-02,05,06**, with β-lactam **8**, giving the corresponding 7-TES-2′-TIPSO-taxoids, **9(a-e)-02,05,06**, followed by silyl deprotection with HF/pyridine in good to high yield for 2 steps (Scheme 2).

2.2. Biological evaluations of new 3rd-generation taxoids

2.2.1. Potency of new 3rd-generation taxoids against human cancer cell lines

The potency (i.e., cytotoxicity) of the new 3rd-generation taxoids was evaluated against various drug-sensitive and drug-resistant cancer cell lines, i.e., MCF-7, NCI/ADR, LCC6-WT, LCC6-MDR, DLD-1 and CFPAC-1. Results are summarized in Table 4 together with the resistance index (*RI*). Paclitaxel and extensively studied 2nd-generation taxoid, **1c**, were used as controls. The IC_{50} values were determined by a standard MTT assay.

As Table 4 shows, all of the new 3rd-generation taxoids possess two

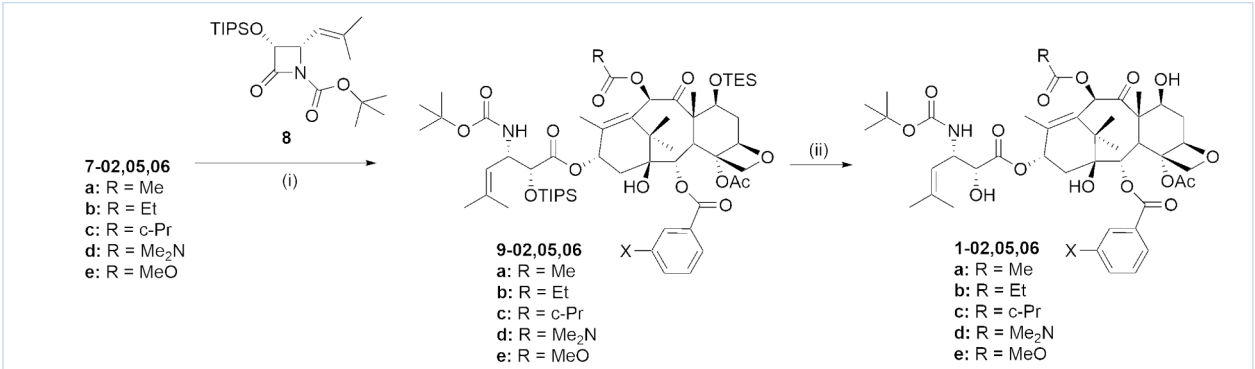

Scheme 2. Synthesis of new 3rd-generation taxoids, **1(a-e)-02,05,06.**

Table 3

New 3rd-generation taxoids.

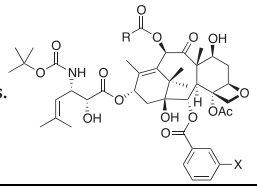

Taxoid	R	X
1a-02	Me	Me
1b-02	Et	Me
1c-02	c-Pr	Me
1d-02	Me_2N	Me
1e-02	MeO	Me
1a-05	Me	OCF_3
1b-05	Et	OCF_3
1c-05	c-Pr	OCF_3
1d-05	Me_2N	OCF_3
1e-05	MeO	OCF_3
1a-06	Ac	OCF_2H
1b-06	Et	OCF_2H
1c-06	c-Pr	OCF_2H
1d-06	Me_2N	OCF_2H
1e-06	MeO	OCF_2H

orders of magnitude greater potency against different drug-resistant cancer cell lines, i.e., NCI/ADR, LCC6/MDR and DLD-1, as compared to the parent compound, paclitaxel. The results clearly indicate that these new taxoids can basically overcome multidrug resistance caused by the overexpression of Pgp and other ABC cassette transporters. Also, all of these new taxoids exhibit subnanomolar IC_{50} values against drug-sensitive cell lines, MCF7 and LCC6-WT, as well as CFPAC-1 which is moderately resistant to paclitaxel.

In general, there is a trend in that the potency of these 3rd-generation taxoids is in the order of preference, OCF_2H (**1-06**) > OCF_3 (**1-05**) > CH_3 (**1-02**), at the 3-position of the C2-benzoate moiety with some exceptions in the drug-sensitive cancer cell lines. For example, **1a-02** and **1d-02** are the two most potent taxoids against LCC6-WT, and **1d-05** and **1e-05** are the two best taxoids against MCF7. However, in all of the drug-resistant cancer cell lines including CFPAC-1, **1(a-e)-06**, exhibit the highest potency. Also, the potency of **1(a-e)-06** is higher than that of excellent 2nd-generation taxoid, **1c**, in all cancer cell lines without exception. [Note: The potency of **1-06** is also higher than that of **1-03** (MeO analogs) (see Table 1) in general. The only minor exception is **1b-03** (*RI* = 2.78) vs. **1b-06** (*RI* = 2.9) in LCC6-WT/LCC6-MDR, but the difference is within the margin of error. Since the data in Table 1 need normalization to make a fair comparison, the normalized values, i.e., IC_{50} and *RI* values, are shown in Table S2 in the Supplementary Material.]

Table 4

IC_{50} values (nM)[a] of new 3rd-generation taxoids against drug-sensitive and drug-resistant human cancer cell lines.

Taxoid	MCF-7[e]	NCI/ADR[f]	*RI*[d]*	LCC6-WT[b]	LCC6-MDR[c]	*RI*[d]	DLD-1[g]	CFPAC-1[h]
PTX	0.9 ± 0.15	130 ± 2.08	*144*	1.81 ± 0.84	619 ± 129	*342*	364 ± 58	60 ± 5.1
1c	0.74 ± 0.56	0.88 ± 0.24	*1.2*	0.91 ± 0.24	3.19 ± 0.66	*3.5*	3.4 ± 0.52	0.71 ± 0.41
1a-02	0.49 ± 0.13	0.78 ± 0.53	*1.6*	0.25 ± 0.06	2.99 ± 1.07	*12*	5.6 ± 1.10	0.59 ± 0.38
1b-02	0.55 ± 0.27	0.59 ± 0.07	*1.1*	0.42 ± 0.30	2.43 ± 0.23	*5.8*	5.5 ± 0.39	0.91 ± 0.74
1c-02	0.56 ± 0.14	0.59 ± 0.26	*1.1*	0.69 ± 0.18	2.15 ± 0.07	*3.1*	3.7 ± 0.75	0.95 ± 0.48
1d-02	0.82 ± 0.32	0.97 ± 0.33	*1.2*	0.27 ± 0.02	3.11 ± 0.93	*12*	3.4 ± 0.46	0.48 ± 0.60
1e-02	0.71 ± 0.07	0.76 ± 0.30	*1.1*	0.47 ± 0.35	2.49 ± 0.85	*5.3*	3.3 ± 0.30	0.61 ± 0.61
1a-05	0.98 ± 0.19	0.83 ± 0.02	*0.85*	0.51 ± 0.18	2.20 ± 0.24	*4.3*	3.0 ± 0.39	0.57 ± 0.32
1b-05	0.37 ± 0.14	0.43 ± 0.20	*1.2*	0.71 ± 0.33	2.40 ± 0.44	*3.4*	3.1 ± 0.26	0.75 ± 0.70
1c-05	0.56 ± 0.16	0.42 ± 0.34	*0.75*	0.58 ± 0.19	2.11 ± 0.08	*3.6*	3.2 ± 0.05	0.79 ± 0.17
1d-05	0.28 ± 0.14	0.66 ± 0.28	*2.4*	0.74 ± 0.06	2.15 ± 0.28	*2.9*	3.3 ± 0.56	0.69 ± 0.59
1e-05	0.32 ± 0.22	0.66 ± 0.18	*2.1*	0.85 ± 0.21	1.96 ± 0.31	*2.3*	3.1 ± 0.47	0.51 ± 0.47
1a-06	0.34 ± 0.21	0.45 ± 0.02	*1.3*	0.42 ± 0.13	2.01 ± 1.26	*4.8*	2.9 ± 0.56	0.48 ± 0.26
1b-06	0.60 ± 0.02	0.26 ± 0.19	*0.43*	0.56 ± 0.25	1.64 ± 0.44	*2.9*	3.0 ± 0.58	0.42 ± 0.29
1c-06	0.37 ± 0.12	0.36 ± 0.11	*0.97*	0.45 ± 0.13	1.80 ± 0.71	*4.0*	3.1 ± 0.44	0.39 ± 0.48
1d-06	0.56 ± 0.3	0.42 ± 0.07	*0.75*	0.40 ± 0.21	1.77 ± 1.39	*4.4*	2.9 ± 0.37	0.44 ± 0.25
1e-06	0.41 ± 0.15	0.39 ± 0.08	*0.95*	0.67 ± 0.03	1.75 ± 0.06	*2.6*	3.0 ± 0.41	0.49 ± 0.37

[a-f]See the captions in Table 1.

[g] multidrug-resistant (Pgp +) human colon cancer cell line.

[h] human pancreatic cancer cell line.

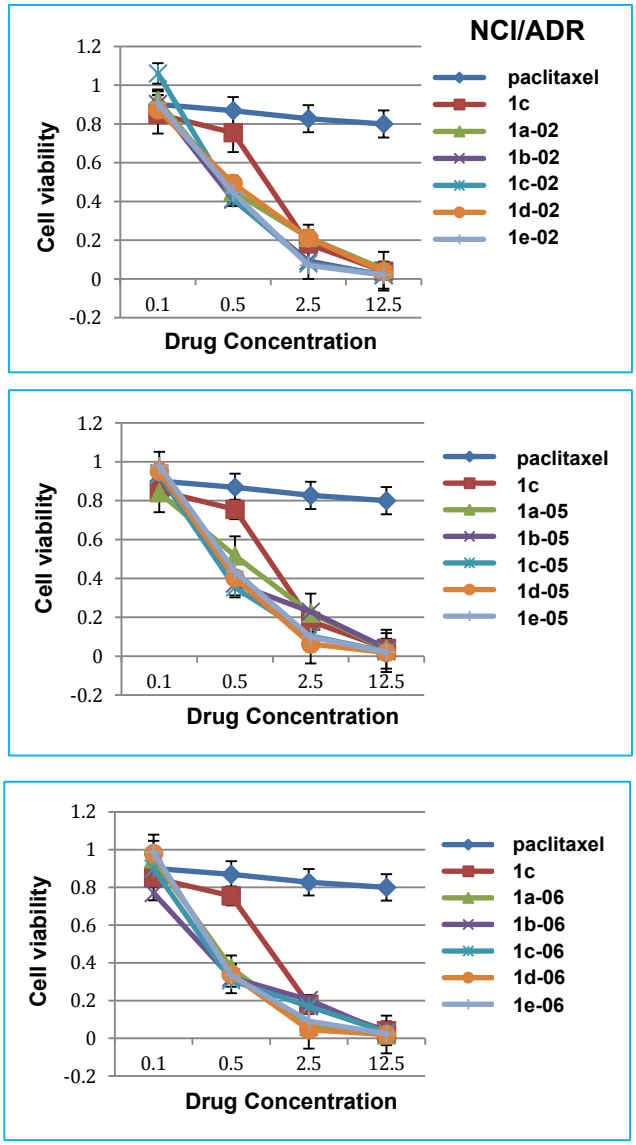

Fig. 3. Dose-response (kill) curves of new 3rd-generation taxoids in NCI/ADR ovarian cancer cell line.

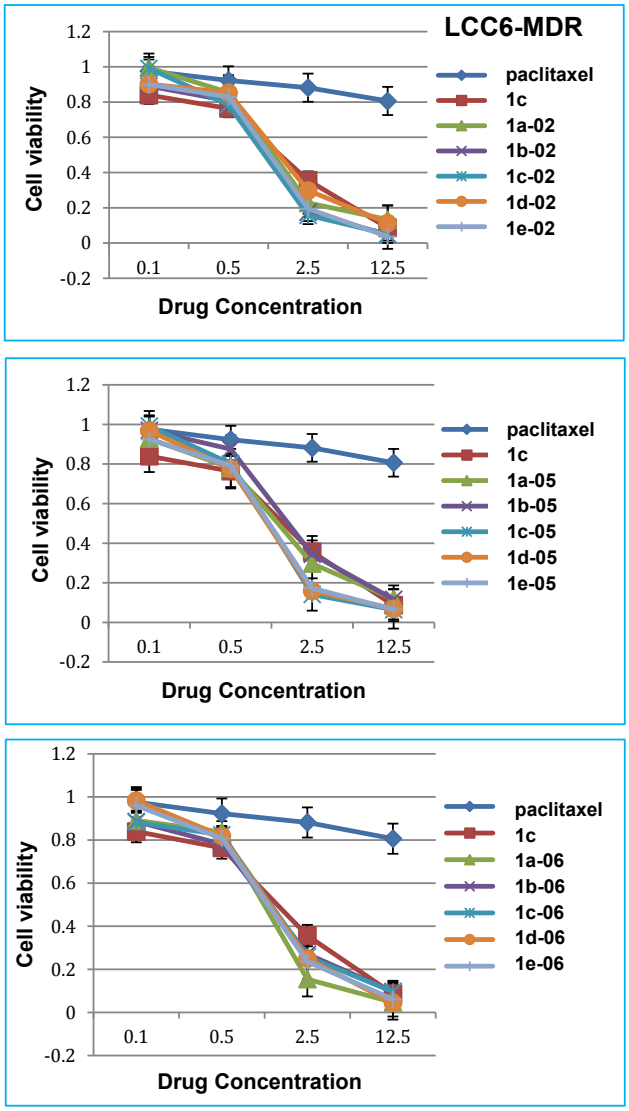

Fig. 4. Dose response curves of new 3rd-generation taxoids in LCC6-MDR lung cancer cell line.

2.2.2. Dose-response (kill) curve analysis of new 3rd-generation taxoids in drug-resistant cancer cell lines

In the NCI/ADR drug-resistant ovarian cancer cell line (Fig. 3), paclitaxel is essentially inactive (IC_{50} 130 nM, Table 4). The new 3rd-generation taxoids showed significantly higher potency than paclitaxel and better dose-response than 2nd-generation taxoid **1c**. It is worthy of note that after 100 nM of paclitaxel treatment, 10% cells were still alive (data not shown). In contrast, after 12.5 nM of next-generation fluorotaxoids treatment, only < 3% cells were alive. Especially, **1b-02**, **1c-02**, **1e-02**, **1d-05**, **1e-05**, **1d-06** and **1e-06** possess very high potency (< 10% cell viability) at 2.5 nM concentration. Overall, **1d-06** and **1d-05** exhibit impressive dose-response (kill) curves as compared to that of paclitaxel and even that of **1c**.

In the LCC6-MDR drug-resistant breast cancer cell line (Fig. 4), paclitaxel was essentially inactive (IC_{50} 619 nM, Table 4) as in the case of the NCI/ADR cell line. Thus, even after 100 nM of paclitaxel treatment, 10% cells were still alive (data not shown), while only < 3% cells were alive after 12.5 nM of new 3rd-generation taxoid treatments. Taxoids **1c-02**, **1c-05**, **1d-05**, **1e-05** and **1a-06** possess high potency (< 15% cell viability) at 2.5 nM concentration, and exhibit impressive dose-response (kill) curves as compared to that of paclitaxel.

In the DLD-1 drug-resistant colon cancer cell line (Fig. 5), paclitaxel was, again, essentially inactive (IC_{50} 364 nM, Table 4). At 12.5 nM paclitaxel concentration, 80% of the cancer cells were alive, while less than 10% cancer cells were alive after treatment with new 3rd-generation taxoids at the same concentration. Taxoids **1d-02**, **1e-02**, **1a-06**, **1d-06**, and **1e-06** possess high potency (< 15% cell viability) at 5 nM concentration, and **1d-06** and **1e-06** exhibit most impressive dose-response (kill) curves as compared to that of paclitaxel and even **1c**. Interestingly, the **1-05** series of taxoids did not show distinct dose-response (kill) curves, compared to that of **1c** against this particular drug-resistant cell line.

2.2.3. Potencies of new 3rd-generation taxoids against CSC-enriched colon cancer cell line HCT-116^{CSC} and patient-derived prostate cancer stem cells PPT2

The potency of select new 3rd-generation taxoids was evaluated against a CSC-enriched colon cancer cell line, HCT116^{CSC} [62,63] and a patient-derived prostate cancer stem cells, PPT2 [61], expressing high levels of CD133, CD44, CD44v6, EpCAM, CD49f and CD166 genes. Since CSC-enriched cancer cells with $CD133^+$ and $CD44^+$ are highly resistant to traditional chemotherapeutic drugs, it was interesting to examine the potency of select new 3rd-generation taxoids against those

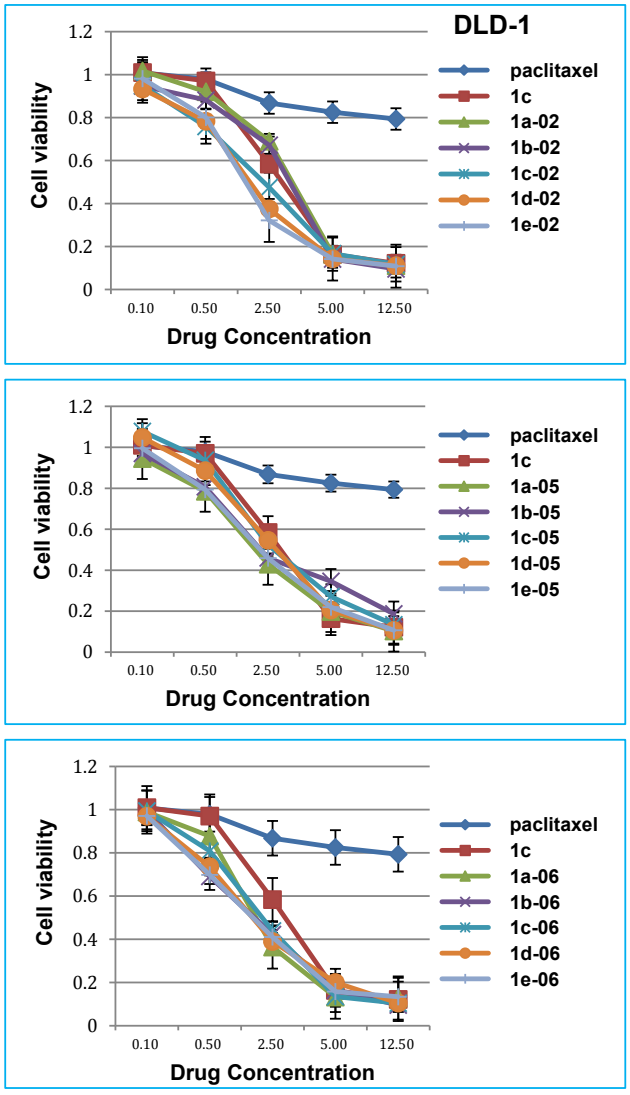

Fig. 5. Dose-response (kill) curves of new 3rd-generation taxoids in DLD-1 colon cancer cell line.

cells.

CSC-enriched colon cancer cell line HCT-116^{CSC}. To maintain its stemness, the CSC-enriched HCT116^{CSC} cell line [38] was cultured in mesenchymal stem cell growth medium (MSCGM™). Since HCT116^{CSC} cells formed 3D spheroids, those cells did not attach well to the bottom of the wells. Three days after treatment with three select taxoids, **1d-05**, **1c-05** and **1c**, much less floating 3D spheroids compared to the control were observed at 10 μM concentration. In the attempted MTT assay (72 h), the cell death rate with 10 μM of taxoids **1d-05** and **1c-05** showed appreciably higher cytotoxicity than carbazitaxel [6], which is the most potent taxane approved by FDA (Fig. 6). Taxoid **1d-05** induced 68% cell death, which is 1.5 times more than that by carbazitaxel. Although 32–40% of HCT116^{CSC} cells survived after treatment with select new 3rd-generation taxoids, it was found that those survived cells showed distinct morphological abnormalities, e.g., enlarged size, severe vacuolization, knobby projections, prolonged size and multiple nuclei. Those abnormalities are characteristic to seriously damaged CSCs, losing pluripotency and ability to form secondary spheroids, reported previously on a HCT116^{CSC} spheroids treated with **1c** [38].

Patient-derived prostate cancer stem cells PPT2. PPT2 cells were also cultivated in the MSCGM™. To estimate approximate IC_{50} values for the new 3rd-generaiton taxoids, three taxoids, **1b-02**, **1b-05** and **1b-06** were selected for an MTT assay. The dose response curves are shown in

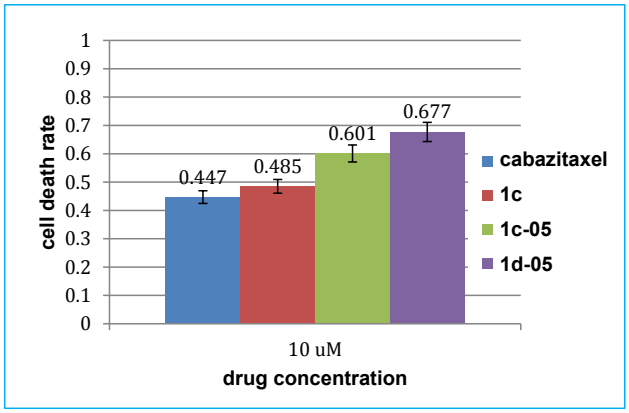

Fig. 6. Cell death rate induced by select taxoids against HCT116^{CSC} cells.

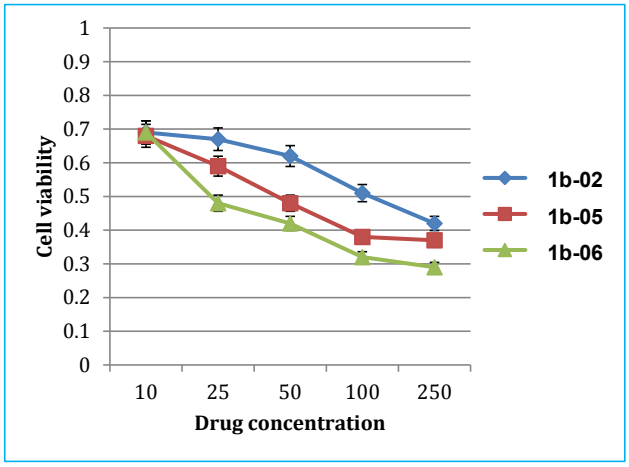

Fig. 7. Dose response curves of select 3rd-generation taxoids against PPT2 CSCs.

Fig. 7. Taxoid **1b-06**, bearing a 3-CHF_2O-benzoyl group at C2, exhibited the best potency (IC_{50} 23 nM) among the three. This pilot study implied that the order of potency is **1-06** series (CHF_2O) > **1-05** series (CF_3O) > **1-02** series (CH_3).

Following up with the pilot study, we examined the cell viability of PPT2 CSCs at 50 nM and 250 nM concentrations of twelve new 3rd-generation taxoids to compare the potencies of **1-02**, **1-05** and **1-06** series and to find if there is a clear structure-activity relationship (SAR). Results are summarized in Fig. 8. As Fig. 8A shows, there is a clear SAR among the twelve taxoids examined wherein the order of potency is **1-06** (CF_2HO) > **1-05** (CF_3O) > **1-02** (CH_3) in all variations at C10 (i.e., **b:** EtCO; **c:** cycloPr-CO; **d:** Me_2NCO; **e:** MeOCO) at 50 nM concentration. At 250 nM concentration (Fig. 8B), however, the relative potency of **1-05** series varies, depending on the C10 substituent although the order of potency among the three series is the same as that observed at 50 nM concentration. The potencies of **1b-02** and **1c-02** are close to those of **1b-05** and **1c-05**, respectively, while the potencies of **1d-05** and **1e-05** are very close to those of **1d-06** and **1e-06**, respectively. Overall, **1e-06** (CF_2HO) exhibited the best potency among the twelve taxoids examined, which caused 62% cell death at 50 nM concentration and 78% cell death at 250 nM concentration.

2.3. Molecular modeling analysis of new 3rd-generation taxoids

We generated a β-tubulin-bound structure of **1a** from the co-crystal structure of β-tubulin and paclitaxel (PDB: 1JFF) [64] using the Avogadro molecular editor [65,66] and MMFF94 force field [67–71], which showed an excellent overlay (see Fig. S1(C) in the Supplementary

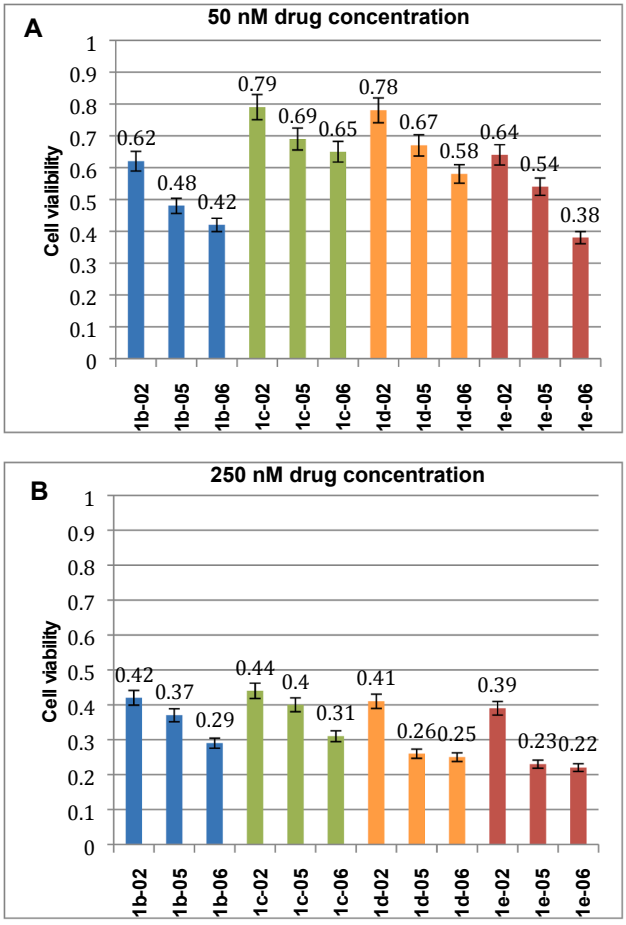

Fig. 8. Cell viability of PPT2 CSCs with 50 nM and 250 nM of new 3rd-generation taxoids (72 h).

Material). Then, the structures of **1a-02**, **1a-03**, **1a-05** and **1a-06** were generated, building upon the β-tubulin-bound **1a** structure in the same manner. Fig. 9 shows (A) the overlays of those 5 taxoids in the proximal binding site and (B) the overlay of **1a-05** and **1a-06**, illustrating the favorable van der Waals (VDW) interactions of the OCF_3 and OCF_2H groups with hydrophobic amino acid residues, Leu230 and Leu275, in the proximal binding site.

Table 5
Relative docking energy scores (kcal/mol) of 3rd-generation taxoids in the proximal and distal sites, in comparison to that of **1a** (kcal/mol).

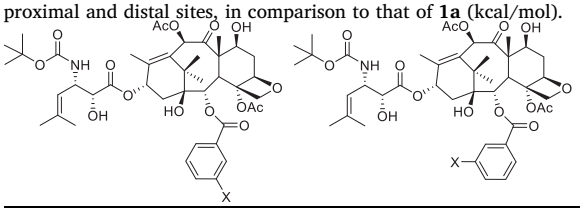

Entry	X	ΔE proximal site	ΔE distal site
1a	H	0	0
1a-02	Me	−0.17	−0.38
1a-03	MeO	−0.01	−0.34
1a-05	OCF_3	−0.54	−0.47
1a-06	OCF_2H	−0.39	−0.40

Docking analyses were performed using AutoDock Vina [72]. Energy-minimized structures were directly used as input for re-orientation. For local search minimization, all possible conformers were used, and data was collected for the conformer in which the pose was most geometrically and energetically favorable. The obtained energy scores of the 4 analogs were compared to that of **1a**, and the relative docking energy scores (ΔE) are summarized in Table 5. Interestingly, the OCF_3 and OCF_2H analogs, i.e., **1a-05** and **1a-06**, orient the X group to the proximal site, while the Me and OMe analogs , i.e., **1a-02** and **1a-03**, tend to place the X groups to the distal site. It is important to point out that all those X groups moderately increase the binding energy, in contrast to bulky X groups such as Br, I, isoPr, *tert*-Bu and CF_3 (see Table S1 in the Supplementary Material). In the proximal site, there is a clear difference in ΔE values between Me/OMe groups vs. OCF_3/OCF_2H groups, while the difference becomes smaller in the distal site although the order of enhancement is the same as that in the proximal site. [*Note*: The distal site is rather shallow and the deviation of binding poses of **1a** analogs from the canonical **1a** structure is large, as compared to that in the proximal site, which show very little deviation. Thus, the results in the proximal site appear to be more reliable. Thus, Fig. 9 only shows docking results in the proximal site.]

Although the predicted affinity is slightly larger for the OCF_3 analog

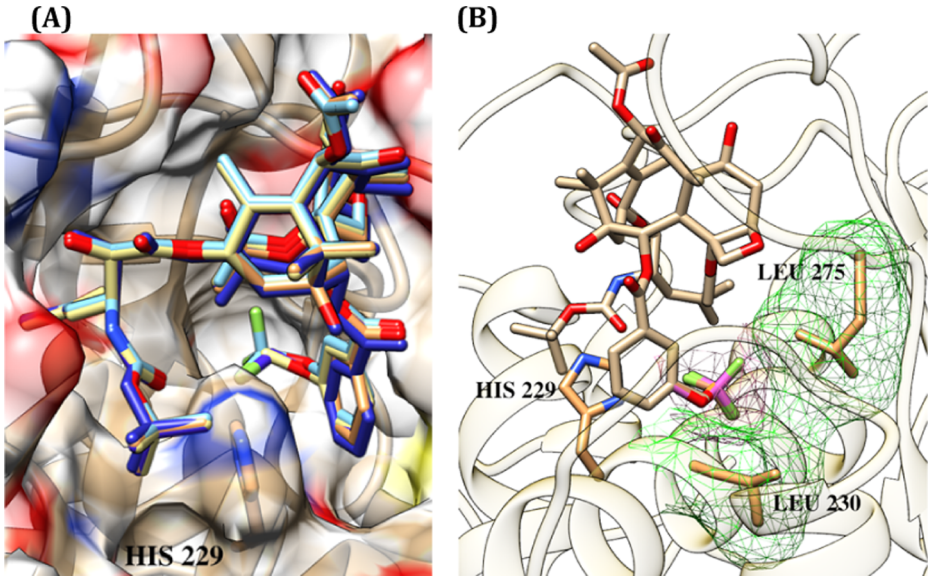

Fig. 9. (A) Overlay of **1a**, **1a-02**, **1a-03**, **1a-05** and **1a-06** in the proximal binding site; (B) Overlay of **1a-05** and **1a-06**, illustrating favorable VDW interactions of the OCF_3 and OCF_2H residues in the proximal binding site.

(**1a-05**) than the OCF_2H analogs (**1a-06**), the observed cytotoxicity of **1a-06** is slightly higher than that of **1a-05** (Table 4). This might be ascribable to a possible difference in cell membrane permeability, i.e., **1a-06** might have a better permeability than **1a-05** though those differences could be within the margin of error.

3. Conclusion

New 3rd-generation taxoids, bearing 3-CH_3, 3-OCF_3 or 3-OCF_2H at the C2 benzoate moiety, were synthesized and fully characterized. These taxoids exhibit up to 7 times better potency (IC_{50}) than paclitaxel against drug-sensitive cancer cell lines, MCF7 (breast) and LCC6-WT (breast), and are 2–3 orders of magnitude more potent than paclitaxel against drug-resistant cancer cell lines, NCI/ADR (ovarian), LCC6-MDR (breast) and LDL-1 (colon) in which P-glycoprotein (Pgp) and other efflux pumps are overexpressed (MDR-phenotype), as well as CFPAC-1 (pancreas). This profile is largely in agreement with those for other 3rd-generation taxoids reported by us previously, wherein the 3-substituents in the C2-benzoate moiety were F, Cl, N_3, MeO and vinyl [31,32]. The new series of taxoids reported in this study expand the SAR studies on 3rd-gneration taxoids, disclosing that CH_3, CF_3O and CHF_2O groups are well tolerated at this position and enhance potency, especially against MDR-cancer cell lines. Importantly, these new taxoids can virtually overcome MDR. Since it has been shown that a vinyl group at this position reduces potency although this group is mildly tolerated, it is a significant finding that rather bulky CF_3O and CHF_2O groups are well tolerated. Molecular modeling analysis of the docked structures and predicted affinity of the new 3rd-generation taxoids, **1a-05** and **1a-06**, in comparison to **1a-02** and **1a-03**, indicated a considerably favorable VDW interactions of OCF_3 and OCF_2H groups with hydrophobic amino acid residues in the binding site, as compared to Me and OMe groups. It has also been shown that inclusion of CF_3O and CHF_2O groups to drug candidates often improve their pharmacological properties, especially metabolic stability, membrane permeability and PK profile [73,74]. Also, the unique non-spherical structure of the $OCHF_2$ group can provide interesting characteristics [54]. Therefore, our finding in this study that the **1-06** series of taxoids, bearing a CHF_2O group at the C2 benzoate position, exhibited the highest potencies against MDR-cancer cell lines and CSC-enriched cancer cell line, HCT-116^{CSC} (colon), as well as patient derived PPT2 CSCs (prostate), is noteworthy. These new 3rd-generation taxoids are promising candidates for highly potent chemotherapeutic agents with proper formulations, especially nanoformulations, and also as payloads (warheads) for tumor-targeting drug conjugates, e.g., antibody-drug conjugates (ADCs).

4. Experimental section

4.1. General methods

Melting points were measured on a Thomas Hoover Capillary melting point apparatus and are uncorrected. NMR spectra were recorded on a Bruker Ascend 700 spectrometer operating at 700 MHz for ^1H and 175 MHz for ^{13}C, a Bruker 500 Advance spectrometer operating at 500 MHz and 125 MHz for ^1H and ^{13}C, respectively, or a Bruker 400 Nanobay spectrometer operating at 400 MHz, 100 MHz, and 376 MHz for ^1H, ^{13}C, and ^{19}F, respectively. Mass to charge values were measured by flow injection analysis on an Agilent Technologies LC/MSD VL. High resolution mass spectrometry (HRMS) analysis was carried out on an Agilent LC-UV-TOF mass spectrometer at the Institute of Chemical Biology and Drug Discovery, Stony Brook, New York. TLC was performed on Merck DC-alufolien with Kieselgel 60F-254 and column chromatography was carried out on silica gel 60 (Merck; 230–400 mesh ASTM). Compound purity was verified by reverse phase HPLC on a Shimadzu LC-2010A machine with a Phenomenex C18 column, Curosil-B 250 × 4.60 mm (acetonitrile-water; flow rate: 0.6 mL/min; UV at 254 and 220/215 nm).

4.2. Materials

The chemicals were purchased from Aldrich Co. and Sigma. Tetrahydrofuran was freshly distilled from sodium metal and benzophenone. Dichloromethane was also distilled immediately prior to use under nitrogen from calcium hydride. 10-DAB III was a gift from the Fujian Yew Park Biological Co. Ltd. (+)-(3*R*,4*S*)-1-Boc-3-TIPS-*O*-4-(2-methylpropen-1-yl)azetidin-2-one (**8**) [34,75], 7,10,13-tris(triethylsilyl)-2-debenzoyl-10-deacetylbaccatin III (**2**) [31], 7,10,13-tris(triethylsilyl)-2-debenzoyl-2-(3-methylbenzoyl)-10-deacetylbaccatin III (**3-02**) [31], 2-debenzoyl-2-(3-methylbenzoyl)-10-deacetylbaccatin III (**4-02**) [31], 2-debenzoyl-2-(3-methylbenzoyl)-10-propanoyl-7-triethylsilyl-10-DAB III (**5a-02**) [31], 2-debenzoyl-2-(3-methylbenzoyl)-10-propanoyl-10-deacetylbaccatin III (**7a-02**) [31], (2′*R*,3′*S*)-2-debenzoyl-2-(3-methylbenzoyl)-7-TES-2′-TIPS-3′-(2-methylpropen-1-yl)-3′-Boc-*N*-3′-dephenyldocetaxel (**9a-02**) [31], (2′*R*,3′*S*)-2-debenzoyl-2-(3-methylbenzoyl)-3′-(2-methylpropen-1-yl)-3′-Boc-*N*-3′-dephenyldocetaxel (**1a-02**) [31] and cabazitaxel [76,77] were prepared by the literature methods. All medium components, buffer and other reagents were obtained from Thermo Fisher Scientific, unless otherwise indicated. 3-(4,5-Dimethylthiazol-2-yl)-2,5-diphenyl-tetrazolium bromide (MTT), hydrochloric acid and isopropyl alcohol were purchased from Aldrich Co. and Sigma.

4.3. Chemical synthesis

4.3.1. 7,10,13-TriTES-2-debenzoyl-2-(3-trifluoromethoxybenzoyl)-10-deacetyl-baccatin III (3-05)

Compound **2** (6.086 g, 7.77 mmol), DMAP (7.594 g, 62.16 mmol) and 3-trifluromethoxybenzoic acid (12.812 g, 62.16 mmol) were dissolved in CH_2Cl_2 (81 mL), and purged with nitrogen. To the mixture DIC (9.71 mL, 62.16 mmol) was added dropwise under inert conditions. The mixture was stirred at room temperature and the reaction progress was monitored by TLC (hexanes:ethyl acetate = 80:20). Upon completion, the reaction was quenched with saturated aqueous NH_4Cl (12 mL), diluted with H_2O (720 mL) and extracted with ethyl acetate (3 × 720 mL). The organic layers were collected, washed with brine (3 × 720 mL), dried over anhydrous $MgSO_4$, and concentrated *in vacuo*. Purification of the crude product by column chromatography on silica gel (hexanes:ethyl acetate = 90:10) to afford **3-05** (7.094 g, 7.31 mmol, 94%) as a white solid: m.p. 189–190 °C; ^1H NMR (400 MHz, $CDCl_3$, ppm) δ 0.56–0.71 (m, 18H), 0.95–1.04 (m, 27H), 1.14 (s, 3H), 1.20 (s, 3H), 1.49 (s, 1H), 1.66 (s, 3H), 1.86–1.93 (m, 1H), 1.99 (d, J = 1.0 Hz, 1H), 2.07–2.24 (m, 2H), 2.28 (s, 3H), 2.50–2.57 (m, 1H), 3.88 (d, J = 7.1 Hz, 1H), 4.14 (AB, J_{AB} = 8.0 Hz, 1H), 4.26 (AB, J_{AB} = 8.0 Hz, 1H), 4.43 (dd, J_1 = 10.5 Hz, J_2 = 6.6 Hz, 1H), 4.91–4.97 (m, 2H), 5.21 (s, 1H), 5.61 (d, J = 7.1 Hz, 1H), 7.44 (d, J = 8.0 Hz, 1H), 7.53 (t, J = 8.0 Hz, 1H), 7.99 (s, 1H), 8.03 (d, J = 8.0 Hz, 1H); ^{19}F NMR (376 MHz, $CDCl_3$, 25 °C) δ −57.92 (3F). HRMS (TOF) *m/z*: Calcd. For $C_{48}H_{77}F_3O11Si_3H^+$, 971.4799. Found, 971.4788.

4.3.2. 7,10,13-TriTES-2-debenzoyl-2-(3-difluromethoxybenzoyl)-10-deacetyl-baccatin III (3-06)

In the same manner as that for **3-05**, **3-06** was synthesized from **2** (1.818 g, 2.32 mmol) and 3-difluromethoxybenzoic acid (1.746 g, 9.28 mmol) in 86% yield (1.903 g) as a white solid: ^1H NMR (400 MHz, $CDCl_3$, ppm) δ 0.55–0.70 (m, 18H), 0.94–1.03 (m, 27H), 1.12 (s, 3H), 1.17 (s, 3H), 1.59 (bs, OH), 1.64 (s, 3H), 1.84–1.91 (m, 1H), 1.98 (s, 3H), 2.06–2.12 (m, 1H), 2.18–2.24 (m, 1H), 2.27 (s, 3H), 2.48–2.56 (m, 1H), 3.86 (d, J = 7.0 Hz, 1H), 4.14 (AB, J_{AB} = 8.2 Hz, 1H), 4.26 (AB,

J_{AB} = 8.2 Hz, 1H), 4.43 (dd, J_1 = 10.5 Hz, J_2 = 6.6 Hz, 1H), 4.90–4.95 (m, 2H), 5.19 (s, 1H), 5.59 (d, J = 7.0 Hz, 1H), 5.59 (d, J = 73.3 Hz, 1H), 7.34 (dd, J_1 = 8.0 Hz, J_2 = 2.0 Hz, 1H), 7.47 (t, J = 8.0 Hz, 1H), 7.88 (s, 1H), 7.94 (d, J = 8.0 Hz, 1H); ^{13}C NMR (100 MHz, $CDCl_3$, ppm) δ 5.02, 5.42, 6.15, 7.05, 7.13, 10.59, 14.76, 20.75, 22.42, 26.49, 37.45, 39.97, 43.15, 47.09, 58.40, 68.47, 72.82, 75.95, 76.17, 76.70, 79.76, 80.92, 84.20, 113.23, 115.83, 118.43, 120.94, 125.14, 127.37, 130.27, 131.68, 135.89, 139.70, 151.23, 166.14, 170.23, 205.79.

*4.3.3. 2-Debenzoyl-2-(3-trifluromethoxybenzoyl)-10-deacetylbaccatin III (**4-05**)*

Compound **3-05** (1.107 g, 1.14 mmol) was dissolved in a 1:1 mixture of acetonitrile:pyridine (50 mL total; 45 mL) and cooled to 0 °C under inert conditions. To the mixture excess HF (70%) in pyridine (11 mL), was added dropwise. The reaction mixture was stirred at room temperature and monitored by TLC (hexanes:ethyl acetate = 50:50). Upon completion, the reaction was quenched with 10% aqueous citric acid (22 mL), diluted with water (220 mL) neutralized with $NaHCO_3$(s) and extracted with ethyl acetate (2 × 220 mL). The organic layer was collected, washed with saturated $CuSO_4$ solution (3 × 70 mL), water (70 mL) and brine (3 × 70 mL). The extract was then dried over anhydrous $MgSO_4$, filtered and the filtrate concentrated *in vacuo*. Purification of the crude product by column chromatography on silica gel (hexanes:ethyl acetate = 50:50) to afford **4-05** (688 mg, 1.095 mmol, 96%) as a white solid: m.p. 224–225 °C; ^{1}H NMR (400 MHz, $CDCl_3$, ppm) δ 0.94 (s, 6H), 1.53 (s, 3H), 1.62–1.68 (m, 1H), 1.90 (s, 3H), 2.13–2.17 (m, 5H), 2.25–2.33 (m, 1H), 3.82 (d, J = 7.1 Hz, 1H), 4.02 (s, 2H), 4.06–4.12 (m, 1H), 4.47 (s, 1H), 4.61–4.62 (m, 1H), 4.78 (d, J = 2.0 Hz, 1H), 4.93 (d, J = 9.1 Hz, 1H), 5.00 (d, J = 7.1 Hz, 1H), 5.14 (d, J = 2.0 Hz, 1H), 5.23 (d, J = 4.4 Hz, 1H), 5.39 (d, J = 7.1 Hz, 1H), 7.72–7.73 (m, 2H), 7.91 (s, 1H), 8.02 (d, J = 8.4 Hz, 1H); ^{13}C NMR (100 MHz, DMSO, ppm) δ 9.66, 14.83, 20.09, 22.03, 26.73, 36.55, 42.39, 46.48, 57.01, 65.98, 70.91, 74.38, 75.39, 75.59, 76.92, 80.08, 83.70, 118.87, 121.41, 126.00, 128.56, 131.11, 132.38, 134.41, 141.59, 148.31, 163.78, 169.39, 210.20; ^{19}F NMR (376 MHz, $CDCl_3$, 25 °C) δ −56.92 (3F). HRMS (TOF) *m/z*: Calcd. For $C_{30}H_{35}F_3O_{11}H^+$, 629.2204. Found, 629.2201.

*4.3.4. 10-Deacetyl-2-debenzoyl-2-(3-difluromethoxybenzoyl)baccatin III (**4-06**)*

In the same manner as that for **4-05**, **4-06** was synthesized from **3-06** (904 mg, 0.948 mmol) in 95% yield (550 mg) as a white solid: m.p. 218–219 °C; ^{1}H NMR (400 MHz, $CDCl_3$, ppm) δ 1.10 (s, 3H), 1.26 (m, 3H), 1.75 (s, 3H), 1.89–1.78 (m, 1H), 2.07 (s, 1H), 2.08 (s, 3H), 2.27 (d, J = 7.7 Hz, 3H), 2.61 (m, 1H), 4.01 (d, J = 7.0 Hz, 1H), 4.20–4.06 (m, 4H), 4.31 (d, J = 8.4 Hz, 1H), 4.87 (s, 1H), 4.99 (d, J = 9.3 Hz, 1H), 5.25 (s, 1H), 5.62 (d, J = 7.0 Hz, 1H), 6.57 (t, J = 73.1 Hz, 1H), 7.38 (d, J = 8.0 Hz, 1H), 7.51 (dd, J_1 = 8.0 Hz, J_2 = 2.0 Hz, 1H), 7.90 (s, 1H), 7.96 (d, J = 8.0 Hz, 1H). HRMS (TOF) *m/z*: Calcd. For $C_{30}H_{36}F_2O_{11}H^+$, 611.2298. Found, 611.2278.

*4.3.5. 2-Debenzoyl-2-(3-methylbenzoyl)-10-deacetyl-10-propanoylbaccatin III (**5b-02**)*

To a solution of **4-02** (92 mg, 0.165 mmol) and cerium(III) chloride hexahydrate (6 mg, 0.017 mmol) in THF (4 mL) was added acetic anhydride (0.16 mL, 1.65 mmol) at 0 °C, the mixture was stirred at room temperature for 3 h. The progress of the reaction was monitored by TLC. Upon completion, the reaction was quenched with saturated NH_4Cl (10 mL), and the aqueous layer was extracted with ethyl acetate (3 × 30 mL). The combined extracts were washed with brine (3 × 30 mL), dried over $MgSO_4$ and concentrated in vacuo. The residue was purified by flash chromatography on silica gel to afford **5b-02** (89 mg, 88%) as a white solid: m.p. 105–107 °C; ^{1}H NMR (500 MHz, $CDCl_3$) δ 1.10 (s, 6H), 1.23(t, J = 7.6 Hz, 3H), 1.66 (m, 6H), 1.86 (m, 1H), 2.04 (s, 3H), 2.19 (d, J = 5 Hz, 1H), 2.28 (m, 5H), 2.42 (s, 3H), 2.53 (m, 5H), 3.87 (d, J = 7.1 Hz, 1H), 4.14 (d, J = 6.4 Hz, 1H), 4.30 (d, J = 8.4 Hz, 1H), 4.46 (m, 1H), 4.88 (dd, J = 7.2 Hz, J = 12.2 Hz, 1H), 4.98 (d, J = 8.0 Hz, 1H), 5.59 (d, J = 7.1 Hz, 1H), 6.33 (s, 1H), 7.35 (t, J = 7.6 Hz, 1H), 7.41 (d, J = 7.6 Hz, 1H), 7.89 (d, J = 7.6 Hz, 1H), 7.91 (s, 1H); ^{13}C NMR (125 MHz, $CDCl_3$) δ 9.2, 9.6, 15.8, 21.1, 21.6, 22.7, 27.2, 27.8, 35.8, 38.8, 42.9, 46.3, 58.9, 68.2, 72.6, 75.0, 76.2, 76.7, 79.3, 81.0, 84.6, 127.4, 128.7, 129.4, 131.0, 132.1, 134.6, 138.6, 146.4, 167.4, 170.8, 174.9, 204.4. HRMS (TOF) Calcd for $C_{33}H_{42}O_{11}NH_4^+$: 632.3065, Found: 632.3066.

*4.3.6. 2-Debenzoyl-2-(3-trifluromethoxybenzoyl)baccatin III (**5a-05**)*

In the same manner as that for **5b-02**, **5a-05** was synthesized from **4-05** (473 mg, 0.752 mmol) and acetic anhydride (0.71 mL, 7.52 mmol)) in 90% yield (453 mg) as a white solid: m.p. 209–210 °C; ^{1}H NMR (400 MHz, $CDCl_3$, ppm) δ 1.11 (s, 6H), 1.67 (s, 3H), 1.83–1.90 (m, 1H), 2.06 (s, 3H), 2.24–2.29 (m, 8H), 2.53–2.61 (m, 1H), 3.89 (d, J = 7.0 Hz, 1H), 4.14 (AB, J_{AB} = 8.2 Hz, 1H), 4.28 (AB, J_{AB} = 8.2 Hz, 1H), 4.47 (dd, J_1 = 10.8 Hz, J_2 = 6.8 Hz, 1H), 4.89 (t, 1H), 4.99 (d, J = 8.8 Hz, 1H), 5.60 (d, J = 7.0 Hz, 1H), 6.33 (s, 1H), 7.46 (d, J = 8.0 Hz, 1H), 7.54 (t, J = 8.0 Hz, 1H), 7.99 (s, 1H), 8.04 (d, J = 8.0 Hz, 1H); ^{13}C NMR δ (100 MHz, $CDCl_3$, ppm) 9.60, 15.83, 21.05, 21.10, 22.56, 27.16, 35.77, 38.71, 42.86, 46.34, 58.87, 68.05, 72.51, 75.71, 76.40, 76.49, 77.44, 79.36, 80.90, 84.66, 119.34, 121.91, 122.35, 126.39, 128.73, 130.50, 131.58, 131.90, 146.75, 149.49, 165.77, 170.85, 171.54, 204.28; ^{19}F NMR (376 MHz, $CDCl_3$, 25 °C) δ −57.86 (3F). HRMS (TOF) *m/z*: Calcd. For $C_{32}H_{37}F_3O_{12}NH_4^+$, 688.2575. Found, 688.2574.

*4.3.7. 2-Debenzoyl-2-(3-trifluromethoxybenzoyl)-10-propanoyl-10-deacetylbaccatin III (**5b-05**)*

In the same manner as that for **5a-05**, **5b-05** was synthesized from **4-05** (431 mg, 0.686 mmol) and propanoic anhydride (0.76 mL, 5.88 mmol) in 88% yield (415 mg) as a white solid: m.p. 124–127 °C; ^{1}H NMR (400 MHz, $CDCl_3$, ppm) δ 1.10 (s, 6H), 1.23 (t, J = 7.6 Hz, 3H), 1.60 (s, 1H), 1.66 (s, 3H), 1.91–1.79 (m, 1H), 2.05 (s, 3H), 2.25 (m, 6H), 2.64–2.47 (m, 4H), 3.89 (d, J = 7.0 Hz, 1H), 4.13 (d, J = 8.2 Hz, 1H), 4.27 (d, J = 8.2 Hz, 1H), 4.49–4.44 (m, 1H), 4.90–4.85 (m, 1H), 4.99 (d, J = 8.1 Hz, 1H), 5.59 (d, J = 7.0 Hz, 1H), 6.33 (s, 1H), 7.45 (d, J = 8.6 Hz, 1H), 7.53 (dd, J_1 = 8.0 Hz, J_2 = 2.0 Hz, 1H), 7.98 (s, 1H), 8.03 (d, J = 7.7 Hz, 1H); ^{13}C NMR δ (100 MHz, $CDCl_3$, ppm) δ 9.03, 9.39, 15.62, 20.86, 22.36, 26.96, 27.60, 35.56, 38.51, 42.65, 46.15, 58.67, 67.85, 72.34, 75.51, 76.00, 76.29, 79.17, 80.70, 84.48, 120.42 (q, J = 259 Hz), 122.15, 126.18, 128.53, 130.30, 131.38, 131.76, 146.43, 149.29, 165.56, 170.65, 174.70, 204.16; ^{19}F NMR (376 MHz, $CDCl_3$, 25 °C) δ −57.86 (3F). HRMS for $C_{33}H_{39}F_3O_{12}^+$ calcd: 684.2637. Found: 684.2389 (Δ = 0.4 ppm).

*4.3.8. 2-Debenzoyl-2-(3-difluromethoxybenzoyl)baccatin III (**5a-06**)*

In the same manner as that for **5a-05**, **5a-06** was synthesized from **4-06** (130 mg, 0.213 mmol) and acetic anhydride (0.2 mL, 2.213 mmol) in 98% yield (133 mg) as a white solid: m.p. 128–130 °C; ^{1}H NMR (700 MHz, $CDCl_3$, ppm) δ 1.07 (m, 6H), 1.23 (m, 3H), 1.63 (s, 3H), 1.85–1.77 (m, 1H), 2.02 (m, 6H), 2.30–2.16 (m, 9H), 2.53 (m, 1H), 3.85 (d, J = 7.0 Hz, 1H), 4.07 (m, 1H), 4.10 (d, J = 8.3 Hz, 1H), 4.26 (d, J = 8.3 Hz, 1H), 4.43 (dd, J = 10.8, 6.8 Hz, 1H), 4.86 (t, J = 7.8 Hz, 1H), 4.96 (d, J = 8.8 Hz, 1H), 5.57 (d, J = 7.0 Hz, 1H), 6.29 (s, 1H), 6.55 (t, J = 73.1 Hz, 1H), 7.35 (d, J = 8.1 Hz, 1H), 7.47 (dd, J_1 = 8.0 Hz, J_2 = 2.0 Hz, 1H), 7.86 (s, 1H), 7.93 (d, J = 7.8 Hz, 1H). HRMS for $C_{32}H_{38}F_2O_{12}^+$ calcd: 652.2336. Found: 652.2331 (Δ = −0.7 ppm).

*4.3.9. 2-Debenzoyl-2-(3-difluromethoxybenzoyl)-10-propanoyl-10-DAB III (**5b-06**)*

In the same manner as that for **5a-05**, **5b-06** was synthesized from **4-06** (316 mg, 0.518 mmol) and propanoic anhydride (0.70 mL, 5.42 mmol) in 95% yield (328 mg) as a white solid: m.p. 140–142 °C; ^{1}H NMR (400 MHz, $CDCl_3$, ppm) δ 1.12 (s, 6H), 1.24 (t, 3H), 1.59 (bs,

1H), 1.68 (s, 3H), 1.84–1.91 (m, 1H), 2.06 (d, J = 1.0 Hz, 3H), 2.28–2.30 (m, 5H), 2.48–2.62 (m, 3H), 3.90 (d, J = 7.0 Hz, 1H), 4.15 (AB, J_{AB} = 8.2 Hz, 1H), 4.31 (AB, J_{AB} = 8.2 Hz, 1H), 4.80 (dd, J_1 = 10.8 Hz, J_2 = 6.8 Hz, 1H), 4.90 (t, 1H), 5.00 (d, J = 7.8 Hz, 1H), 5.61 (d, J = 7.0 Hz, 1H), 6.35 (s, 1H), 6.58 (d, J = 73.2 Hz, 1H), 7.38 (d, J = 7.8 Hz, 1H), 7.51 (t, J = 7.8 Hz, 1H), 7.91 (s, 1H), 7.97 (d, J = 7.8 Hz, 1H); ^{13}C NMR (100 MHz, $CDCl_3$, ppm) δ 9.26, 9.61, 15.82, 21.08, 22.64, 27.20, 27.82, 35.80, 38.72, 42.89, 46.34, 58.93, 68.15, 72.56, 75.59, 76.20, 76.55, 79.38, 80.97, 84.70, 113.19, 115.79, 118.40, 121.18, 126.37, 127.42, 130.41, 131.41, 132.09, 146.51, 151.23, 166.15, 170.92, 174.88, 204.37; ^{19}F NMR (376 MHz, $CDCl_3$, 25 °C) δ −81.54 to −80.63 (2F). HRMS (TOF) *m/z*: Calcd. For $C_{33}H_{40}F_2O_{12}NH_4^+$, 684.2826. Found, 684.2833.

*4.3.10. 2-Debenzoyl-2-(3-trifluromethoxybenzoyl)-7-triethylsilyl-10-deacetylbaccatin III (**6-05**)*

Compound **4-05** (2.118 g, 3.37 mmol) was dissolved in DMF (46 mL) and cooled to 0 °C under inert conditions. To this mixture was added 4 eq of imidazole (990 mg, 14.60 mmol) and allowed to stir 5 min. Then TES-Cl (1.84 mL, 10.95 mmol) was added dropwise. The mixture was stirred and allowed to warm to room temperature while being monitored by TLC (hexanes: ethyl acetate = 60:40). Upon completion the reaction was quenched with saturated NH_4Cl (12 mL) and extracted with ethyl acetate (3 × 200 mL). The organic layer was collected, washed with brine (3 × 250 mL), dried over anhydrous $MgSO_4$, and concentrated *in vacuo*. Purification of the crude product by column chromatography on silica gel (hexanes: ethyl acetate = 65:35) to afford **6-05** (2.302 g, 3.10 mmol, 92%) as a white solid: ^{1}H NMR (400 MHz, $CDCl_3$, ppm) δ 0.53–0.62 (m, 6H), 0.93–0.97 (m, 9H), 1.09 (s, 6H), 1.74 (s, 3H), 1.88–1.94 (m, 1H), 2.05–2.06 (m, 1H), 2.09 (s, 3H), 2.25–2.27 (m, 5H), 2.45–2.53 (m, 1H), 3.97 (d, J = 7.0 Hz, 1H), 4.15 (AB, J_{AB} = 8.2 Hz, 1H), 4.25–4.30 (m, 2H), 4.42 (dd, J_1 = 10.5 Hz, J_2 = 6.6 Hz, 1H), 4.86–4.89 (m, 1H), 4.97 (d, J = 8.0 Hz, 1H), 5.18 (d, J = 2.0 Hz, 1H), 5.58 (d, J = 7.0 Hz, 1H), 7.46 (d, J = 8.0 Hz, 1H), 7.54 (t, J = 8.0 Hz, 1H), 8.00 (s, 1H), 8.05 (d, J = 8.0 Hz, 1H). HRMS (TOF) *m/z*: Calcd. For $C_{36}H_{49}F_3O_{11}SiH^+$, 743.3069. Found, 743.3072.

*4.3.11. 2-Debenzoyl-2-(3-difluromethoxybenzoyl)-7-triethylsilyl-10-deacetylbaccatin III (**6-06**)*

In the same manner as that for **6-02**, **6-06** was synthesized from **4-06** (1.195 g, 1.96 mmol) and TES-Cl (0.40 mL, 2.35 mmol) in 97% yield (1.377 g) as a white solid: ^{1}H NMR (400 MHz, $CDCl_3$, ppm) δ; δ 0.52–0.62 (m, 6H), 0.92–0.96 (m, 9H), 1.09 (s, 6H), 1.74 (s, 3H), 1.87–1.94 (m, 1H), 2.02–2.09 (m, 4H), 2.25–2.29 (m, 5H), 2.45–2.53 (m, 1H), 3.96 (d, J = 7.0 Hz, 1H), 4.15 (AB, J_{AB} = 8.2 Hz, 1H), 4.25 (d, J = 2.0 Hz, 1H), 4.15 (AB, J_{AB} = 8.2 Hz, 1H), 4.41 (dd, J_1 = 10.5 Hz, J_2 = 6.6 Hz, 1H), 4.86–4.88 (m, 1H), 4.97 (d, J = 8.0 Hz, 1H), 5.18 (d, J = 2.0 Hz, 1H), 5.59 (d, J = 7.0 Hz, 1H), 6.57 (d, J = 73.2 Hz, 1H), 7.36 (d, J = 8.0 Hz, 1H), 7.50 (t, J = 8.0 Hz, 1H), 7.90 (s, 1H), 7.94 (d, J = 8.0 Hz, 1H); ^{13}C NMR (100 MHz, $CDCl_3$, ppm) δ 5.02, 5.42, 6.15, 7.05, 7.13, 10.59, 14.76, 20.75, 22.42, 26.49, 37.45, 39.97, 43.15, 47.09, 58.40, 68.47, 72.82, 75.95, 76.17, 76.70, 79.76, 80.92, 84.20, 113.23, 115.83 (t, J = 260 Hz), 118.43, 120.94, 125.14, 127.37, 130.27, 131.68, 135.89, 139.70, 151.23, 166.14, 170.23, 205.79; ^{19}F NMR (376 MHz, $CDCl_3$, 25 °C) δ −80.99 (ABq, J = 167 Hz, 2F).

*4.3.12. 2-Debenzoyl-7-TES-2-(3-methylbenzoyl)-10-deacetyl-10-propanoylbaccatin III (**7b-02**)*

To a solution of **5b-02** (72 mg, 0.117 mmol) and imidazole (32 mg, 0.469 mmol) in DMF (6 mL) was added TES-Cl (58 μl, 0.351 mmol) dropwise at 0 °C. The mixture was stirred at 0 °C for 45 min. The progress of the reaction was monitored by TLC. Upon completion, the reaction was quenched with saturated NH_4Cl (10 mL), and the aqueous layer was extracted with ethyl acetate (3 × 30 mL). The combined extracts were washed with brine (3 × 30 mL), dried over $MgSO_4$ and concentrated in vacuo. The residue was purified by flash chromatography on silica gel to afford **7b-02** (64 mg, 75%) as a white solid: m.p. 105–107 °C; ^{1}H NMR (700 MHz, $CDCl_3$) δ 0.57 (m, 6H), 0.91 (t, J = 8.0 Hz, 9H), 1.02 (s, 3H), 1.20 (m, 6H), 1.67 (m, 4H), 1.86 (m, 1H), 2.18 (d, J = 4.8 Hz, 1H), 2.19 (d, J = 1.1 Hz, 3H), 2.28 (m, 5H), 2.42 (m, 3H), 2.52 (m, 2H), 3.87 (d, J = 7.0 Hz, 1H), 4.13 (d, J = 8.5 Hz, 1H), 4.29 (d, J = 8.5 Hz, 1H), 4.48 (dd, J = 6.7 Hz, J = 10.5 Hz, 1H), 4.82 (m, 1H), 4.96 (d, J = 8.2 Hz, 1H), 5.60 (d, J = 7.1 Hz, 1H), 6.47 (s, 1H), 7.35 (t, J = 7.5 Hz, 1H), 7.40 (d, J = 7.5 Hz, 1H), 7.90 (d, J = 7.5 Hz, 1H), 7.93 (s, 1H); ^{13}C NMR (175 MHz, $CDCl_3$) δ 5.5, 6.9, 9.4, 10.1, 15.1, 20.3, 21.6, 22.8, 27.0, 37.4, 38.4, 42.9, 47.5, 58.8, 68.1, 72.6, 74.8, 76.0, 76.7, 79.0, 81.1, 84.4, 127.4, 128.7, 129.5, 131.0, 132.9, 134.6, 138.5, 144.1, 167.4, 170.9, 173.0, 202.45. HRMS (TOF) Calcd for $C_{39}H_{56}O_{11}SiH^+$ 729.3665, Found: 729.3669 (Δ = −0.55 ppm).

*4.3.13. 2-Debenzoyl-7-TES-2-(3-methylbenzoyl)-10-deacetyl-10-cyclopropane-carbonylbaccatin III (**7c-02**)*

To a solution of **6-02** (193 mg, 0.287 mmol) in THF (6 mL) was added LiHMDS (1.0 M in THF, 0.32 mL, 0.320 mmol) dropwise at −40 °C. The mixture was stirred at −40 °C for 5 min. Then cyclopropane-carbonyl chloride (27 μl, 0.301 mmol) was added dropwise and the reaction mixture was stirred at −40 °C for 30 min. The progress of the reaction was monitored by TLC. Upon completion, the reaction was quenched with saturated NH_4Cl (10 mL), and the aqueous layer was extracted with ethyl acetate (3 × 30 mL). The combined extracts were washed with brine (3 × 30 mL), dried over $MgSO_4$ and concentrated in vacuo. The residue was purified by flash chromatography on silica gel to afford **7b-02** (178 mg, 84%) as a white solid: m.p. 132–133 °C; ^{1}H NMR (500 MHz, $CDCl_3$) δ 0.56 (m, 6H), 0.91 (m, 10H), 1.02 (m, 5H), 1.17 (m, 4H), 1.67 (m, 4H), 1.75 (m, 1H), 1.87 (m, 1H), 2.19 (s, 3H), 2.26 (m, 6H), 2.41 (s, 3H), 2.51 (m, 1H), 3.87 (d, J = 7.0 Hz, 1H), 4.13 (d, J = 8.4 Hz, 1H), 4.30 (d, J = 8.4 Hz, 1H), 4.47 (dd, J = 6.8 Hz, J = 10.5 Hz, 1H), 4.82 (t, J = 8.0 Hz, 1H), 4.96 (d, J = 8.7 Hz, 1H), 5.61 (d, J = 7.1 Hz, 1H), 6.45 (s, 1H), 7.35 (t, J = 7.7 Hz, 1H), 7.40 (d, J = 7.7 Hz, 1H), 7.89 (d, J = 7.7 Hz, 1H), 7.93 (s, 1H); ^{13}C NMR (125 MHz, $CDCl_3$) δ 5.5, 7.0, 8.8, 8.9, 10.1, 13.2, 15.1, 20.4, 21.6, 22.8, 27.0, 37.4, 38.4, 43.0, 47.5, 58.8, 68.2, 72.6, 74.8, 75.7, 76.8, 79.0, 81.1, 84.4, 127.4, 128.7, 129.5, 131.0, 133.0, 134.6, 138.5, 144.1, 167.4, 170.9, 173.4, 202.5. HRMS (TOF) Calcd for $C_{40}H_{57}O_{11}Si^+$:741.3665, Found: 741.3673 (Δ = −1.08 ppm).

*4.3.14. 2-Debenzoyl-7-TES-2-(3-methylbenzoyl)-10-deacetyl-10-N,N-dimethyl-carbamoyl-baccatin III (**7d-02**)*

In the same manner as that for **7c-02**, **7d-02** was synthesized from **6-02** (101 mg, 0.150 mmol) and *N,N*-dimethylcarbamoyl chloride (15 μl, 0.158 mmol) in 94% yield (454 mg) as a white solid: m.p. 146–148 °C; ^{1}H NMR (500 MHz, $CDCl_3$) δ 0.58 (m, 6H), 0.91 (t, J = 8.1 Hz, 9H), 1.04 (s, 3H), 1.19 (s, 3H), 1.64 (s, 1H), 1.65 (s, 3H), 1.67 (s, 3H), 1.86 (m, 1H), 2.12 (d, J = 4.8 Hz, 1H), 2.25 (m, 8H), 2.41 (s, 3H), 2.51 (m, 1H), 2.93 (s, 3H), 3.07 (s, 3H), 3.88 (d, J = 7.0 Hz, 1H), 4.13 (d, J = 8.3 Hz, 1H), 4.29 (d, J = 8.3 Hz, 1H), 4.47 (dd, J = 6.8 Hz, J = 10.5 Hz, 1H), 4.81 (br s, 1H), 4.96 (d, J = 8.1 Hz, 1H), 5.60 (d, J = 7.1 Hz, 1H), 6.37 (s, 1H), 7.34 (t, J = 7.6 Hz, 1H), 7.39 (d, J = 7.6 Hz, 1H), 7.89 (d, J = 7.6 Hz, 1H), 7.93 (s, 1H); ^{13}C NMR (125 MHz, $CDCl_3$) δ 5.4, 5.5, 6.9, 10.1, 15.0, 20.4, 21.6, 22.8, 27.1, 36.4, 36.7, 37.4, 38.4, 42.9, 47.5, 58.6, 68.2, 72.5, 74.8, 76.8, 79.0, 81.1, 84.5, 127.4, 128.7, 129.5, 131.0, 133.4, 134.5, 138.5, 143.8, 155.5, 167.4, 170.9, 203.5. HRMS (TOF) Calcd for $C_{39}H_{57}NO_{11}SiNa^+$ 766.3593, Found: 766.3594 (Δ = −0.1 ppm).

*4.3.15. 2-Debenzoyl-7-TES-2-(3-methylbenzoyl)-10-deacetyl-10-methoxycarbonyl-baccatin III (**7e-02**)*

In the same manner as that for **7c-02**, **7e-02** was synthesized from **6-02** (102 mg, 0.152 mmol) and methyl chloroformate (13 μl, 0.159 mmol) in 72% yield (80 mg) as a white solid: m.p. 110–112 °C ^{1}H

NMR (500 MHz, $CDCl_3$) δ 0.59 (m, 6H), 0.93 (t, J = 8.2 Hz, 9H), 1.05 (s, 3H), 1.17 (s, 3H), 1.63 (s, 1H), 1.68 (s, 3H), 1.88 (m, 1H), 2.10 (br s, 1H), 2.20 (s, 3H), 2.27 (m, 5H), 2.42 (s, 3H), 2.53 (m, 1H), 3.81 (s, 3H), 3.84 (d, J = 7.1 Hz, 1H), 4.13 (d, J = 8.4 Hz, 1H), 4.30 (d, J = 8.4 Hz, 1H), 4.48 (dd, J = 6.9 Hz, J = 10.5 Hz, 1H), 4.86 (m, 1H), 4.96 (d, J = 8.2 Hz, 1H), 5.60 (d, J = 7.1 Hz, 1H), 6.28 (s, 1H), 7.35 (t, J = 7.7 Hz, 1H), 7.41 (d, J = 7.7 Hz, 1H), 7.89 (d, J = 7.7 Hz, 1H), 7.93 (s, 1H); ^{13}C NMR (125 MHz, $CDCl_3$) δ 5.4, 5.5, 6.9, 10.1, 15.0, 20.4, 21.6, 22.8, 27.1, 36.4, 36.7, 37.4, 38.4, 42.9, 47.5, 58.6, 68.2, 72.5, 74.8, 76.8, 79.0, 81.1, 84.5, 127.4, 128.7, 129.5, 131.0, 133.4, 134.5, 138.5, 143.8, 155.5, 167.4, 170.9, 203.5. HRMS (TOF) Calcd for $C_{37}H_{56}NO_{12}Si^+$ 748.3723, Found: 748.3727 (Δ = −0.53 ppm).

*4.3.16. 2-Debenzoyl-2-(3-trifluromethoxybenzoyl)-7-TES-baccatin III (**7a-05**)*

Compound **5a-05** (400 mg, 0.596 mmol) was dissolved in DMF (8 mL) and cooled to 0 °C under inert conditions. To this mixture was added 4 equiv. of imidazole (162 mg, 2.39 mmol) and the mixtures was allowed to stir for 5 min. Then, TES-Cl (0.30 mL, 1.79 mmol) was added dropwise. The mixture was stirred and allowed to warm to room temperature while being monitored by TLC (hexanes: ethyl acetate = 60:40). Upon completion the reaction was quenched with saturated aqueous NH_4Cl (2 mL) and extracted with ethyl acetate (3 × 35 mL). The organic layer was collected, washed with brine (3 × 45 mL), dried over anhydrous $MgSO_4$, and concentrated *in vacuo*. Purification of the crude product by column chromatography on silica gel (hexanes: ethyl acetate = 60:40) to afford **7a-05** (409 mg, 0.521 mmol, 88%) as a white solid: ^{1}H NMR (400 MHz, $CDCl_3$, ppm) δ 0.56–0.62 (m, 6H), 0.93 (t, J = 8.0 Hz, 9H), 1.05 (s, 3H), 1.20 (s, 3H), 1.69 (s, 3H), 1.85–1.92 (m, 1H), 2.07 (d, J = 4.8 Hz, 1H), 2.19 (s, 3H), 2.20 (d, J = 1.0 Hz, 1H), 2.26–2.27 (m, 4H), 2.51–2.59 (m, 1H), 3.90 (d, J = 7.0 Hz, 1H), 4.14 (AB, J_{AB} = 8.1 Hz, 1H), 4.28 (AB, J_{AB} = 8.1 Hz, 1H), 4.47 (dd, J_1 = 10.5 Hz, J_2 = 6.8 Hz, 1H), 4.83–4.86 (m, 1H), 4.98 (d, J = 8.1 Hz, 1H), 5.62 (d, J = 7.0 Hz, 1H), 6.47 (s, 1H), 7.46 (d, J = 8.0 Hz, 1H), 7.54 (t, J = 8.0 Hz, 1H), 8.00 (s, 1H), 8.04 (d, J = 8.0 Hz, 1H); ^{13}C NMR (100 MHz, $CDCl_3$, ppm) δ 5.50, 6.96, 10.12, 15.20, 20.25, 21.16, 22.68, 27.04, 37.43, 38.36, 42.95, 47.47, 58.86, 68.12, 72.57, 75.53, 75.96, 76.60, 77.44, 79.05, 81.02, 84.44, 122.40, 126.35, 128.77, 130.46, 131.66, 132.84, 144.23, 149.50, 165.84, 169.56, 170.96, 202.29. HRMS (TOF) *m/z*: Calcd. For $C_{38}H_{51}F_3O_{12}SiH^+$, 785.3175. Found, 785.3178.

*4.3.17. 2-Debenzoyl-7-TES-2-(3-trifluromethoxybenzoyl)-10-propanoyl-10-deacetylbaccatin III (**7b-05**)*

In the same manner as that for **7a-05**, **7b-05** was synthesized from **5b-05** (400 mg, 0.605 mmol) and TES-Cl (0.32 mL, 1.82 mmol) in 94% yield (454 mg) as a white solid: m.p. 202–205 °C; ^{1}H NMR (400 MHz, $CDCl_3$, ppm) δ 0.58 (d, J = 7.1 Hz, 6H), 0.92 (t, J = 7.8 Hz, 9H), 1.03 (s, 3H), 1.25–1.19 (m, 6H), 1.65 (m, 3H), 1.87 (m, 1H), 2.26 (m, 9H), 2.39–2.60 (m, 4H), 3.89 (d, J = 6.8 Hz, 1H), 4.12 (d, J = 8.0 Hz, 1H), 4.26 (d, J = 8.0 Hz, 1H), 4.49 (dd, J = 9.8, 6.9 Hz, 1H), 4.83 (s, 1H), 4.96 (d, J = 9.0 Hz, 1H), 5.61 (d, J = 6.8 Hz, 1H), 6.47 (s, 1H), 7.45 (d, J = 7.6 Hz, 1H), 7.52 (dd, J = 8.0, 2.0 Hz, 1H), 7.99 (s, 1H), 8.04 (d, J = 7.5 Hz, 1H); ^{13}C NMR (100 MHz, $CDCl_3$, ppm) δ 5.3, 6.7, 9.2, 9.9, 14.9, 20.1, 26.8, 27.7, 37.2, 42.7, 47.3, 58.6, 67.8, 72.3, 75.3, 75.6, 76.4, 76.7, 77.2, 77.3, 116.5, 116.7, 121.7 (q, J = 259 Hz), 122.2, 124.5, 126.1, 128.5, 130.2, 131.5, 132.6, 144.1, 149.3, 165.6, 170.7, 172.7, 202.2; ^{19}F NMR (376 MHz, $CDCl_3$) δ −57.87 (s, 3F). HRMS (TOF) *m/z*: Calcd. For $C_{39}H_{53}F_3O_{12}Si^+$, 798.3445. Found, 798.3477 (Δ = 4.0 ppm).

*4.3.18. 2-Debenzoyl-2-(3-trifluromethoxybenzoyl)-7-TES-10-cyclopropanecarbonyl-10-deacetyl-baccatin III (**7c-05**)*

Compound **6c-05** (123 mg, 0.166 mmol) was dissolved in THF (3.7 mL) and cooled to −40 °C under inert conditions. To the mixture 1.0 M LiHMDS in *tert*-butyl methyl ether (0.2 mL) was added dropwise, followed by the dropwise addition of 1.2 equiv. of cyclopropanecarbonyl chloride (19 µl, 0.199 mmol). The mixture was stirred and the progress of the reaction was monitored by TLC (hexanes:ethyl acetate = 70:30). Upon completion, the reaction was quenched with saturated NH_4Cl (5 mL), diluted with water and extracted with ethyl acetate (3 × 5 mL). The organic layers were collected and combined, washed with brine (2 × 5 mL), dried over anhydrous $MgSO_4$, and concentrated *in vacuo*. Purification of the crude product by column chromatography on silica gel (hexanes:ethyl acetate = 67:33) to afford **7c-05** (0.154 mmol, 93%) as a white solid: m.p. 201–202 °C; ^{1}H NMR (400 MHz, $CDCl_3$, ppm) δ 0.65–0.50 (m, 6H), 0.92 (t, J = 7.9 Hz, 9H), 1.06 (s, 3H), 1.20 (s, 3H), 1.68 (s, 2H), 1.76 (m, 1H), 1.83–1.93 (m, 1H), 2.20 (d, J = 1.2 Hz, 2H), 2.30–2.23 (m, 4H), 2.53 (ddd, J = 14.4, 9.6, 6.8 Hz, 1H), 3.89 (d, J = 7.0 Hz, 1H), 4.13 (d, J = 7.7 Hz, 1H), 4.27 (d, J = 8.1 Hz, 1H), 4.48 (dd, J = 10.4, 6.7 Hz, 1H), 4.84 (t, J = 8.1 Hz, 1H), 4.97 (d, J = 7.8 Hz, 1H), 5.61 (d, J = 7.1 Hz, 1H), 6.47 (s, 1H), 7.45 (d, J = 8.9 Hz, 1H), 7.53 (dd, J = 10.6, 5.3 Hz, 1H), 8.00 (s, 1H), 8.04 (dd, J = 7.7, 1.2 Hz, 1H); ^{13}C NMR (100 MHz, $CDCl_3$, ppm) δ 5.42, 6.91, 8.72, 8.84, 10.05, 13.15, 15.08, 20.29, 22.53, 26.91, 37.32, 38.42, 42.86, 47.43, 58.71, 67.90, 72.49, 75.53, 75.71, 76.52, 78.97, 80.86, 84.41, 119.28, 121.85 (q, J = 259 Hz), 122.29, 126.24, 128.67, 130.40, 131.64, 132.60, 144.53, 149.42, 165.71, 170.81, 173.36, 202.62; ^{19}F NMR (376 MHz, $CDCl_3$) δ −57.87 (s, 3F). HRMS (TOF) *m/z*: Calcd. For $C_{40}H_{53}F_3O_{12}SiNa^+$, 833.3150. Found, 833.3150.

*4.3.19. 2-Debenzoyl-2-(3-trifluromethoxybenzoyl)-7-TES-10-(N,N-dimethylcarbamoyl)-10-deacetylbaccatin III (**7d-05**)*

In the same manner as that for **7c-05**, **7d-05** was synthesized from **6d-05** (394 mg, 0.530 mmol) and *N,N*-dimethylcarbamoyl chloride (0.059 mL, 0.636 mmol) in 77% yield (332 mg) as a white solid: ^{1}H NMR (400 MHz, $CDCl_3$, ppm) δ 0.57–0.64 (m, 6H), 0.91–0.95 (m, 9H), 1.06 (s, 3H), 1.20 (s, 9H), 1.69 (s, 3H), 1.85–1.91 (m, 1H), 2.26–2.27 (m, 7H), 2.51–2.58 (m, 1H), 2.95 (s, 3H), 3.09 (s, 3H), 3.92 (d, J = 7.0 Hz, 1H), 4.14 (AB, J_{AB} = 8.2 Hz, 1H), 4.28 (AB, J_{AB} = 8.2 Hz, 1H), 4.50 (dd, J_1 = 10.4 Hz, J_2 = 6.7 Hz, 1H), 4.84 (t, J = 8.0 Hz, 1H), 4.98 (d, J = 8.3 Hz, 1H), 6.40 (s, 1H), 5.62 (d, J = 7.0 Hz, 1H), 7.46 (d, J = 8.0 Hz, 1H), 7.54 (t, J = 8.0 Hz, 1H), 8.01 (s, 1H), 8.06 (d, J = 8.0 Hz, 1H);^{13}C NMR (100 MHz, $CDCl_3$, ppm) δ 5.49, 6.95, 10.14, 15.09, 20.39, 22.70, 27.10, 36.44, 36.78, 37.42, 38.35, 42.92, 47.48, 58.64, 68.20, 72.56, 75.60, 76.62, 77.43, 79.13, 81.05, 84.51, 121.92, 122.42, 126.33, 128.75, 130.44, 131.71, 133.28, 143.92, 149.49, 155.52, 165.86, 170.94, 203.39.

*4.3.20. 10-Deacetyl-2-debenzoyl-10-methoxycarbonyl-7-TES-2-(3-trifluoromethoxybenzoyl)-baccatin III (**7e-05**)*

In the same manner as that for **7c-05**, **7e-05** was synthesized from **6e-05** (364 mg, 0.490 mmol) and methyl chloroformate (0.045 mL, 0.59 mmol) in 89% yield (351 mg) as a white solid: ^{1}H NMR (400 MHz, $CDCl_3$, ppm) δ 0.58–0.64 (m, 6H), 0.90–0.97 (m, 9H), 3.04 (s, 3H), 1.18 (s, 3H), 1.70 (s, 3H), 1.86–1.92 (m, 1H), 2.21 (d, J = 1.0 Hz, 1H), 2.26–2.28 (m, 5H), 2.52–2.59 (m, 1H), 3.83 (s, 3H), 3.86 (d, J = 7.0 Hz, 1H), 4.13 (AB, J_{AB} = 8.2 Hz, 1H), 4.28 (AB, J_{AB} = 8.2 Hz, 1H), 4.50 (dd, J_1 = 10.4 Hz, J_2 = 6.7 Hz, 1H), 4.87 (t, J = 8.0 Hz, 1H), 4.98 (d, J = 8.1 Hz, 1H), 5.61 (d, J = 7.0 Hz, 1H), 6.30 (s, 1H), 7.46 (d, J = 8.2 Hz, 1H), 7.54 (t, J = 8.0 Hz, 1H), 8.00 (s, 1H), 8.05 (dd, J_1 = 7.7 Hz, J_2 = 1.2 Hz, 1H).

*4.3.21. 2-Debenzoyl-7-TES-2-(3-difluromethoxybenzoyl)baccatin III (**7a-06**)*

In the same manner as that for **7a-05**, **7a-06** was synthesized from **5a-06** (133 mg, 0.204 mmol) and TES-Cl (0.11 mL, 0.61 mmol) in 93% yield (148 mg) as a white solid: m.p. 197–198 °C; ^{1}H NMR (400 MHz, $CDCl_3$, ppm) δ 0.55–0.61 (m, 6H), 0.92 (t, J = 7.9 Hz, 9H), 1.04 (s, 3H), 1.19 (s, 3H), 1.57 (d, J = 8.1 Hz, 2H), 1.68 (s, 3H), 1.84–1.96 (m, 1H), 2.07 (d, J = 5.0 Hz, 1H), 2.18 (m, 6H), 2.26 (d, J = 7.5 Hz, 5H), 2.49–2.57 (m, 1H), 3.88 (d, J = 7.0 Hz, 1H), 4.13 (d, J = 8.2 Hz, 1H),

4.29 (d, J = 8.2 Hz, 1H), 4.49 (dd, J = 10.4, 6.7 Hz, 1H), 4.83 (dd, J = 13.0, 6.8 Hz, 1H), 4.96 (d, J = 7.9 Hz, 1H), 5.61 (d, J = 7.0 Hz, 1H), 6.46 (s, 1H), 6.66 (t, J = 72.0 Hz, 1H), 7.37 (d, J = 7.8 Hz, 1H), 7.49 (dd, J_1 = 8.0 Hz, J_1 = 2.0 Hz, 1H), 7.90 (s, 1H), 7.96 (d, J = 7.8 Hz, 1H); ^{13}C NMR (100 MHz, $CDCl_3$, ppm) δ 5.29, 6.75, 9.92, 14.97, 20.05, 20.95, 22.52, 26.83, 37.23, 38.19, 42.76, 47.25, 58.66, 67.93, 72.36, 75.20, 75.76, 76.44, 76.70, 77.22, 77.34, 78.81, 80.81, 84.24, 115.60 (t, J = 263 Hz), 120.97, 125.10, 127.23, 130.16, 131.28, 132.65, 144.00, 151.02, 165.98, 169.35, 170.82, 202.11; ^{19}F NMR (376 MHz, $CDCl_3$) δ −81.06 (ABq, J = 169 Hz, 2F). HRMS (TOF) m/z: Calcd. For $C_{38}H_{52}F_2O_{12}Si^+$, 766.3212. Found, 767.322 (Δ = 1 ppm).

4.3.22. 2-Debenzoyl-7-TES-2-(3-difluromethoxybenzoyl)-10-propanoyl-10-deacetyl-baccatin III (**7b-06**)

In the same manner as that for **7a-05**, **7b-06** was synthesized from **5b-06** (323 mg, 0.484 mmol) and TES-Cl (0.25 mL, 1.45 mmol) in 85% yield (321 mg) as a white solid: m.p. 104–106 °C; ^{1}H NMR (400 MHz, $CDCl_3$, ppm) δ 0.56–0.62 (m, 6H), 0.91–0.95 (m, 9H), 1.04 (s, 3H), 1.20–1.24 (m, 6H), 1.59 (bs, OH), 1.68 (s, 3H), 1.85–1.91 (m, 1H), 2.21 (s, 3H), 2.26–2.28 (m, 5H), 2.40–2.55 (m, 1H), 3.90 (d, J = 7.0 Hz, 1H), 4.14 (AB, J_{AB} = 8.2 Hz, 1H), 4.30 (AB, J_{AB} = 8.2 Hz, 1H), 4.50 (dd, J_1 = 10.4 Hz, J_2 = 6.7 Hz, 1H), 4.84 (t, 1H), 4.98 (d, J = 8.1 Hz, 1H), 5.62 (d, J = 7.0 Hz, 1H), 6.49 (s, 1H), 6.58 (d, J = 73.2 Hz, 1H), 7.37 (dd, J_1 = 8.0 Hz, J_1 = 2.0 Hz, 1H), 7.50 (t, J = 7.8 Hz, 1H), 7.91 (s, 1H), 7.97 (d, J = 7.8 Hz, 1H); ^{13}C NMR (100 MHz, $CDCl_3$, ppm) δ 5.50, 6.97, 9.44, 10.13, 15.17, 20.28, 22.77, 27.03, 27.91, 37.43, 38.40, 42.95, 47.46, 58.84, 68.13, 72.56, 75.42, 75.77, 76.65, 77.43, 79.04, 81.02, 84.46, 113.20, 115.80, 118.41, 121.17, 125.29, 127.43, 130.36, 131.48, 132.90, 144.17, 151.22, 166.19, 171.02, 172.98, 202.41; ^{19}F NMR (376 MHz, $CDCl_3$) δ −81.06 (ABq, J = 167 Hz, 2F). HRMS (TOF) m/z: Calcd. For $C_{39}H_{54}F_2O_{12}SiH^+$, 781.3425. Found, 781.3425.

4.3.23. 2-Debenzoyl-2-(3-difluromethoxybenzoyl)-7-TES-10-deacetyl-10-cyclopropane-carbonylbaccatin III (**7c-06**)

In the same manner as that for **7c-05**, **7c-06** was synthesized from **6e-06** (338 mg, 0.466 mmol) and cyclopropanecarbonyl chloride (58 mg, 0.559 mmol) in 86% yield (318 mg) as a white solid: ^{1}H NMR (400 MHz, $CDCl_3$, ppm) δ 0.56–0.61 (m, 6H), 0.93 (t, J = 7.9 Hz, 9H), 1.06 (s, 3H), 1.20 (s, 3H), 1.69 (s, 2H), 1.73 (m, 1H), 1.80–1.91 (m, 1H), 2.20 (d, J = 1.2 Hz, 2H), 2.26–2.28 (m, 4H), 2.50–2.54 (m, 1H), 3.89 (d, J = 7.0 Hz, 1H), 4.14 (d, J = 8.0 Hz, 1H), 4.30 (d, J = 8.0 Hz, 1H), 4.48 (dd, J = 10.4, 6.7 Hz, 1H), 4.85 (t, J = 8.1 Hz, 1H), 4.97 (d, J = 7.8 Hz, 1H), 5.62 (d, J = 7.0 Hz, 1H), 6.47 (s, 1H), 6.58 (t, J = 73.1 Hz, 1H), 7.37 (dd, J_1 = 8.0 Hz, J_1 = 2.0 Hz, 1H), 7.48 (t, J = 8.0 Hz, 1H), 7.91 (s, 1H), 7.97 (d, J = 8.0 Hz, 1H); ^{19}F NMR (376 MHz, $CDCl_3$) δ −57.87 (s, 3F). ^{19}F NMR (376 MHz, $CDCl_3$, 25 °C) δ −81.05 (ABq, J = 167 Hz, 2F).

4.3.24. 2-Debenzoyl-2-(3-difluromethoxybenzoyl)-7-TES-10-deacetyl-10-N,N-demthyl-carbamoylbaccatin III (**7d-06**)

In the same manner as that for **7c-05**, **7d-06** was synthesized from **6d-06** (349 mg, 0.481 mmol) and *N,N*-demthylcarbamoyl chloride (62 mg, 0.577 mmol) in 84% yield (321 mg) as a white solid: H-NMR (400 MHz, $CDCl_3$, ppm) δ 0.56–0.62 (m, 6H), 0.90–0.94 (m, 9H), 1.04 (s, 3H), 1.18 (s, 3H), 1.67 (s, 3H), 1.82–1.92 (m, 1H), 2.24 (s, 3H), 2.26–2.28 (m, 5H), 2.48–2.57 (m, 1H), 2.93 (s, 3H), 3.07 (s, 3H), 3.90 (d, J = 7.0 Hz, 1H), 4.13 (AB, J_{AB} = 8.2 Hz, 1H), 4.28 (AB, J_{AB} = 8.2 Hz, 1H), 4.49 (dd, J_1 = 10.4 Hz, J_2 = 6.8 Hz, 1H), 4.81 (t, 1H), 4.97 (d, J = 8.2 Hz, 1H), 5.61 (d, J = 7.0 Hz, 1H), 6.39 (s, 1H), 6.57 (d, J = 73.2 Hz, 1H), 7.36 (dd, J_1 = 8.0 Hz, J_1 = 2.0 Hz, 1H), 7.48 (t, J = 8.0 Hz, 1H), 7.90 (s, 1H), 7.96 (d, J = 8.0 Hz, 1H); ^{13}C NMR (100 MHz, $CDCl_3$, ppm) δ 5.45, 5.98, 6.77, 6.92, 10.11, 15.05, 17.88, 20.38, 22.69, 22.80, 27.04, 36.40, 37.39, 38.42, 42.89, 47.44, 58.60, 68.09, 72.52, 75.48, 76.64, 77.43, 79.05, 80.98, 84.49, 113.19, 115.79, 118.39, 121.12, 125.22, 127.37, 130.32, 131.51, 133.15, 144.06, 151.18, 151.21, 155.51, 166.16, 170.95, 203.46. ^{19}F NMR (376 MHz, $CDCl_3$, 25 °C) δ −81.06 (ABq, J = 167 Hz, 2F).

4.3.25. 2-Debenzoyl-2-(3-difluromethoxybenzoyl)-10-deacetyl-10-methoxycarbonyl-7-TES-baccatin III (**7e-06**)

In the same manner as that for **7c-05**, **7e-06** was synthesized from **6e-06** (355 mg, 0.462 mmol) and methyl chloroformate (53 mg, 0.554 mmol) in 87% yield (321 mg) as a white solid: m.p. 115–117 °C; ^{1}H NMR (400 MHz, $CDCl_3$, ppm) δ 0.58–0.64 (m, 6H), 0.92–0.96 (m, 9H), 1.06 (s, 3H), 1.18 (s, 3H), 1.69 (s, 3H), 1.85–1.91 (m, 1H), 2.20 (s, 3H), 2.26–2.28 (m, 5H), 2.51–2.59 (m, 1H), 3.82 (s, 3H), 3.86 (d, J = 7.0 Hz, 1H), 4.13 (AB, J_{AB} = 8.2 Hz, 1H), 4.29 (AB, J_{AB} = 8.2 Hz, 1H), 4.50 (dd, J_1 = 10.4 Hz, J_2 = 6.8 Hz, 1H), 4.86 (t, 1H), 4.97 (d, J = 9.0 Hz, 1H), 5.61 (d, J = 7.0 Hz, 1H), 6.30 (s, 1H), 6.58 (d, J = 73.2 Hz, 1H), 7.37 (dd, J_1 = 8.0 Hz, J_1 = 2.0 Hz, 1H), 7.49 (t, J = 8.0 Hz, 1H), 7.90 (s, 1H), 8.05 (d, J = 8.0 Hz, 1H); ^{13}C NMR (100 MHz, $CDCl_3$, ppm) δ 5.55, 6.98, 10.10, 15.27, 20.15, 22.71, 26.93, 37.41, 38.38, 42.86, 47.40, 55.26, 58.74, 68.10, 72.57, 75.36, 76.64, 77.43, 79.00, 79.36, 80.98, 84.42, 113.20, 115.81, 118.41, 121.15, 125.30, 127.43, 130.36, 131.46, 132.50, 145.05, 151.19, 151.22, 155.05, 166.15, 171.04, 201.79; ^{19}F NMR (376 MHz, $CDCl_3$, 25 °C) δ −81.06 (ABq, J = 167 Hz, 2F). HRMS (TOF) m/z: Calcd. For $C_{38}H_{52}F_2NO_{13}SiNH_4^+$, 800.8483. Found, 800.8486.

4.3.26. 2-Debenzoyl-2-(3-methylbenzoyl)-7-TES-10-deacetyl-10-propanoyl-2′-TIPS-3′-(2-methylpropen-1-yl)-3′-dephenyldocetaxel (**9b-02**)

To a solution of **7b-02** (64 mg, 0.088 mmol) and **8** (42 mg, 0.105 mmol) in THF (2 mL) was added LiHMDS (1.0 M in THF, 105 μl, 0.105 mmol) dropwise at −40 °C. The mixture was stirred at −40 °C for 2 h. The progress of the reaction was monitored by TLC. Upon completion, the reaction was quenched with saturated NH_4Cl (10 mL), and the aqueous layer was extracted with ethyl acetate (3 × 30 mL). The combined extracts were washed with brine (3 × 30 mL), dried over $MgSO_4$ and concentrated in vacuo. The residue was purified by flash chromatography on silica gel to afford **9b-02** (83 mg, 84%) as a white solid: m.p. 140–142 °C; ^{1}H NMR (500 MHz, $CDCl_3$) δ 0.57 (m, 6H), 0.91 (t, J = 8.1 Hz, 9H), 1.11 (m, 21H), 1.16 (s, 3H), 1.17 (s, 1H), 1.21 (m, 6H), 1.25 (s, 1H), 1.33 (s, 9H), 1.59 (s, 1H), 1.67 (m, 4H), 1.74 (s, 3H), 1.78 (d, J = 0.9 Hz, 3H), 1.88 (m, 1H), 2.01 (d, J = 0.9 Hz, 3H), 2.36 (m, 5H), 2.42 (s, 3H), 2.52 (m, 3H), 3.84 (d, J = 7.1 Hz, 1H), 4.18 (d, J = 8.6 Hz, 1H), 4.31 (d, J = 8.5 Hz, 1H), 4.43 (d, J = 2.9 Hz, 1H), 4.47 (dd, J = 6.7 Hz, J = 10.6 Hz, 1H), 4.78 (m, 2H), 4.94 (d, J = 8.2 Hz, 1H), 5.33 (d, J = 8.7 Hz, 1H), 5.67 (d, J = 7.1 Hz, 1H), 6.08 (t, J = 9.3 Hz, 1H), 6.49 (s, 1H), 7.34 (t, J = 7.7 Hz, 1H), 7.41 (d, J = 7.7 Hz, 1H), 7.90 (d, J = 7.7 Hz, 1H), 7.93 (s, 1H); ^{13}C NMR (125 MHz, $CDCl_3$) δ 5.5, 7.0, 9.4, 10.3, 12.8, 14.6, 18.2, 18.3, 18.8, 21.5, 21.6, 22.8, 25.9, 26.5, 27.8, 28.5, 29.9, 35.7, 37.4, 43.5, 47.0, 52.2, 58.6, 72.1, 72.5, 75.1, 75.1, 75.6, 76.8, 79.1, 79.6, 84.5, 122.4, 127.6, 128.7, 129.5, 131.0, 133.6, 134.5, 136.4, 138.5, 141.1, 155.4, 167.2, 170.0, 172.1, 172.9, 202.2. HRMS (TOF) m/z: Calcd. For $C_{60}H_{95}NO_{15}Si_2Na^+$ 1148.6132, Found: 1148.6133 (Δ = −0.04 ppm).

4.3.27. 2-Debenzoyl-2-(3-methylbenzoyl)-7-TES-10-deacetyl-10-cyclopropane-carbonyl-2′-TIPS-3′-(2-methylpropen-1-yl)-3′-dephenyldocetaxel (**9c-02**)

In the same manner as that for **9b-02**, **9c-02** was synthesized from **7c-02** (178 mg, 0.240 mmol) and **8** (115 mg, 0.289 mmol) in 81% yield (222 mg) as a white solid: m.p. 153–154 °C; ^{1}H NMR (500 MHz, $CDCl_3$) δ 0.56 (m, 6H), 0.91 (m, 11*H*), 1.10 (m, 21H), 1.19 (m, 4H), 1.23 (s, 3H), 1.33 (s, 9H), 1.68 (m, 4H), 1.74 (m, 4H), 1.77 (d, J = 1.1 Hz, 3H), 1.88 (m, 1H), 2.00 (d, J = 1.1 Hz, 3H), 2.36 (m, 5H), 2.41 (s, 3H), 2.49 (m, 1H), 3.83 (d, J = 7.1 Hz, 1H), 4.17 (d, J = 8.4 Hz, 1H), 4.30 (d, J = 8.4 Hz, 1H), 4.45 (m, 2H), 4.76 (m, 1H), 4.81 (m, 1H), 4.94 (d, J = 7.8 Hz, 1H), 5.33 (d, J = 8.7 Hz, 1H), 5.67 (d, J = 7.2 Hz, 1H), 6.08 (t, J = 8.9 Hz, 1H), 6.48 (s, 1H), 7.34 (t, J = 7.7 Hz, 1H), 7.40 (d, J = 7.7 Hz, 1H), 7.90 (d, J = 7.7 Hz, 1H), 7.93 (s, 1H); ^{13}C NMR

(125 MHz, $CDCl_3$) δ 5.5, 7.0, 8.8, 9.0, 10.3, 12.7, 13.2, 14.5, 18.17, 18.24, 18.8, 21.5, 22.7, 25.9, 26.5, 28.5, 35.7, 37.4, 43.4, 47.0, 52.2, 58.5, 72.1, 72.4, 75.0, 75.1, 75.5, 76.8, 79.1, 79.6, 81.3, 84.5, 122.4, 127.6, 128.7, 129.5, 131.0, 133.6, 134.5, 136.3, 138.4, 141.1, 155.3, 167.2, 169.9, 172.1, 173.3, 202.3. HRMS (TOF) *m/z*: Calcd. For $C_{61}H_{95}NO_{15}Si_2Na^+$ 1160.6132, Found: 1160.6132 (Δ = 0.07 ppm).

*4.3.28. 2-Debenzoyl-2-(3-methylbenzoyl)-7-TES-10-deacetyl-10-N,N-dimethyl-carbamoyl-2′-TIPS-3′-(2-methylpropen-1-yl)-3′-dephenyldocetaxel (**9d-02**)*

In the same manner as that for **9b-02**, **9d-02** was synthesized from **7-02d** (67 mg, 0.090 mmol) and **8** (43 mg, 0.108 mmol) in 92% yield (94 mg) as a white solid: m.p. 167–169 °C; ^{1}H NMR (700 MHz, $CDCl_3$) δ 0.58 (m, 6H), 0.90 (t, J = 8.0 Hz, 9H), 1.11 (m, 21H), 1.18 (s, 3H), 1.21 (s, 3H), 1.32 (s, 9H), 1.67 (s, 3H), 1.73 (m, 4H), 1.76 (s, 3H), 1.87 (m, 1H), 2.04 (s, 3H), 2.31 (m, 1H), 2.38 (m, 7H), 2.50 (m, 1H), 2.92 (s, 3H), 3.04 (s, 3H), 3.84 (d, J = 7.0 Hz, 1H), 4.17 (d, J = 8.5 Hz, 1H), 4.29 (d, J = 8.5 Hz, 1H), 4.42 (d, J = 2.9 Hz, 1H), 4.46 (dd, J = 6.7 Hz, J = 10.5 Hz, 1H), 4.75 (br s, 1H), 4.81 (br s, 1H), 4.93 (d, J = 7.9 Hz, 1H), 5.32 (d, J = 8.8 Hz, 1H), 5.66 (d, J = 7.2 Hz, 1H), 6.08 (t, J = 8.6 Hz, 1H), 6.39 (s, 1H), 7.32 (t, J = 7.7 Hz, 1H), 7.38 (d, J = 7.7 Hz, 1H), 7.88 (d, J = 7.7 Hz, 1H), 7.92 (s, 1H); ^{13}C NMR (175 MHz, $CDCl_3$) δ 5.5, 6.9, 10.2, 12.7, 14.5, 18.1, 18.2, 18.8, 21.5, 21.6, 22.7, 25.9, 26.5, 28.4, 35.7, 36.3, 36.8, 37.3, 43.4, 46.9, 58.3, 72.0, 72.4, 75.1, 75.4, 76.5, 76.7, 79.0, 79.5, 81.2, 84.5, 122.3, 127.5, 128.6, 129.5, 130.9, 133.9, 134.5, 136.3, 138.4, 140.8, 155.3, 167.2, 169.9, 172.0, 203.2. HRMS (TOF) *m/z*: Calcd. For $C_{60}H_{96}N_2O_{15}Si_2H^+$ calcd: 1141.6422, Found: 1141.6422 (Δ = −0.26 ppm).

*4.3.29. 2-Debenzoyl-2-(3-methylbenzoyl)-7-TES-10-deacetyl-10-methoxycarbonyl-2′-TIPS-3′-(2-methylpropen-1-yl)-3′-dephenyldocetaxel (**9e-02**)*

In the same manner as that for **9b-02**, **9e-02** was synthesized from **7e-02** (67 mg, 0.092 mmol) and **8** (44 mg, 0.110 mmol) in 84% yield (87 mg) as a white solid: m.p. 151–152 °C; ^{1}H NMR (500 MHz, $CDCl_3$) δ 0.58 (m, 6H), 0.92 (t, J = 8.1 Hz, 9H), 1.11 (m, 21H), 1.19 (s, 3H), 1.20 (s, 3H), 1.33 (s, 9H), 1.68 (s, 3H), 1.76 (m, 7H), 1.89 (m, 1H), 2.02 (s, 3H), 2.36 (m, 5H), 2.40 (s, 3H), 2.50 (m, 1H), 3.80 (m, 4H), 4.17 (d, 8.4 Hz, 1H), 4.30 (d, J = 8.4 Hz, 1H), 4.45 (m, 2H), 4.76 (m, 1H), 4.81 (m, 1H), 4.93 (d, J = 8.3 Hz, 1H), 5.33 (d, J = 8.8 Hz, 1H), 5.66 (d, J = 7.2 Hz, 1H), 6.08 (t, J = 8.6 Hz, 1H), 6.27 (s, 1H), 7.33 (t, J = 7.7 Hz, 1H), 7.40 (d, J = 7.7 Hz, 1H), 7.89 (d, J = 7.7 Hz, 1H), 7.92 (s, 1H). ^{13}C NMR (125 MHz, $CDCl_3$) δ 5.6, 7.0, 10.2, 12.5, 12.7, 14.6, 18.0, 18.1, 18.17, 18.24, 18.8, 21.3, 21.5, 22.7, 23.5, 24.9, 25.9, 26.4, 28.5, 29.9, 35.6, 36.8, 37.4, 43.4, 46.9, 52.2, 55.3, 58.5, 72.1, 72.5, 75.0, 75.5, 76.8, 78.8, 79.0, 79.7, 81.3, 84.4, 122.4, 127.5, 128.7, 129.5, 131.0, 133.2, 134.5, 136.4, 138.4, 141.9, 155.1, 155.4, 167.2, 170.0, 172.1, 201.5; HRMS (TOF) *m/z*: Calcd. For $C_{59}H_{93}NO_{16}Si_2H^+$ calcd: 1128.6106. Found: 1128.6093 (Δ = 1.15 ppm).

*4.3.30. 2-Debenzoyl-2-(3-trifluoromethoxybenzoyl)-7-TES-10-propanoyl-2′-TIPS-3′-(2-methyl-propen-1-yl)-3′-dephenyldocetaxel (**9b-05**)*

In the same manner as that for **9b-02**, **9b-05** was synthesized from **7b-05** (307 mg, 0.393 mmol) and **8** (188 mg, 0.472 mmol) in 77% yield (355 mg) as a white solid: ^{1}H NMR (400 MHz, $CDCl_3$, ppm) δ 0.54–0.60 (m, 1H), 0.90 (t, J = 8.0 Hz, 1H), 1.11 (s, 21H), 1.16 (s, 3H), 1.17–1.26 (m, 6H), 1.31 (s, 9H), 1.68 (s, 3H), 1.73–1.76 (m, 7H), 1.75 (s, 3H), 1.85–1.92 (m, 1H), 2.02 (s, 3H), 2.23–2.41 (m, 5H), 2.41–2.53 (m, 1H), 3.82 (d, J = 7.0 Hz, 1H), 4.16 (AB, J_{AB} = 8.3 Hz, 1H), 4.30 (AB, J_{AB} = 8.3 Hz, 1H), 4.43 (d, J = 2.68 Hz, 1H), 4.45–4.50 (m, 1H), 4.76–4.85 (m, 2H), 4.95 (d, J = 8.2 Hz, 1H), 5.32 (d, J = 8.7 Hz, 1H), 5.67 (d, J = 7.0 Hz, 1H), 6.08 (t, J = 8.9 Hz, 1H), 6.49 (s, 1H), 7.35 (dd, J_1 = 8.0 Hz, J_1 = 2.0 Hz, 1H), 7.47 (t, J = 8.0 Hz, 1H), 7.88 (s, 1H), 7.95 (d, J = 7.8 Hz, 2H); ^{13}C NMR (100 MHz, $CDCl_3$, ppm) δ 5.50, 6.93, 9.37, 10.22, 12.74, 14.52, 18.14, 18.22, 18.64, 21.48, 22.64, 22.83, 25.85, 27.80, 28.41, 35.52, 37.32, 43.42, 46.87, 52.15, 58.51, 71.96, 72.39, 75.00, 75.49, 75.68, 76.60, 115.93, 120.41, 122.23, 124.87, 127.41, 130.35, 131.48, 133.44, 136.39, 141.19, 151.42, 155.37, 165.95, 170.06, 172.10, 172.81, 202.12.

*4.3.31. 2-Debenzoyl-2-(3-trifluoromethoxybenzoyl)-7-TES-10-cyclopropanecarbonyl-2′-TIPS-3′-(2-methylpropen-1-yl)-3′-dephenyldocetaxel (**9c-05**)*

In the same manner as that for **9b-02**, **9c-05** was synthesized from **7c-05** (121 mg, 0.15 mmol) and **8** (72 mg, 0.18 mmol) in 88% yield (159 mg) as a white solid: ^{1}H NMR (400 MHz, $CDCl_3$) δ 0.55 (m, 6H), 0.90 (m, 9H), 1.10 (s, 21H), 1.33 (s, 3H), 1.61–1.79 (m, 9H), 2.01 (d, J = 8.4 Hz, 3H), 2.33 (s, 5H), 2.50 (m, 1H), 3.84 (d, J = 6.4 Hz, 1 H), 4.06–4.17(m, 2 H), 4.26 (d, J = 8.0 Hz, 1 H), 4.44 (m, 2 H), 4.74 (s, 1H), , 4.83 (m, 1 H), 4.94 (d, J = 8.8 Hz, 1 H), 5.32 (d, J = 8.4 Hz, 1 H), 5.66 (d, J = 6.8 Hz, 1H), 6.04 (t, J = 8.8 Hz, 1 H), 6.48 (s, 1H), 7.44 (d, J = 7.6 Hz, 1 H), 7.51 (t, J = 7.6 Hz, 1H), 7.97 (s, 1H), 8.04 (d, J = 7.6 Hz, 1H); ^{13}C NMR (100 MHz, $CDCl_3$) δ 201.98, 173.01, 171.93, 171.12, 169.71, 165.32, 155.16, 149.15, 141.08, 136.32, 133.16, 131.44, 130.19, 128.66, 125.95, 122.14, 121.94, 121.67, 119.10, 84.26, 80.98, 79.36, 78.79, 77.32, 77.20, 77.00, 76.68, 76.34, 75.51, 75.26, 74.74, 72.18, 71.89, 60.35, 58.27, 52.00, 46.67, 43.18, 37.09, 35.30, 28.19, 26.21, 25.58, 22.30, 21.21, 20.97, 18.33, 17.98, 17.91, 14.31, 14.14, 12.90, 12.51, 9.95, 8.71, 8.61, 6.70, 5.26; ^{19}F NMR (376 MHz, CDCl3) δ −57.83 (s, 3 F).

*4.3.32. 2-Debenzoyl-2-(3-trifluoromethoxybenzoyl)-7-TES-10-N,N-dimethylcarbamoyl-2′-TIPS-3′-(2-methylpropen-1-yl)-3′-dephenyldocetaxel (**9d-05**)*

In the same manner as that for **9b-02**, **9d-05** was synthesized from **7d-05** (110 mg, 0.135 mmol) and **8** (65 mg, 0.162 mmol) in 91% yield (149 mg) as a white solid: ^{1}H NMR (500 MHz, $CDCl_3$) δ 0.57–0.62 (m, 6H), 0.90–0.93 (m, 9H), 1.10–1.14 (m, 21H), 1.19 (s, 3H), 1.23 (s, 3H), 1.33 (s, 9H), 1.65–1.68 (m, 4H), 1.74 (s, 3H), 1.76 (s, 3H), 1.86–1.91 (m, 1H), 2.06 (s, 3H), 2.34–2.39 (m, 1H), 2.49–2.55 (m, 1H), 2.94 (s, 3H), 3.06 (s, 3H), 3.87 (d, J = 7.0 Hz, 1H), 4.16 (AB, J_{AB} = 8.2 Hz, 1H), 4.28 (AB, J_{AB} = 8.2 Hz, 1H), 4.42 (d, J = 2.7 Hz, 1H), 4.47 (dd, J_1 = 10.5 Hz, J_2 = 6.7 Hz, 1H), 4.75–4.84 (m, 2H), 4.96 (d, J = 8.6 Hz, 1H), 5.33 (d, J = 8.6 Hz, 1H), 5.68 (d, J = 7.0 Hz, 1H), 6.07 (t, J = 8.8 Hz, 1H), 6.42 (s, 1H), 7.45 (d, J = 8.0 Hz, 1H), 7.52 (t, J = 8.0 Hz, 1H), 7.99 (s, 1H), 8.05 (d, J = 8.0 Hz, 1H);^{13}C NMR (125 MHz, $CDCl_3$) δ 5.25, 5.49, 5.72, 6.93, 10.21, 12.51, 12.75, 12.99, 14.31, 14.53, 18.16, 18.24, 18.58, 20.89, 21.60, 22.56, 22.85, 25.47, 25.83, 26.46, 28.44, 31.79, 34.86, 35.60, 36.37, 36.79, 37.33, 43.40, 46.91, 52.19, 58.33, 72.05, 72.40, 75.45, 75.82, 75.82, 76.50, 76.60, 79.10, 79.53, 81.23, 84.54, 117.54, 119.60, 121.65, 122.22, 122.40, 123.70, 126.19, 128.89, 130.43, 131,70, 133.73, 136.50, 141.11, 149.40, 149.41, 155.35, 165.61, 169.91, 172.05, 203.19.

*4.3.33. 2-Debenzoyl-2-(3-trifluoromethoxybenzoyl)-7-TES-10-methoxycarbonyl-2′-TIPS-3′-(2-methylpropen-1-yl)-3′-dephenyldocetaxel (**9e-05**)*

In the same manner as that for **9b-02**, **9e-05** was synthesized from **7e-05** (351 mg, 0.438 mmol) and **8** (225 mg, 0.567 mmol) in 91% yield (474 mg) as a white solid: m.p. 103–105 °C; ^{1}H NMR (400 MHz, $CDCl_3$, ppm) δ 0.57–0.63 (m, 6H), 0.94 (m, 9H), 1.11–1.12 (m, 21H), 1.20 (s, 3H), 1.21 (s, 3H), 1.34 (s, 9H), 1.69 (s, 3H), 1.72 (s, 2H), 1.75 (s, 3H), 1.76 (s, 3H), 1.87–1.93 (m, 1H), 2.03 (s, 3H), 2.31–2.38 (m, 5H), 2.50–2.58 (m, 1H), 3.83 (m, 4H), 4.16 (AB, J_{AB} = 8.2 Hz, 1H), 4.28 (AB, J_{AB} = 8.2 Hz, 1H), 4.42–4.49 (m, 2H), 4.76–4.84 (m, 2H), 4.95 (d, J = 8.6 Hz, 1H), 5.33 (d, J = 8.6 Hz, 1H), 5.67 (d, J = 7.0 Hz, 1H), 6.07 (t, J = 8.8 Hz, 1H), 6.30 (s, 1H), 7.46 (d, J = 8.0 Hz, 1H), 7.53 (t, J = 8.0 Hz, 1H), 7.98 (s, 1H), 8.06 (d, J = 8.0 Hz, 1H);^{13}C NMR (100 MHz, $CDCl_3$, ppm) δ 5.57, 6.96, 10.18, 12.76, 14.65, 18.16, 18.23, 18.59, 21.27, 22.56, 25.83, 26.37, 28.45, 35.45, 37.33, 43.37, 46.87, 52.24, 55.29, 58.47, 72.16, 72.45, 75.52, 75.67, 76.59, 77.43, 78.78, 79.02, 79.64, 81.22, 84.46, 119.35, 121.92, 122.19, 122.38, 126.22,

130.45, 131.67, 133.03, 136.57, 142.12, 149.40, 155.04, 155.39, 165.55, 170.02, 172.20, 201.46; ^{19}F NMR (376 MHz, $CDCl_3$) δ −57.81 (3F). HRMS (TOF) *m/z*: Calcd. For $C_{59}H_{90}F_3NO_{17}Si_2Na^+$, 1220.5592. Found, 1220.5587.

*4.3.34. 2-Debenzoyl-2-(3-difluoromethoxybenzoyl)-7-TES-10-acetyl-2′-TIPS-3′-(2-methyl-propen-1-yl)-3′-dephenyldocetaxel (**9a-06**)*

In the same manner as that for **9b-05**, **9a-06** was synthesized from **7a-06** (150 mg, 0.186 mmol) and **8** (92 mg, 0.222 mmol) in 92% yield (199 mg) as a white solid: m.p. 123–125 °C; ^{1}H NMR (400 MHz, $CDCl_3$) δ 0.60–0.54 (m, 6H), 0.92 (m, 9H), 1.14–1.07 (m, 21H), 1.20 (d, J = 12.9 Hz, 6H), 1.31 (s, 9H), 1.67 (s, 6H), 1.75 (d, J = 8.2 Hz, 6H), 1.94–1.84 (m, 1H), 2.00 (s, 3H), 2.17 (s, 3H), 2.36 (s, 3H), 2.55–2.48 (m, 1H), 3.84 (d, J = 7.0 Hz, 1H), 4.16 (d, J = 8.2 Hz, 1H), 4.30 (d, J = 8.2 Hz, 1H), 4.43 (d, J = 2.7 Hz, 1H), 4.47 (dd, J = 10.6, 6.6 Hz, 1H), 4.86–4.76 (m, 2H), 4.95 (d, J = 7.9 Hz, 1H), 5.32 (d, J = 8.6 Hz, 1H), 5.67 (d, J = 7.0 Hz, 1H), 6.08 (t, J = 8.8 Hz, 1H), 6.47 (s, 1H), 6.75 (t, J = 73.4 Hz, 1H), 7.35 (d, J = 7.8 Hz, 1H), 7.48 (t, J = 7.8 Hz, 1H), 7.88 (s, 1H), 7.96 (d, J = 7.8 Hz, 1H). ^{13}C NMR (126 MHz, $CDCl_3$) δ5.31. 6.74, 10.04, 12.55, 14.34, 17.97, 18.03, 18.47, 20.87, 21.29, 22.46, 25.67, 26.30, 28.23, 29.71, 34.67, 35.32, 37.14, 43.25, 46.68, 51.94, 58.35, 71.73, 72.21, 75.03, 75.31, 75.47, 76.42, 76.77, 77.28, 78.89, 79.42, 81.00, 84.27, 115.74 (t, J = 263 Hz), 120.23, 122.04, 124.73, 127.25, 130.18, 131.27, 133.16, 136.24, 141.09, 151.23, 155.20, 165.79, 169.25, 169.91, 171.90, 201.89.^{19}F NMR (376 MHz, $CDCl_3$) δ −81.57 (dd, J = 526 Hz, 169 Hz, 2F). HRMS (TOF) *m/z*: Calcd. For $C_{59}H_{91}F_2NO_{16}Si_2^+$, 1164.5917. Found: 1164.5908.

*4.3.35. 2-Debenzoyl-2-(3-difluoromethoxybenzoyl)-7-TES-10-propanoyl-2′-TIPS-3′-(2-methyl-propen-1-yl)-3′-dephenyldocetaxel (**9b-06**)*

In the same manner as that for **9b-05**, **9b-06** was synthesized from **7b-06** (307 mg, 0.393 mmol) and **8** (188 mg, 0.472 mmol) in 77% yield (355 mg) as a white solid: ^{1}H NMR (400 MHz, CDCl3, ppm) δ 0.54–0.60 (m, 1H), 0.90 (t, J = 8.0 Hz, 1H), 1.11 (s, 21H), 1.16 (s, 3H), 1.17–1.26 (m, 6H), 1.31 (s, 9H), 1.68 (s, 3H), 1.73–1.76 (m, 7H), 1.75 (s, 3H), 1.85–1.92 (m, 1H), 2.02 (s, 3H), 2.23–2.41 (m, 5H), 2.41–2.53 (m, 1H), 3.82 (d, J = 7.0 Hz, 1H), 4.16 (AB, J_{AB} = 8.3 Hz, 1H), 4.30 (AB, J_{AB} = 8.3 Hz, 1H), 4.43 (d, J = 2.7 Hz, 1H), 4.45–4.50 (m, 1H), 4.76–4.85 (m, 2H), 4.95 (d, J = 8.2 Hz, 1H), 5.32 (d, J = 8.7 Hz, 1H), 5.67 (d, J = 7.0 Hz, 1H), 6.08 (t, J = 8.9 Hz, 1H), 6.49 (s, 1H), 6.66 (t, J = 73.4 Hz, 1H), 7.35 (dd, J_1 = 8.0 Hz, J_1 = 2.0 Hz, 1H), 7.47 (t, J = 8.0 Hz, 1H), 7.88 (s, 1H), 7.95 (d, J = 8.0 Hz, 2H); ^{13}C NMR (100 MHz, CDCl3, ppm) δ 5.50, 6.93, 9.37, 10.22, 12.74, 14.52, 18.14, 18.22, 18.64, 21.48, 22.64, 22.83, 25.85, 27.80, 28.41, 35.52, 37.32, 43.42, 46.87, 52.15, 58.51, 71.96, 72.39, 75.00, 75.49, 75.68, 76.60, 115.93, 120.41, 122.23, 124.87, 127.41, 130.35, 131.48, 133.44, 136.39, 141.19, 151.42, 155.37, 165.95, 170.06, 172.10, 172.81, 202.12.

*4.3.36. 2-Debenzoyl-2-(3-difluoromethoxybenzoyl)-7-TES-10-cyclopropanecarbonyl-2′-TIPS-3′-(2-methylpropen-1-yl)-3′-dephenyldocetaxel (**9c-06**)*

In the same manner as that for **9b-02**, **9c-06** was synthesized from **7c-06** (312 mg, 0.393 mmol) and **8** (188 mg, 0.472 mmol) in 90% yield (422 mg) as a white solid: m.p. 127–129 °C; ^{1}H NMR (400 MHz, $CDCl_3$, ppm) δ 0.52–0.62 (m, 6H), 0.90–0.94 (m, 9H), 1.11–1.14 (m, 21H), 1.21 (s, 3H), 1.24 (s, 3H), 1.33 (s, 9H), 1.59 (s, 3H), 1.69 (s, 3H), 1.75–1.77 (m, 7H), 1.86–1.93 (m, 1H), 2.02 (s, 3H), 2.32–2.37 (m, 5H), 2.48–2.54 (m, 1H), 3.86 (d, J = 7.0 Hz, 1H), 4.17 (AB, J_{AB} = 8.1 Hz, 1H), 4.32 (AB, J_{AB} = 8.1 Hz, 1H), 4.44–4.50 (m, 2H), 4.77–4.83 (m, 2H), 4.96 (d, J = 8.0 Hz, 1H), 5.33 (d, J = 8.6 Hz, 1H), 5.68 (d, J = 7.0 Hz, 1H), 6.10 (t, J = 8.8 Hz, 1H), 6.50 (s, 1H), 6.67 (d, J = 73.4 Hz, 1H), 7.37 (dd, J_1 = 8.0 Hz, J_1 = 2.0 Hz, 1H), 7.49 (t, J = 8.0, 1H), 7.89 (s, 1H), 7.97 (d, J = 7.8 Hz, 1H);^{13}C NMR (100 MHz, $CDCl_3$, ppm) δ 5.53, 6.98, 8.88, 8.99, 10.25, 12.78, 13.17, 14.52, 18.18, 18.26, 18.69, 21.56, 22.68, 25.89, 26.53, 28.45, 35.56, 37.36, 43.45, 46.91, 52.18, 58.53, 71.98, 72.41, 74.97, 75.51, 75.70, 76.60, 77.43, 79.16, 79.60, 81.23, 84.52, 113.36, 115.95, 118.54, 120.47, 122.27, 124.94, 127.47, 130.40, 131.49, 133.44, 136.42, 141.29, 151.45, 155.39, 166.02, 170.09, 172.13, 173.28, 202.25; ^{19}F NMR (376 MHz, $CDCl_3$) δ −81.08 (ABq, J = 167 Hz, 2F). HRMS (TOF) *m/z*: Calcd. For $C_{61}H_{93}F_2NO_{16}Si_2H^+$, 1190.6074. Found, 1190.6075.

*4.3.37. 2-Debenzoyl-2-(3-difluoromethoxybenzoyl)-7-TES-10-N,N-dimethyl-carbamoyl-2′-TIPS-3′-(2-methylpropen-1-yl)-3′-dephenyldocetaxel (**9d-06**)*

In the same manner as that for **9b-02**, **9d-06** was synthesized from **7d-06** (268 mg, 0.337 mmol) and **8** (161 mg, 0.404 mmol) in 85% yield (341 mg) as a white solid: ^{1}H NMR (700 MHz, $CDCl_3$, ppm) δ 0.56–0.62 (m, 6H), 0.90–0.93 (m, 9H), 1.06–1.14 (m, 21H), 1.19 (s, 3H), 1.21 (s, 3H), 1.31 (s, 9H), 1.68 (s, 4H), 1.74 (s, 3H), 1.76 (s, 3H), 1.84–1.90 (m, 1H), 2.06 (s, 3H), 2.31–2.38 (m, 5H), 2.50–2.55 (m, 1H), 2.94 (s, 3H), 3.06 (s, 3H), 3.86 (d, J = 7.0 Hz, 1H), 4.16 (AB, J_{AB} = 8.4 Hz, 1H), 4.30 (AB, J_{AB} = 8.4 Hz, 1H), 4.43 (d, J = 2.8 Hz, 1H), 4.47 (dd, J_1 = 10.5 Hz, J_2 = 6.7 Hz, 1H), 4.77–4.84 (m, 2H), 4.95 (d, J = 8.7 Hz, 1H), 5.32 (d, J = 8.7 Hz, 1H), 5.68 (d, J = 7.0 Hz, 1H), 6.10 (t, J = 8.8 Hz, 1H), 6.41 (s, 1H), 7.35 (dd, J_1 = 8.0 Hz, J_1 = 2.0 Hz, 1H), 7.48 (t, J = 8.0 Hz, 1H), 7.88 (s, 1H), 8.05 (d, J = 8.0 Hz, 1H);^{13}C NMR (175 MHz, $CDCl_3$, ppm) δ 5.29, 5.46, 5.62, 6.92, 10.23, 12.56, 12.73, 12.90, 14.47, 18.15, 18.22, 18.64, 21.66, 22.65, 25.87, 26.49, 28.41, 35.57, 36.36, 36.78, 37.30, 43.39, 46.86, 52.07, 58.27, 71.89, 72.35, 75.42, 75.73, 76.45, 76.60, 79.12, 79.53, 81.18, 84.51, 114.44, 115.92, 117.40, 120.33, 122.22, 124.86, 127.40, 130.35, 131,47, 133.75, 136.34, 141.00, 151.42, 155.38, 165.98, 170.02, 171.99, 203.19; ^{19}F NMR (376 MHz, $CDCl_3$) δ −81.12 (ABq, J = 167 Hz, 2F). HRMS (TOF) *m/z*: Calcd. For $C_{60}H_{94}F_2N_2O_{16}Si_2Na^+$, 1215.6002. Found, 1215.5994.

*4.3.38. 2-Debenzoyl-2-(3-difluoromethoxybenzoyl)-7-TES-10-methoxycarbonyl-2′-TIPS-3′-(2-methylpropen-1-yl)-3′-dephenyldocetaxel (**9e-06**)*

In the same manner as that for **9b-02**, **9e-06** was synthesized from **7e-06** (148 mg, 0.190 mmol) and **8** (84 mg, 0.228 mmol) in 69% yield (155 mg) as a white solid: m.p. 115–117 °C; ^{1}H NMR (400 MHz, $CDCl_3$, ppm) δ 0.59–0.63 (m, 6H), 0.92–0.96 (m, 9H), 1.11–1.14 (m, 21H), 1.21 (s, 6H), 1.32 (s, 9H), 1.63 (s, 3H), 1.67 (s, 1H), 1.70 (s, 3H), 1.75 (s, 3H), 1.77 (s, 3H), 1.87–1.94 (m, 1H), 2.03 (s, 3H), 2.34–2.37 (m, 5H), 2.50–2.58 (m, 1H), 2.94 (s, 3H), 3.81–3.83 (m, 4H), 4.17 (AB, J_{AB} = 8.4 Hz, 1H), 4.32 (AB, J_{AB} = 8.4 Hz, 1H), 4.44–4.50 (m, 2H), 4.77–4.97 (m, 2H), 5.33 (d, J = 8.7 Hz, 1H), 5.68 (d, J = 7.0 Hz, 1H), 6.11 (t, J = 8.8 Hz, 1H), 6.29 (s, 1H), 6.66 (t, J = 73.4 Hz, 1H), 7.37 (dd, J = 8.0 Hz, J = 2.0 Hz, 1H), 7.48 (t, J = 8.0 Hz, 1H), 7.89 (s, 1H), 7.97 (d, J = 8.0 Hz, 1H);^{13}C NMR (100 MHz, $CDCl_3$, ppm) δ 5.58, 6.97, 10.22, 12.78, 14.62, 18.18, 18.25, 18.68, 21.36, 22.67, 25.89, 26.43, 28.45, 35.46, 37.35, 43.39, 46.86, 52.19, 55.30, 58.46, 72.02, 72.43, 75.52, 75.62, 76.63, 77.44, 78.76, 79.09, 79.67, 81.21, 84.47, 113.37, 115.96, 118.55, 120.46, 122.24, 124.94, 127.48, 130.39, 131,48, 133.08, 136.44, 142.07, 151.44, 155.06, 155.41, 165.96, 170.15, 172.15, 201.48; ^{19}F NMR (376 MHz, $CDCl_3$) δ −81.07 (ABq, J = 167 Hz, 2F). HRMS (TOF) *m/z*: Calcd. For $C_{59}H_{91}F_2NO_{17}Si_2Na^+$, 1202.5686. Found, 1202.5673.

*4.3.39. 2-Debenzoyl-2-(3-methylbenzoyl)-10-propanoyl-3′-(2-methylpropen-1-yl)-3′-dephenyl-docetaxel (**1b-02**)*

To a solution of **9b-02** (74 mg, 0.066 mmol) in 5 mL pyridine/acetonitrile (1/1) was added dropwise HF/pyridine (70%, 0.74 mL) at 0 °C. The mixture was stirred at room temperature for 21 h. The progress of the reaction was monitored by TLC. Upon completion, the reaction was quenched with saturated aqueous $NaHCO_3$. The reaction mixture was diluted with EtOAc, washed with aqueous saturated $CuSO_4$ and water, dried over $MgSO_4$, and concentrated in vacuo. The residue was purified by flash chromatography on silica gel to afford **1b-02** (44 mg, 77%) as a white solid: m.p. 169–172°C; ^{1}H NMR (700 MHz, $CDCl_3$) δ

1.14 (s, 3H), 1.23 (m, 6H), 1.34 (s, 9H), 1.67 (s, 3H), 1.74 (s, 3H), 1.76 (s, 3H), 1.87 (m, 4H), 2.37 (m, 5H), 2.42 (s, 3H), 2.53 (m, 4H), 3.39 (br s, 1H), 3.81 (d, J = 7.1 Hz, 1H), 4.17 (d, 8.5 Hz, 1H), 4.20 (dd, J = 2.5 Hz, J = 6.7 Hz, 1H), 4.30 (d, J = 8.5 Hz, 1H), 4.42 (m, 1H), 4.74 (t, J = 6.9 Hz, 1H), 4.81 (d, J = 8.7 Hz, 1H), 4.96 (d, J = 8.1 Hz, 1H), 5.32 (d, J = 7.6 Hz, 1H), 5.64 (d, J = 7.1 Hz, 1H), 6.16 (t, J = 9.0 Hz, 1H), 6.31 (s, 1H), 7.34 (t, J = 7.6 Hz, 1H), 7.41 (d, J = 7.6 Hz, 1H), 7.89 (d, J = 7.6 Hz, 1H), 7.92 (s, 1H); ^{13}C NMR (700 MHz) δ 9.3, 9.7, 15.1, 18.8, 21.5, 22.0, 22.5, 25.9, 26.8, 27.8, 28.4, 35.7, 35.8, 43.4, 45.9, 51.7, 58.7, 72.4, 72.6, 73.9, 75.1, 75.6, 76.7, 79.3, 80.1, 81.3, 84.6, 120.8, 127.5, 128.7, 129.3, 131.0, 133.1, 134.6, 138.0, 138.5, 142.7, 155.6, 167.2, 170.2, 173.4, 174.8, 204.0. HRMS (TOF) *m/z*: Calcd. For $C_{45}H_{61}NO_{15}H^+$ calcd: 856.4129. Found: 856.4129 (Δ = 0.01 ppm).

*4.3.40. 2-Debenzoyl-2-(3-methylbenzoyl)-10-cyclopropanecarbonyl-3′-(2-methylpropen-1-yl)-3′-dephenyldocetaxel (**1c-02**)*

In the same manner as that for **1b-02**, **1c-02** was synthesized from **9c-02** (195 mg, 0.171 mmol) and HF/pyridine (70%, 2.2 mL) in 77% yield (115 mg) as a white solid: m.p. 178–179 °C; ^{1}H NMR (500 MHz, $CDCl_3$) δ 0.99 (m, 2H), 1.14 (m, 5H), 1.25 (s, 3H), 1.34 (s, 9H), 1.66 (s, 3H), 1.71 (s, 1H), 1.77 (m, 7H), 1.86 (m, 4H), 2.37 (m, 5H), 2.41 (s, 3H), 2.52 (m, 1H), 2.57 (d, J = 4.0 Hz, 1H), 3.38 (d, J = 5.3 Hz, 1H), 3.80 (d, J = 7.1 Hz, 1H), 4.17 (d, J = 8.5 Hz, 1H), 4.20 (dd, J = 6.9 Hz, J = 6.9 Hz, 1H), 4.30 (d, J = 8.5 Hz, 1H), 4.40 (m, 1H), 4.74 (m, 1H), 4.80 (d, J = 6.4 Hz, 1H), 4.96 (d, J = 4.3 Hz, 1H), 5.32 (d, J = 8.4 Hz, 1H), 5.64 (d, J = 7.1 Hz, 1H), 6.17 (t, J = 9.0 Hz, 1H), 6.30 (s, 1H), 7.35 (t, J = 7.7 Hz, 1H), 7.41 (d, J = 7.7 Hz, 1H), 7.89 (d, J = 7.7 Hz, 1H), 7.93 (s, 1H); ^{13}C NMR (125 MHz) δ 9.4, 9.6, 9.7, 13.2, 15.2, 18.8, 21.6, 22.2, 22.5, 25.9, 26.9, 28.4, 35.7, 35.8, 43.4, 45.9, 51.7, 58.7, 72.4, 72.6, 73.9, 75.1, 75.6, 76.7, 79.4, 80.1, 81.3, 84.6, 120.9, 127.5, 128.7, 129.3, 131.0, 133.1, 134.6, 138.0, 138.5, 142.8, 155.6, 167.3, 170.2, 173.3, 175.3, 204.1. HRMS (TOF) *m/z*: Calcd. For $C_{46}H_{61}NO_{15}H$ + calcd: 868.4114. Found: 868.4122 (Δ = −0.94 ppm).

*4.3.41. 2-Debenzoyl-2-(3-methylbenzoyl)-10-N,N-dimethylcarbamoyl-3′-(2-methylpropen-1-yl)-3′-dephenyldocetaxel (**1d-02**)*

In the same manner as that for **1b-02**, **1d-02** was synthesized from **9d-02** (93 mg, 0.082 mmol) and HF/pyridine (70%, 1.0 mL) in 89% yield (63 mg) as a white solid: m.p. 158–160°C; ^{1}H NMR (700 MHz, $CDCl_3$) δ 1.15 (s, 3H), 1.24 (s, 3H), 1.34 (s, 9H), 1.66 (s, 3H), 1.74 (s, 3H),1.75 (s, 3H) 1.85 (m, 3H), 1.91 (s, 3H), 2.36 (m, 5H), 2.41 (s, 3H), 2.52 (m, 1H), 2.95 (s, 3H), 3.04 (s, 3H), 3.24 (br s, 1H), 3.46 (br s, 1H), 3.80 (d, J = 7.0 Hz, 1H), 4.17 (d, 8.5 Hz, 1H), 4.20 (d, J = 3.9 Hz, 1H), 4.30 (d, J = 8.5 Hz, 1H), 4.44 (dd, J = 6.8 Hz, J = 10.9 Hz, 1H), 4.74 (t, J = 7.6 Hz, 1H), 4.83 (d, J = 8.6 Hz, 1H), 4.97 (d, J = 8.4 Hz, 1H), 5.32 (d, J = 7.8 Hz, 1H), 5.63 (d, J = 7.1 Hz, 1H), 6.17 (t, J = 8.9 Hz, 1H), 6.25 (s, 1H), 7.34 (t, J = 7.7 Hz, 1H), 7.40 (d, J = 7.7 Hz, 1H), 7.89 (d, J = 7.7 Hz, 1H), 7.92 (s, 1H); ^{13}C NMR (175 MHz) δ 9.5, 15.2, 18.7, 21.5, 22.5, 25.9, 27.0, 28.4, 35.6, 35.8, 36.2, 36.8, 43.4, 45.8, 51.7, 58.6, 72.7, 73.9, 75.2, 76.4, 76.6, 77.0, 77.2, 77.4, 79.4, 80.1, 81.3, 84.8, 120.8, 127.5, 128.7, 129.3, 131.0, 133.4, 134.6, 138.0, 138.5, 143.1, 155.6, 156.3, 167.2, 170.1, 173.3, 205.9. HRMS (TOF) *m/z*: Calcd. For $C_{45}H_{62}N_2O_{15}Na$ + calcd: 893.4042. Found: 893.4054 (Δ = −1.3 ppm).

*4.3.42. 2-Debenzoyl-2-(3-methylbenzoyl)-10-methoxycarbonyl-3′-(2-methylpropen-1-yl)-3′-dephenyldocetaxel (**1e-02**)*

In the same manner as that for **1b-02**, **1e-02** was synthesized from **9e-02** (81 mg, 0.072 mmol) and HF/pyridine (70%, 1.1 mL) in 84% yield (52 mg) as a white solid: m.p. 150–152 °C; ^{1}H NMR (700 MHz, $CDCl_3$) δ 1.15 (s, 3H), 1.24 (s, 3H), 1.34 (s, 9H), 1.64 (s, 1H), 1.69 (s, 3H), 1.71 (s, 1H), 1.75 (s, 3H), 1.76 (s, 3H), 1.88 (m, 1H), 1.93 (s, 3H), 2.36 (m, 5H), 2.42 (s, 3H), 2.46 (d, J = 4.1 Hz, 1H), 2.56 (m, 1H), 3.39 (br s, 1H), 3.78 (d, J = 7.1 Hz, 1H), 3.87 (s, 3H), 4.17 (d, J = 8.5 Hz, 1H), 4.21 (dd, J = 2.7 Hz, J = 7.1 Hz, 1H), 4.31 (d, J = 8.5 Hz, 1H), 4.39 (m, 1H), 4.75 (m, 2H), 5.32 (d, J = 7.4 Hz, 1H), 5.65 (d, J = 7.1 Hz, 1H), 6.12 (s, 1H), 6.16 (t, J = 9.0 Hz, 1H), 7.35 (t, J = 7.7 Hz, 1H), 7.41 (d, J = 7.7 Hz, 1H), 7.89 (d, J = 7.7 Hz, 1H), 7.93 (s, 1H); ^{13}C NMR (175 MHz) δ 9.6, 15.2, 18.7, 21.5, 21.9, 22.5, 25.9, 26.7, 28.4, 35.7, 35.8, 43.3, 45.8, 51.7, 55.8, 58.7, 72.3, 72.5, 73.9, 75.0, 76.6, 77.0, 77.2, 77.4, 78.5, 79.3, 80.1, 81.2, 84.5, 120.8, 127.5, 128.7, 129.3, 131.0, 132.7, 134.7, 138.0, 138.5, 143.7, 155.6, 156.0, 167.2, 170.3, 173.3, 204.2. HRMS (TOF) *m/z*: Calcd. For $C_{44}H_{59}NO_{16}Na^+$ calcd: 880.3726. Found: 880.3742 (Δ = −1.8 ppm).

*4.3.43. 2-Debenzoyl-2-(3-trifluoromethoxybenzoyl)-10-acetyl-3′-(2-methylpropen-1-yl)-3′-dephenyldocetaxel (**1a-05**)*

In the same manner as that for **9b-02**, **9a-05** was synthesized from **7a-05** (188 mg, 0.241 mmol) and **8** (101 mg, 0.253 mmol) as a white solid, which was immediately subjected to deprotection with HF-pyridine in the same manner as that for **1b-02** to give **1a-05** (202 mg, 0.221 mmol, 92% for 2 steps) as a white solid: m.p. 149–151 °C; ^{1}H NMR (400 MHz, $CDCl_3$, ppm) δ 1.16 (s, 3H), 1.27 (s, 3H), 1.35 (s, 9H), 1.65 (s, 1H), 1.69 (s, 3H), 1.74 (s, 3H), 1.77 (s, 3H), 1.85–1.91 (m, 4H), 2.25 (s, 3H), 2.27–2.46 (m, 5H), 2.50 (broad, OH), 2.53–2.61 (m, 1H), 3.34 (d, J = 6.5 Hz, 1H), 3.84 (d, J = 7.0 Hz, 1H), 4.16–4.20 (m, 2H), 4.29 (AB, J_{AB} = 8.2 Hz, 1H), 4.43 (t, J = 7.0 Hz, 1H), 4.71–4.76 (m, 2H), 4.99 (d, J = 7.8 Hz, 1H), 5.34 (d, J = 4.5 Hz, 1H), 5.66 (d, J = 7.0 Hz, 1H), 6.15 (t, J = 8.5 Hz, 1H), 6.32 (s, 1H), 7.47 (d, J = 8.0 Hz, 1H), 7.54 (t, J = 8.0 Hz, 1H), 7.99 (s, 1H), 8.06 (d, J = 8.0 Hz, 1H); ^{13}C NMR (100 MHz, $CDCl_3$, ppm) δ 9.69, 15.20, 18.60, 21.06, 21.99, 22.39, 25.87, 26.79, 28.40, 35.60, 35.74, 43.37, 45.85, 51.80, 58.76, 72.39, 72.59, 73.84, 75.83, 76.51, 77.43, 79.40, 80.10, 81.21, 84.63, 119.34, 120.73, 121.91, 122.36, 126.37, 128.86, 130.53, 131.49, 132.86, 138.28, 143.10, 149.46, 149.48, 155.59, 165.67, 170.23, 171.48, 173.48, 203.90; ^{19}F NMR (376 MHz, $CDCl_3$, 25 °C) δ −57.82 (3F). HRMS (TOF) *m/z*: Calcd. For $C_{44}H_{56}F_3NO_{16}H^+$, 912.3624. Found, 912.3629.

*4.3.44. 2-Debenzoyl-2-(3-trifluoromethoxybenzoyl)-10-propanoyl-3′-(2-methylpropen-1-yl)-3′-dephenyldocetaxel (**1b-05**)*

In the same manner as that for **1b-02**, **1b-05** was synthesized from **9b-05** (246 mg, 0.207 mmol) and HF/pyridine (70%, 2.5 mL) in 94% yield (180 mg) as a white solid: ^{1}H NMR (500 MHz, $CDCl_3$) 1.17 (s, 3H), 1.32 (m, 6H),1.36 (s, 9H), 1.71 (m, 3H),1.77 (m, 3H), 1.92 (s, 3H), 2.35 (s, 3H), 2.06 (s, 1H), 2.63–2.47 (m, 4H), 3.37 (s, 1H), 3.85 (d, J = 7.0 Hz, 1H), 4.14 (q, J = 8.0 Hz, 1H), 4.18 (d, J = 8.0 Hz, 1H), 4.21 (d, J = 4.7 Hz, 1H), 4.30 (d, J = 8.3 Hz, 1H), 4.47–4.43 (m, 1H),4.75 (dt, J = 8.5, 5.4 Hz, 2H), 5.00 (d, J = 8.1 Hz, 1H), 5.35 (d, J = 7.4 Hz, 1H), 5.67 (d, J = 7.0 Hz, 1H), 6.17 (t, J = 8.8 Hz, 1H), 6.34 (s, 1H), 7.48 (d, J = 8.0 Hz, 1H), 7.55 (dd, J = 8.0, 2.0 Hz, 1H), 8.00 (s, 1H), 8.07 (d, J = 8.0 Hz, 1H). ^{13}C NMR (125 MHz, $CDCl_3$) δ 9.03, 9.48, 14.95, 18.38, 21.79, 22.17, 25.27, 25.65, 26.57, 27.56, 28.18, 34.66, 35.42, 35.54, 43.15, 45.69, 51.58, 58.50, 72.18, 72.37, 73.64, 75.43, 75.66, 76.29, 79.15, 79.84, 80.99, 84.45,119.86 (q, J = 259 Hz), 121.44, 122.15, 126.13,128.65, 130.31, 131.30, 137.98, 132.74,142.71, 149.24, 155.38, 165.44,170.02, 173.28, 174.60, 203.74. ^{19}F NMR (376 MHz, $CDCl_3$) δ −57.83 (s, 3F). HRMS (TOF) *m/z*: Calcd. For $C_{45}H_{58}F_3NO_{16}^+$, 926.3780. Found, 926.3791.

*4.3.45. 2-Debenzoyl-2-(3-trifluoromethoxybenzoyl)-10-cyclopropanecarbonyl-3′-(2-methyl-propen-1-yl)-3′-dephenyldocetaxel (**1c-05**)*

In the same manner as that for **1b-02**, **1c-05** was synthesized from **9c-05** (670 mg, 0.55 mmol) and HF/pyridine (70%, 6.5 mL) in 98% yield (511 mg) as a white solid: m.p. 145–146 °C; ^{1}H NMR (400 MHz, $CDCl_3$, ppm) δ 0.99–1.01 (m, 1H), 1.12–1.17 (m, 4H), 1.27 (s, 3H), 1.36 (s, 9H), 1.60 (s, 3H), 1.64 (s, 1H), 1.68 (s, 3H), 1.75 (s, 3H), 1.78 (s, 3H), 1.79–1.82 (m, 1H), 1.85–1.91 (m, 4H), 2.32–2.45 (m, 5H), 2.53–2.59 (m, 2H), 3.32 (d, J = 6.4 Hz, 1H), 3.83 (d, J = 7.0 Hz, 1H), 4.17 (AB, J_{AB} = 8.2 Hz, 1H), 4.19 (d, J = 9.6 Hz, 1H), 4.29 (AB,

J_{AB} = 8.2 Hz, 1H), 4.43 (dd, J_1 = 10.8 Hz, J_2 = 6.6 Hz, 1H), 4.74 (d, J = 3.4 Hz, 1H), 4.99 (d, J = 7.9 Hz, 1H), 5.34 (s, 1H), 5.66 (d, J = 7.0 Hz, 1H), 6.16 (t, J = 8.0 Hz, 1H), 6.32 (s, 1H), 7.47 (d, J = 8.0 Hz, 1H), 7.55 (t, J = 8.0 Hz, 1H), 8.00 (s, 1H), 8.06 (d, J = 8.0 Hz, 1H); ^{13}C NMR (125 MHz, $CDCl_3$) δ 9.43, 9.67, 13.24, 15.23, 18.61, 22.11, 22.40, 25.88, 26.86, 28.41(3C of the *t*-butyl group), 35.62, 35.68, 43.38, 45.84, 51.78, 58.77, 72.47, 72.65, 73.84, 75.63, 75.84, 76.51, 79.44, 80.12, 81.23, 84.68, 119.61, 120.72, 121.66, 122.37, 126.39, 128.87, 130.54, 131.49, 132.93, 138.32, 143.15, 149.47, 155.59, 165.68, 170.21, 174.10, 175.37, 204.09; ^{19}F NMR (376 MHz, $CDCl_3$, 25 °C) δ −57.83 (3F). HRMS (TOF) *m/z*: Calcd. For $C_{46}H_{58}F_3NO_{16}H^+$, 938.3780. Found, 938.3778.

4.3.46. 2-Debenzoyl-2-(3-trifluoromethoxybenzoyl)-10-N,N-dimethylcarbamoyl-3′-(2-methylpropen-1-yl)-3′-dephenyldocetaxel (1d-05)

In the same manner as that for **1b-02**, **1d-05** was synthesized from **9d-05** (491 mg, 0.405 mmol) and HF/pyridine (70%, 5 mL) in 96% yield (366 mg) as a white solid: m.p. 170–172 °C; ^{1}H NMR (400 MHz, $CDCl_3$, ppm) δ 1.17 (s, 3H), 1.26 (s, 3H), 1.35 (s, 9H), 1.67 (s, 3H), 1.75 (s, 3H), 1.77 (s, 3H), 1.86–1.93 (m, 4H), 2.29–2.42 (m, 5H), 2.51–2.59 (m, 1H), 2.97 (s, 3H), 3.05 (s, 3H), 3.83 (d, J = 7.0 Hz, 1H), 4.16–4.20 (m, 2H), 4.28 (AB, J_{AB} = 8.2 Hz, 1H), 4.46 (dd, J_1 = 10.8 Hz, J_2 = 6.6 Hz, 1H), 4.73–4.79 (m, 2H), 4.99 (d, J = 8.2 Hz, 1H), 5.34 (d, J = 6.3 Hz, 1H), 5.65 (d, J = 7.0 Hz, 1H), 6.17 (t, J = 8.7 Hz, 1H), 6.27 (s, 1H), 7.47 (d, J = 8.0 Hz, 1H), 7.54 (t, J = 8.0 Hz, 1H), 8.00 (s, 1H), 8.06 (d, J = 8.0 Hz, 1H); ^{13}C NMR (100 MHz, $CDCl_3$, ppm) δ 9.51, 15.27, 18.60, 22.39, 25.87, 27.00, 28.41, 35.55, 35.66, 36.23, 36.86, 43.38, 45.80, 51.81, 58.71, 72.65, 72.70, 73.86, 75.96, 76.41, 76.51, 77.43, 79.52, 80.08, 81.29, 84.86, 120.75, 122.39, 126.34, 128.86, 130.51, 131.52, 133.23, 138.29, 143.41, 149.46, 155.59, 156.33, 165.69, 170.16, 173.47, 205.87; ^{19}F NMR (376 MHz, $CDCl_3$, 25 °C) δ −57.82 (3F). HRMS (TOF) *m/z*: Calcd. For $C_{45}H_{59}F_3N_2O_{16}H^+$, 941.3889. Found, 941.3893.

4.3.47. 2-Debenzoyl-2-(3-trifluoromethoxybenzoyl)-10-methoxycarbonyl-3′-(2-methyl-propen-1-yl)-3′-dephenyldocetaxel (1e-05)

In the same manner as that for **1b-02**, **1e-05** was synthesized from **9e-05** (246 mg, 0.207 mmol) and HF/pyridine (70%, 2.5 mL) in 95% yield (183 mg) as a white solid: m.p. 121–123 °C; ^{1}H NMR (400 MHz, $CDCl_3$, ppm) δ 1.16 (s, 3H), 1.25 (s, 3H), 1.35 (s, 9H), 1.70 (s, 3H), 1.74 (s, 3H), 1.77 (s, 3H), 1.86–1.94 (m, 4H), 2.29–2.50 (m, 5H), 2.53–2.61 (m, 1H), 3.81 (d, J = 7.0 Hz, 1H), 3.88 (s, 3H), 4.17–4.21 (m, 2H), 4.32 (AB, J_{AB} = 8.4 Hz, 1H), 4.46 (dd, J_1 = 10.8 Hz, J_2 = 6.6 Hz, 1H), 4.73–4.79 (m, 2H), 4.98 (d, J = 8.2 Hz, 1H), 5.34 (d, J = 7.1 Hz, 1H), 5.66 (d, J = 7.0 Hz, 1H), 6.13 (s, 1H), 6.18 (t, J = 8.8 Hz, 1H), 6.67 (t, J = 73.4 Hz, 1H), 7.37 (dd, J_1 = 8.0 Hz, J_2 = 2.0 Hz, 1H), 7.50 (t, J = 8.0 Hz, 1H), 7.89 (s, 1H), 7.96 (d, J = 8.0 Hz, 1H); ^{13}C NMR (100 MHz, $CDCl_3$, ppm) δ 9.67, 15.23, 18.68, 21.99, 22.48, 25.90, 26.76, 28.40, 35.57, 35.78, 43.27, 45.79, 51.67, 55.81, 58.75, 72.27, 72.48, 73.84, 75.69, 76.53, 77.49, 78.49, 79.43, 80.11, 81.14, 84.60, 113.30, 115.89, 118.48, 120.34, 120.75, 125.13, 127.42, 130.46, 131.26, 132.60, 138.20, 143.85, 151.43, 155.61, 155.98, 166.03, 170.38, 173.54, 204.16; ^{19}F NMR (376 MHz, CDCl3) δ −57.82 (s, 3F); HRMS (TOF) *m/z*: Calcd. For $C_{44}H_{56}F_3NO_{17}H^+$, 928.3573. Found, 928.3576.

4.3.48. 2-Debenzoyl-2-(3-difluoromethoxybenzoyl)-10-acetyl-3′-(2-methylpropen-1-yl)-3′-dephenyl-docetaxel (1a-06)

In the same manner as that for **1b-02**, **1a-06** was synthesized from **9a-06** (187 mg, 0.163 mmol) and HF/pyridine (70%, 1.6 mL) in 96% yield (140 mg) as a white solid: ^{1}H NMR (400 MHz, $CDCl_3$) δ1.14 (s, 3H), 1.24 (m, 3H), 1.31 (s, 9H), 1.66 (s, 3H), 1.74 (m, 3H), 1.77 (m, 3H), 1.84–1.80 (m, 1H), 1.87 (m, 3H), 2.03 (s, 1H), 2.23 (s, 3H), 2.36 (m, 6H), 2.58–2.50 (m, 2H), 3.40 (d, J = 6.7 Hz, 1H), 3.81 (d, J = 7.0 Hz, 1H), 4.15 (d, J = 8.3 Hz, 1H), 4.29 (d, J = 8.3 Hz, 1H), 4.44–4.38 (m, 1H), 4.74 (dd, J = 8.8, 2.5 Hz, 1H), 4.82 (d, J = 8.8 Hz, 1H), 4.96 (d, J = 7.8 Hz, 1H), 5.32 (d, J = 8.3 Hz, 1H), 5.64 (d, J = 7.0 Hz, 1H), 6.16 (dd, J = 9.1, 7.9 Hz, 1H), 6.29 (s, 1H), 6.66 (t, J = 73.2 Hz, 1H), 7.35 (d, J = 8.0 Hz, 1H), 7.47 (t, J = 8.0 Hz, 1H), 7.86 (s, 1H), 7.94 (d, J = 8.0 Hz, 1H); ^{13}C NMR (100 MHz, $CDCl_3$) δ 9.52, 14.19, 14.92, 18.46, 20.85, 21.04, 21.86, 22.27, 25.69, 26.62, 28.19, 35.43, 35.53, 43.16, 45.63, 51.46, 58.49, 60.41, 72.11, 72.30, 73.63, 75.57, 75.61, 76.32, 76.72, 77.36, 79.17, 79.85, 80.97, 84.42, 115.69 (t, J = 263 Hz), 124.88, 127.20, 130.24, 131.09, 132.75, 137.91, 142.74, 151.21, 155.40, 165.81, 170.14, 171.26, 203.70; ^{19}F NMR (376 MHz, $CDCl_3$) δ −81.23 (ABq, J = 167 Hz, 2F); HRMS (TOF) *m/z*: Calcd. for $C_{44}H_{57}F_2NO_{16}{}^+$, 94.3718. Found: 894.3727.

4.3.49. 2-Debenzoyl-2-(3-difluoromethoxybenzoyl)-10-propanoyl-3′-(2-methylpropen-1-yl)-3′-dephenyl-docetaxel (1b-06)

In the same manner as that for **1b-02**, **1b-06** was synthesized from **9b-06** (350 mg, 0.297 mmol) and HF/pyridine (70%, 3.4 mL) in 92% yield (248 mg) as a white solid: m.p. 126–128 °C; ^{1}H NMR (400 MHz, $CDCl_3$, ppm) δ 1.15 (s, 3H), 1.21–1.26 (m, 6H), 1.33 (s, 9H), 1.68 (s, 3H), 1.75 (s, 3H), 1.77 (s, 3H), 1.85–1.92 (m, 4H), 2.30–2.38 (m, 5H), 2.47–2.60 (m, 3H), 3.83 (d, J = 7.0 Hz, 1H), 4.17 (AB, J_{AB} = 8.3 Hz, 1H), 4.21 (d, J = 2.2 Hz, 1H), 4.31 (AB, J_{AB} = 8.3 Hz, 1H), 4.44 (dd, J_1 = 10.8 Hz, J_2 = 6.7 Hz, 1H), 4.75–4.81 (m, 2H), 4.98 (d, J = 7.8 Hz, 1H), 5.34 (d, J = 7.8 Hz, 1H), 5.66 (d, J = 7.0 Hz, 1H), 6.18 (t, J = 8.5 Hz, 1H), 6.67 (d, J = 73.4 Hz, 1H), 7.36–7.38 (dd, J_1 = 8.0 Hz, J_2 = 2.0 Hz, 1H), 7.49 (t, J = 8.0 Hz, 1H), 7.89 (s, 1H), 7.96 (d, J = 7.8 Hz, 1H); ^{13}C NMR (100 MHz, $CDCl_3$, ppm) δ 9.23, 9.72,15.12, 18.67, 22.08, 22.48, 25.89, 26.83, 27.77, 28.39, 35.63, 35.73, 43.37, 45.83, 51.66, 58.72, 72.37, 72.54, 73.83, 75.61, 75.76, 76.53, 77.43, 79.42, 80.07, 81.18, 84.65, 113.29, 115.88, 118.48, 120.36, 120.77, 125.11, 127.41, 130.45, 131.28, 133.01, 138.17, 142.84, 151.42, 155.59, 166.03, 170.33, 173.48, 174.82, 203.98; ^{19}F NMR (376 MHz, $CDCl_3$, 25 °C) δ −81.13 (ABq, J = 167 Hz, 2F); HRMS (TOF) *m/z*: Calcd. For $C_{45}H_{59}F_2NO_{16}H^+$, 908.3875. Found, 908.3882.

4.3.50. 2-Debenzoyl-2-(3-difluoromethoxybenzoyl)-10-cyclopropanecarbonyl-3′-(2-methylpropen-1-yl)-3′-dephenyl-docetaxel (1c-06)

In the same manner as that for **1b-02**, **1c-06** was synthesized from **9c-06** (418 mg, 0.351 mmol) and HF/pyridine (70%, 4.1 mL) in 91% yield (294 mg) as a white solid: m.p. 145–147 °C; ^{1}H NMR (400 MHz, $CDCl_3$, ppm) δ 0.98–1.02 (m, 2H), 1.11–1.15 (m, 4H), 1.26 (s, 3H), 1.32 (s, 9H), 1.66 (s, 3H), 1.74 (s, 3H), 1.76 (s, 3H), 1.78–1.82 (m, 1H), 1.86–1.89 (m, 4H), 2.30–2.38 (m, 5H), 2.50–2.58 (m, 2H), 3.81 (d, J = 7.0 Hz, 1H), 4.16 (AB, J_{AB} = 8.3 Hz, 1H), 4.20 (d, J = 2.6 Hz, 1H), 4.29 (AB, J_{AB} = 8.3 Hz, 1H), 4.39–4.43 (m, 1H), 4.72–4.77 (m, 1H), 4.83 (d, J = 8.7 Hz, 1H), 4.97 (d, J = 8.0 Hz, 1H), 5.33 (d, J = 8.4 Hz, 1H), 5.65 (d, J = 7.0 Hz, 1H), 6.17 (t, J = 9.0 Hz, 1H), 6.66 (t, J = 73.4 Hz, 1H), 7.36 (dd, J_1 = 8.0 Hz, J_2 = 2.0 Hz, 1H), 7.48 (t, J = 8.0 Hz, 1H), 7.87 (s, 1H), 7.95 (d, J = 7.8 Hz, 1H); ^{13}C NMR (100 MHz, $CDCl_3$, ppm) δ 9.20, 9.43, 9.50, 13.04, 14.93, 18.46, 21.97, 22.27, 25.69, 26.68, 28.19, 35.46, 35.49, 43.17, 45.64, 51.45, 58.49, 72.14, 72.34, 73.63, 75.40, 75.60, 76.33, 77.25, 79.18, 79.87, 80.99, 84.47, 113.10, 115.69, 118.29, 120.15, 120.59, 124.88, 127.20, 130.24, 131.10, 132.83, 137.92, 142.74, 151.21, 155.41, 165.81, 170.13, 173.27, 175.12, 203.86; ^{19}F NMR (376 MHz, $CDCl_3$) δ −81.24 (ABq, J = 167 Hz, 2F); HRMS (TOF) *m/z*: Calcd. For $C_{46}H_{59}F_2NO_{16}Na^+$, 942.3694. Found, 942.3694.

4.3.51. 2-Debenzoyl-2-(3-difluoromethoxybenzoyl)-10-N,N-dimethylcarbamoyl-3′-(2-methyl-propen-1-yl)-3′-dephenyl-docetaxel (1d-06)

In the same manner as that for **1b-02**, **1d-06** was synthesized from **9d-06** (157 mg, 0.132 mmol) and HF/pyridine (70%, 1.7 mL) in 92% yield (112 mg) as a white solid: m.p. 150–152 °C; ^{1}H NMR (400 MHz, $CDCl_3$, ppm) δ 1.16 (s, 3H), 1.26 (s, 3H), 1.33 (s, 9H), 1.67 (s, 3H), 1.75

(s, 3H), 1.77 (s, 3H), 1.85–1.92 (m, 4H), 2.30–2.41 (m, 5H), 2.50–2.58 (m, 1H), 2.96 (s, 3H), 3.05 (s, 3H), 3.82 (d, J = 7.0 Hz, 1H), 4.16–4.21 (m, 2H), 4.30 (AB, J_{AB} = 8.3 Hz, 1H), 4.46 (dd, J_1 = 10.9 Hz, J_2 = 6.6 Hz, 1H), 4.75–4.82 (m, 2H), 4.99 (d, J = 7.9 Hz, 1H), 5.33 (d, J = 8.1 Hz, 1H), 5.65 (d, J = 7.0 Hz, 1H), 6.19 (t, J = 8.0 Hz, 1H), 6.67 (t, J = 73.4 Hz, 1H), 7.37 (dd, J_1 = 8.0 Hz, J_2 = 2.0 Hz, 1H), 7.49 (t, J = 8.0 Hz, 1H), 7.88 (s, 1H), 7.96 (d, J = 7.80 Hz, 1H); ^{13}C NMR (100 MHz, $CDCl_3$, ppm) δ 9.54, 15.19, 18.67, 22.48, 25.89, 27.02, 28.39, 35.55, 35.68, 36.23, 36.85, 43.37, 45.77, 51.65, 58.66, 72.62, 73.84, 75.89, 76.39, 76.52, 77.43, 79.51, 80.05, 81.24, 84.86, 113.30, 115.89, 118.48, 120.36, 120.78, 125.08, 127.40, 130.43, 131.31, 133.30, 138.16, 143.26, 151.42, 155.60, 156.33, 166.04, 170.27, 173.48, 205.86; ^{19}F NMR (376 MHz, $CDCl_3$) δ −81.23 (ABq, J = 167 Hz, 2F). HRMS (TOF) m/z: Calcd. For $C_{45}H_{60}F_2N_2O_{16}Na^+$, 945.3803. Found, 945.3794.

4.3.52. 2-Debenzoyl-2-(3-difluoromethoxybenzoyl)-10-methoxycarbonyl-3′-(2-methyl-propen-1-yl)-3′-dephenyl-docetaxel (*1e-06*)

In the same manner as that for **1b-02**, **1e-06** was synthesized from **9e-06** (89 mg, 0.075 mmol) and HF/pyridine (70%, 0.9 mL) in 90% yield (61 mg) as a white solid: m.p. 170–172 °C; ^{1}H NMR (400 MHz, $CDCl_3$, ppm) δ 1.16 (s, 3H), 1.26 (s, 3H), 1.33 (s, 9H), 1.70 (s, 3H), 1.75 (s, 3H), 1.77 (s, 3H), 1.86–1.94 (m, 4H), 2.30–2.42 (m, 5H), 2.53–2.61 (m, 1H), 3.81 (d, J = 7.0 Hz, 1H), 3.88 (s, 3H), 4.17–4.21 (m, 2H), 4.32 (AB, J_{AB} = 8.4 Hz, 1H), 4.46 (dd, J_1 = 10.8 Hz, J_2 = 6.6 Hz, 1H), 4.73–4.79 (m, 2H), 4.98 (d, J = 8.2 Hz, 1H), 5.34 (d, J = 7.1 Hz, 1H), 5.66 (d, J = 7.0 Hz, 1H), 6.13 (s, 1H), 6.18 (t, J = 8.8 Hz, 1H), 6.67 (t, J = 73.4 Hz, 1H), 7.37 (dd, J_1 = 8.0 Hz, J_2 = 2.0 Hz, 1H), 7.50 (t, J = 8.0 Hz, 1H), 7.89 (s, 1H), 7.96 (d, J = 7.80 Hz, 1H); ^{13}C NMR (100 MHz, $CDCl_3$, ppm) δ 9.67, 15.23, 18.68, 21.99, 22.48, 25.90, 26.76, 28.40, 35.57, 35.78, 43.27, 45.79, 51.67, 55.81, 58.75, 72.27, 72.48, 73.84, 75.69, 76.53, 77.49, 78.49, 79.43, 80.11, 81.14, 84.60, 113.30, 115.89, 118.48, 120.34, 120.75, 125.13, 127.42, 130.46, 131.26, 132.60, 138.20, 143.85, 151.43, 155.61, 155.98, 166.03, 170.38, 173.54, 204.16; ^{19}F NMR (376 MHz, $CDCl_3$) δ −81.24 (ABq, J = 167 Hz, 2F); HRMS (TOF) m/z: Calcd. For $C_{44}H_{57}F_2NO_{17}H^+$, 910.3667. Found, 910.3671.

4.4. In vitro cell growth inhibition assay

Tumor cell growth inhibition was determined according to the method established by Skehan et al. [78]. Human cancer cells DLD-1, NCI/ADR, LCC6-MDR were cultured and maintained in Roswell Park Memorial Institute growth medium RPMI1640 supplemented by 10% fetal bovine serum (FBS) and 1% penicillin (PenStrip). Human cancer cells CFPAC-1 were cultured and maintained in Iscove's modified Dulbecco's medium (IDMEM) supplemented by 2 mM glutamine and 10% fetal bovine serum (FBS). CSC-enriched HCT116^{CSC} colon cancer cells were cultured in Mesenchymal stem cell growth medium (MSCGM™). Patient-derived CSC-enriched PPT2 prostate cancer cells were cultured in serum-free Mesenchymal stem cell basal medium (MSCBM).

Cells were plated at a density of 2000–5000 cells/well in 96-well plates and allowed to attach overnight and reach 50% confluency. Taxoids were dissolved in sterilized DMSO and further diluted with the corresponding medium. The concentration of DMSO was restricted to be below 99.5% culture medium/0.5% DMSO to avoid DMSO's effect on cell growth. Quintuplicate wells were exposed to various treatments. After 72 h of incubation, plates were washed with DPBS buffer to remove drug and serum proteins in medium. Then MTT solution was added into each well. Following 3 h incubation avoiding light, the remaining MTT solution was discarded. The dye was dissolved in 0.04 M HCl in isopropanol. And the 96-well plate was shaken for 10 min. Optical density (OD) was tested under 570 nm. A dose-response (kill) curve was built by applying gradient drug concentration as x axis and related cell viability as y axis. The curve was then fitted with Sigmoid-Emax model in Sigmaplot 12.5 to calculate IC_{50} value of a given compound.

4.5. Molecular modeling analysis

The structures of 3rd-generation taxoids were adapted from the co-crystal coordinates of paclitaxel in β-tubulin (PDB ID: 1JFF) [64]. The Avogadro molecular editor [79] was used to fix co-crystal structure of paclitaxel, manually build each functional group augmentation, assign Marsilli-Gasteiger partial charges [65,66], and minimize the unconstrained atoms with the organic molecule force field MMFF94 [67–71]. For most taxoids, only two conformers were generated, with the C2 benzoate group substituent orientated to the proximal and distal binding sites. However, for more complicated substituents with added rotatable bonds, e.g. OCF_3 and OCF_2H, relevant gauche and eclipsed conformations were also identified and built in accordance to the local minima from the force field.

Docking calculations were performed using AutoDock Vina [72] where typical re-orientation calculations, the local search algorithm, and direct rescoring were utilized. Energy-minimized structures were directly used as input for re-orientation calculations. For local search minimization and rescoring calculations, the adapted crystal coordinate structures for all conformers were used. Data was collected for the conformer in which the pose was geometrically and energetically most favorable. All calculations used default parameters (see Supplementary Material) of the scoring function. All visualization and analysis of binding poses was performed in UCSF Chimera [80].

Declaration of Competing Interest

The authors declare that they have no known competing financial interests or personal relationships that could have appeared to influence the work reported in this paper.

Acknowledgements

This work was supported by grants from the National Cancer Institute (CA 103314 to IO) and the Natural Science Foundation of Guangdong Province, China (2015B020211012 and 2016A050502039 to CW). The authors would like to thank Dr. Bela Ruzsiczka, Institute of Chemical Biology and Drug Discovery, Stony Brook University, for his advice and technical help for LC/HRMS analysis and the Fujian Yew Park Biological Co. Ltd., China for generous gift of 10-deacetylbaccatin III used in this work.

Appendix A. Supplementary material

Supplementary data to this article can be found online at https://doi.org/10.1016/j.bioorg.2019.103523.

References

[1] I. Ojima, B. Lichtenthal, S. Lee, C.W. Wang, X. Wang, Taxane anticancer agents: a patent perspective, Exp. Opin. Ther. Pat. 26 (2016) 1–20.
[2] I. Ojima, X. Wang, Y.R. Jing, C.W. Wang, Quest for efficacious next-generation taxoid anticancer agents and their tumor-targeted delivery, J. Nat. Prod. 81 (2018) 703–721.
[3] N. Desai, Nanoparticle albumin-bound paclitaxel (Abraxane®), in: M. Otagiri, V. Tuan, G. Chuang (Eds.), Albumin in Medicine: Pathological and Clinical Applications, Springer, New York, 2016, pp. 101–119.
[4] I. Cucinotto, L. Fiorillo, S. Gualtieri, M. Arbitrio, D. Ciliberto, N. Staropoli, A. Grimaldi, A. Luce, P. Tassone, M. Caraglia, P. Tagliaferri, Nanoparticle albumin bound Paclitaxel in the treatment of human cancer: nanodelivery reaches prime-time? J. Drug Deliv. 2013 (2013) 905091.
[5] A.E. Quinton, S.H. Gwynne, K.L. Yim, Nab-paclitaxel in combination with gemcitabine for the treatment of metastatic pancreas cancer: the South Wales experience, Med. Oncol. 35 (2018) 115.
[6] J.S. Bono, S. Oudard, M. Ozguroglu, Prednisone plus cabazitaxel or mitoxantrone

for metastatic castration-resistant prostate cancer progressing after docetaxel treatment: a randomised open-label trial, Lancet 376 (2010) 1147–1154.
[7] P. Vrignaud, D. Sémiond, P. Lejeune, H. Bouchard, L. Calvet, C. Combeau, J.-F. Riou, A. Commerçon, F. Lavelle, M.-C. Bissery, Preclinical antitumor activity of cabazitaxel, a semisynthetic taxane active in taxane-resistant tumors, Clin. Cancer Res. 19 (2013) 2973–2983.
[8] M.C. Bissery, G. Nohynek, G.J. Sanderink, F. Lavelle, Docetaxel (Taxotere): a review of preclinical and clinical experience, Part I and Part II: preclinical experience, Anticanc. Drugs 6 (1995) 339–355 (pp. 356–368).
[9] A.T. Fojo, K. Ueda, D.J. Slamon, D.G. Poplack, M.M. Gottesman, I. Pastan, Expression of a multidrug-resistance gene in human-tumors and tissues, Proc. Natl. Acad. Sci. USA 84 (1987) 265–269.
[10] M.M. Gottesman, I. Pastan, Biochemistry of multidrug-resistance mediated by the multidrug transporter, Annu. Rev. Biochem. 62 (1993) 385–427.
[11] Y. Tang, J. Rodriguez-Salarichs, Y. Zhao, P. Cai, J. Estevez-Gallego, F. Balaguer-Perez, M.R. Horcajo, D. Lucena-Agell, I. Barasoain, J.F. Diaz, W.S. Fang, Modification of C-seco taxoids through ring tethering and substituent replacement leading to effective agents against tumor drug resistance mediated by beta III-Tubulin and P-glycoprotein (P-gp) overexpressions, Eur. J. Med. Chem. 137 (2017) 488–503.
[12] W.Q. Qiu, Y.M. Cui, P. Tang, Y.Y. Qiu, H.X. Lin, Synthesis and biological evaluation of novel A-seco-taxoids derived from 1-deoxybaccatin VI, Nat. Prod. Res. 32 (2018) 121–127.
[13] I. Ojima, Strategic incorporation of fluorine into taxoid anticancer agents for medicinal chemistry and chemical biology studies, J. Fluorine Chem. 198 (2017) 10–23.
[14] B. Mohelnikova-Duchonova, M. Kocik, B. Duchonova, V. Brynychova, M. Oliverius, J. Hlavsa, E. Honsova, J. Mazanec, Z. Kala, I. Ojima, D.J. Hughes, J.E. Doherty, H.A. Murray, M.A. Crockard, R. Lemstrova, P. Soucek, Hedgehog pathway over-expression in pancreatic cancer is abrogated by new-generation taxoid SB-T-1216, Pharmacogen. J. 17 (2017) 452–460.
[15] S.R. Wang, P.A. Sanchez-Murcia, F. Gago, W.S. Fang, A novel C, D-spirodioxene taxoid synthesized through an unexpected Pd-mediated ring cyclization, Org. Biomol. Chem. 14 (2016) 345–352.
[16] J.D. Seitz, T. Wang, J.G. Vineberg, T. Honda, I. Ojima, Synthesis of a next-generation taxoid by rapid methylation amenable for (11)C-labeling, J. Org. Chem. 83 (2018) 2847–2857.
[17] K. Haranahalli, T. Honda, I. Ojima, Recent progress in the strategic incorporation of fluorine into medicinally active compounds, J. Fluorine Chem. 217 (2019) 29–40.
[18] Z. Luo, L. Jiang, C. Ding, B. Hu, X.J. Loh, Z. Li, Y.L. Wu, Surfactant free delivery of docetaxel by poly[(R)-3-hydroxybutyrate-(R)-3-hydroxyhexanoate]-based polymeric micelles for effective melanoma treatments, Adv. Healthc. Mater. 7 (2018) e1801221.
[19] A.A. Asmawi, N. Salim, C.L. Ngan, H. Ahmad, E. Abdulmalek, M.J. Masarudin, M.B.A. Rahman, Excipient selection and aerodynamic characterization of nebulized lipid-based nanoemulsion loaded with docetaxel for lung cancer treatment, Drug Deliv. Transl. Res. 9 (2019) 543–554.
[20] C.C. Feng, X.X. Han, L.L. Chi, J. Sun, F.R. Gong, Y.L. Shen, Synthesis, characterization, and in vitro evaluation of TRAIL-modified, cabazitaxel -loaded polymeric micelles for achieving synergistic anticancer therapy, J. Biomater. Sci. Polym. Ed. 29 (2018) 1729–1744.
[21] J.E. Egan, I. Ojima, M.M. Amiji, G.I. Botchkina, Nanoemulsion compositions of taxoid drugs, and methods for the use thereof to target cancer cells and cancer stem cells, WIPO, 2017, WO2017214260.
[22] L. Zhou, F. Lv, L. Liu, G. Shen, X. Yan, G.C. Bazan, S. Wang, Cross-linking of thiolated paclitaxel-oligo(p-phenylene vinylene) conjugates aggregates inside tumor cells leads to “Chemical Locks” that increase drug efficacy, Adv. Mater. 30 (2018) 1704888.
[23] T. Yu, C. Wu, C. Zhu, Y. He, D. Yang, Y. Cheng, X. Gao, Oral administration of liposome-apatinib and locally delivery of docetaxel/MPEG-PCL by fibrin glue synergistically improve therapeutic effect in colorectal cancer, J. Biomed. Nanotechnol. 14 (2018) 2077–2091.
[24] X. Lu, T. Meng, Depletion of tumor-associated macrophages enhances the anti-tumor effect of docetaxel in a murine epithelial ovarian cancer, Immunobiology 224 (2019) 355–361.
[25] G. Ahmed, G.G. Mackenzie, J. Egan, M.M. Amiji, DHA-SBT-1214 taxoid nanoemulsion and anti-PD-L1 antibody combination therapy enhances anti-tumor efficacy in a syngeneic pancreatic adenocarcinoma model, Mol. Cancer Ther. 18 (2019) 1961–1972.
[26] D.A. Yardley, L.L. Hart, P.J. Ward, G.L. Wright, M. Shastry, L. Finney, L.M. DeBusk, J.D. Hainsworth, Cabazitaxel plus lapatinib as therapy for HER2(+) metastatic breast cancer with intracranial metastases: results of a dose-finding study, Clin. Breast Cancer 18 (2018) E781–E787.
[27] G. Ahmad, F. Gattacecca, R. El Sadda, G. Botchkina, I. Ojima, J. Egan, M. Amiji, Biodistribution and pharmacokinetic evaluations of a novel taxoid DHA-SBT-1214 in an oil-in-water nanoemulsion formulation in naive and tumor-bearing mice, Pharm. Res. 35 (2018) 91.
[28] J.E. Egan, M.M. Amiji, I. Ojima, Combination taxoid nanoemulsion with immunotherapy in cancer, US Paten Appl., 2019, US20190183796.
[29] S. Jaracz, J. Chen, L.V. Kuznetsova, L. Ojima, Recent advances in tumor-targeting anticancer drug conjugates, Bioorg Med. Chem. 13 (2005) 5043–5054.
[30] T. Wang, Y. Zhang, L. Wei, Y.G. Teng, T. Honda, I. Ojima, Design, synthesis, and biological evaluations of asymmetric bow-tie PAMAM dendrimer-based conjugates for tumor-targeted drug delivery, ACS Omega 3 (2018) 3717–3736.
[31] I. Ojima, J. Chen, L. Sun, C.P. Borella, T. Wang, M.L. Miller, S.N. Lin, X.D. Geng, L.R. Kuznetsova, C.X. Qu, D. Gallager, X.R. Zhao, I. Zanardi, S.J. Xia, S.B. Horwitz, J. Mallen-St Clair, J.L. Guerriero, D. Bar-Sagi, J.M. Veith, P. Pera, R.J. Bernacki, Design, synthesis, and biological evaluation of new-generation taxoids, J. Med. Chem. 51 (2008) 3203–3221.
[32] L. Kuznetsova, L. Sun, J. Chen, X.R. Zhao, J. Seitz, M. Das, Y. Li, J.M. Veith, P. Pera, R.J. Bernacki, S.J. Xia, S.B. Horwitz, I. Ojima, Synthesis and biological evaluation of novel 3 '-difluorovinyl taxoids, J. Fluorine Chem. 143 (2012) 177–188.
[33] L.V. Kuznetsova, A. Pepe, L.M. Ungureanu, P. Pera, R.J. Bernacki, I. Ojima, Syntheses and structure-activity relationships of novel 3 '-difluoromethyl and 3 '-trifluoromethyl-taxoids, J. Fluorine Chem. 129 (2008) 817–828.
[34] I. Ojima, J.C. Slater, S.D. Kuduk, C.S. Takeuchi, R.H. Gimi, C.M. Sun, Y.H. Park, P. Pera, J.M. Veith, R.J. Bernacki, Syntheses and structure-activity relationships of taxoids derived from 14 beta-hydroxy-10-deacetylbaccatin III, J. Med. Chem. 40 (1997) 267–278.
[35] I. Ojima, C. Wang, X. Wang, Third generation taxoids and methods of using same, WIPO, 2017, WO2017004478.
[36] L. Kuznetsova, J. Chen, L. Sun, X.Y. Wu, A. Pepe, J.A. Veith, P. Pera, R.J. Bernacki, I. Ojima, Syntheses and evaluation of novel fatty acid-second-generation taxoid conjugates as promising anticancer agents, Bioorg. Med. Chem. Lett. 16 (2006) 974–977.
[37] G. Ahmad, R. El Sadda, G. Botchkina, I. Ojima, J. Egan, M. Amiji, Nanoemulsion formulation of a novel taxoid DHA-SBT-1214 inhibits prostate cancer stem cell-induced tumor growth, Cancer Lett. 406 (2017) 71–80.
[38] G.I. Botchkina, E.S. Zuniga, M. Das, Y.A. Wang, H.C. Wang, S. Zhu, A.G. Savitt, R.A. Rowehl, Y. Leyfman, J.F. Ju, K. Shroyer, I. Ojima, New-generation taxoid SB-T-1214 inhibits stem cell-related gene expression in 3D cancer spheroids induced by purified colon tumor-initiating cells, Mol. Cancer 9 (2010).
[39] D.S. Sonnichsen, Q. Liu, E.G. Schuetz, J.D. Schuetz, A. Pappo, M.V. Relling, Variability in human cytochrome P450 paclitaxel metabolism, J. Pharmacol. Exp. Ther. 275 (1995) 566–575.
[40] A.G. Chaudhary, M.M. Gharpure, J.M. Rimoldi, M.D. Chordia, A.A.L. Gunatilaka, D.G.I. Kingston, S. Grover, C.M. Lin, E. Hamel, Unexpectedly facile hydrolysis of the 2-benzoate group of taxol and syntheses of analogs with increased activities, J. Am. Chem. Soc. 116 (1994) 4097–4098.
[41] D.G.I. Kingston, A.G. Chaudhary, M.D. Chordia, M. Gharpure, A.A.L. Gunatilaka, P.I. Higgs, J.M. Rimoldi, L. Samala, P.G. Jagtap, Y.Q. Jiang, C.M. Lin, E. Hamel, B.H. Long, C.R. Fairchild, K.A. Johnston, Synthesis and biological evaluation of 2-acyl analogues of paclitaxel (taxol), J. Med. Chem. 41 (1998) 3715–3726.
[42] F.P. Guengerich, M.R. Waterman, M. Egli, Recent structural insights into cytochrome P450 function, Trends Pharmacol. Sci. 37 (2016) 625–640.
[43] I. Ojima, Fluorine in Medicinal Chemistry and Chemical Biology, Wiley-Blackwell, Chichester, 2009.
[44] K. Muller, C. Faeh, F. Diederich, Fluorine in pharmaceuticals: Looking beyond intuition, Science 317 (2007) 1881–1886.
[45] J.P. Begue, D. Bonnet-Delpon, Recent advances (1995–2005) in fluorinated pharmaceuticals based on natural products, J. Fluorine Chem. 127 (2006) 992–1012.
[46] C. Isanbor, D. O'Hagan, Fluorine in medicinal chemistry: A review of anti-cancer agents, J. Fluorine Chem. 127 (2006) 303–319.
[47] J. Wang, M. Sanchez-Rosello, J.L. Acena, C. del Pozo, A.E. Sorochinsky, S. Fustero, V.A. Soloshonok, H. Liu, Fluorine in pharmaceutical industry: fluorine-containing drugs introduced to the market in the last decade (2001–2011), Chem. Rev. 114 (2014) 2432–2506.
[48] F. Cottet, M. Marull, O. Lefebvre, M. Schlosser, Recommendable routes to trifluoromethyl-substituted pyridine- and quinolinecarboxylic acids, Eur. J. Org. Chem. (2003) 1559–1568.
[49] K.L. Kirk, Fluorine in medicinal chemistry: recent therapeutic applications of fluorinated small molecules, J. Fluorine Chem. 127 (2006) 1013–1029.
[50] T. Yamazaki, T. Taguchi, I. Ojima, Unique properties of fluorine and their relevance to medicinal chemistry and chemical biology, in: I. Ojima (Ed.), Fluorine in Medicinal Chemistry and Chemical Biology, Wiley-Blackwell, Chichester, 2009, pp. 1–46.
[51] L. Xing, D.C. Blakemore, A. Narayanan, R. Unwalla, F. Lovering, R.A. Denny, H.Y. Zhou, M.E. Bunnage, Fluorine in drug design: a case study with fluoroanisoles, ChemMedChem 10 (2015) 715–726.
[52] H.J. Bohm, D. Banner, S. Bendels, M. Kansy, B. Kuhn, K. Muller, U. Obst-Sander, M. Stahl, Fluorine in medicinal chemistry, ChemBioChem 5 (2004) 637–643.
[53] F. Leroux, P. Jeschke, M. Schlosser, alpha-fluorinated ethers, thioethers, and amines: anomerically biased species, Chem. Rev. 105 (2005) 827–856.
[54] K. Muller, Simple vector considerations to assess the polarity of partially fluorinated alkyl and alkoxy groups, Chimia 68 (2014) 356–362.
[55] J. Pollock, D. Borkin, G. Lund, T. Purohit, E.Y. Dyguda-Kazimierowicz, J. Grembecka, T. Cierpicki, Rational design of orthogonal multipolar interactions with fluorine in protein-ligand complexes, J. Med. Chem. 58 (2015) 7465–7474.
[56] L. Xing, C. Keefer, M.E. Brown, Fluorine multipolar interaction: Toward elucidating its energetics in binding recognition, J. Fluorine Chem. 198 (2017) 47–53.
[57] R. Paulini, K. Muller, F. Diederich, Orthogonal multipolar interactions in structural chemistry and biology, Angew. Chem. 44 (2005) 1788–1805.
[58] J. Olsen, P. Seiler, B. Wagner, H. Fischer, T. Tschopp, U. Obst-Sander, D.W. Banner, M. Kansy, K. Muller, F. Diederich, A fluorine scan of the phenylamidinium needle of tricyclic thrombin inhibitors: effects of fluorine substitution on pKa and binding affinity and evidence for intermolecular C-F...CN interactions, Org. Biomol. Chem. 2 (2004) 1339–1352.
[59] J.A. Olsen, D.W. Banner, P. Seiler, U.O. Sander, A. D'Arcy, M. Stihle, K. Muller, F. Diederich, A fluorine scan of thrombin inhibitors to map the fluorophilicity/fluorophobicity of an enzyme active site: evidence for C-F center dot center dot center dot C=O interactions, Angew. Chem. 42 (2003) 2507–2511.
[60] X.W. Zheng, C.W. Wang, Y.M. Xing, S.Y. Chen, T. Meng, H.S. You, I. Ojima,

Y.L. Dong, SB-T-121205, a next-generation taxane, enhances apoptosis and inhibits migration/invasion in MCF-7/PTX cells, Int. J. Oncol. 50 (2017) 893–902.
[61] G.I. Botchkina, E.S. Zuniga, R.H. Rowehl, R. Park, R. Bhalla, A.B. Bialkowska, F. Johnson, L.M. Golub, Y. Zhang, I. Ojima, K.R. Shroyer, Prostate cancer stem cell-targeted efficacy of a new-generation taxoid, SBT-1214 and novel polyenolic zinc-binding curcuminoid, CMC2.24, Plos One 8 (2013) e69884.
[62] R.A. Rowehl, H. Crawford, A. Dufour, J. Ju, G.I. Botchkina, Genomic analysis of prostate cancer stem cells isolated from a highly metastatic cell line, Cancer Genom. Proteom. 5 (2008) 301–310.
[63] I.L. Botchkina, R.A. Rowehl, D.E. Rivadeneira, M.S. Karpeh Jr., H. Crawford, A. Dufour, J. Ju, Y. Wang, Y. Leyfman, G.I. Botchkina, Phenotypic subpopulations of metastatic colon cancer stem cells: genomic analysis, Cancer Genom. Proteom. 6 (2009) 19–29.
[64] J. Lowe, H. Li, K.H. Downing, E. Nogales, Refined structure of alpha beta-tubulin at 3.5 A resolution, J. Mol. Biol. 313 (2001) 1045–1057.
[65] J. Gasteiger, M. Marsili, A new model for calculating atomic charges in molecules, Tetrahedr. Lett. 19 (1978) 3181–3184.
[66] J. Gasteiger, M. Marsili, Iterative partial equalization of orbital electronegativity—a rapid access to atomic charges, Tetrahedr. Lett. 36 (1980) 3219–3228.
[67] T.A. Halgren, Merck molecular force field. 1. Basis, form, scope, parameterization, and performance of MMFF94, J. Comput. Chem. 17 (1996) 490–519.
[68] T.A. Halgren, Merck molecular force field. 2. MMFF94 van der Waals and electrostatic parameters for intermolecular interactions, J. Comput. Chem. 17 (1996) 520–552.
[69] T.A. Halgren, Merck molecular force field. 3. Molecular geometries and vibrational frequencies for MMFF94, J. Comput. Chem. 17 (1996) 553–586.
[70] T.A. Halgren, R.B. Nachbar, Merck molecular force field. 4. Conformational energies and geometries for MMFF94, J. Comput. Chem. 17 (1996) 587–615.
[71] T.A. Halgren, Merck molecular force field. 5. Extension of MMFF94 using experimental data, additional computational data, and empirical rules, J. Comput. Chem. 17 (1996) 616–641.
[72] O. Trott, A.J. Olson, AutoDock Vina: improving the speed and accuracy of docking with a new scoring function, efficient optimization, and multithreading, J. Comput. Chem. 31 (2010) 455–461.
[73] I. Ojima, D. Awasthi, L. Wei, K. Haranahalli, Strategic incorporation of fluorine in the drug discovery of new-generation antitubercular agents targeting bacterial cell division protein FtsZ, J. Fluorine Chem. 196 (2017) 44–56.
[74] N.A. Meanwell, Fluorine and fluorinated motifs in the design and application of bioisosteres for drug design, J. Med. Chem. 61 (2018) 5822–5880.
[75] I. Ojima, S.D. Kuduk, P. Pera, J.M. Veith, R.J. Bernacki, Synthesis and structure-activity relationships of nonaromatic taxoids: effects of alkyl and alkenyl ester groups on cytotoxicity, J. Med. Chem. 40 (1997) 279–285.
[76] Y.R. Jing, W. Zhou, W.L. Li, L.X. Zhao, Y.F. Wang, The synthesis of novel taxoids for oral administration, Bioorg. Med. Chem. 22 (2014) 194–203.
[77] H. Bouchard, J.-D. Bourzat, A. Commercon, Methods of treating cell lines expressing multidrug resistance P-glycoprotein, US Patent, 2002, US6,372,780.
[78] P. Skehan, R. Storeng, D. Scudiero, A. Monks, J. McMahon, D. Vistica, J.T. Warren, H. Bokesch, S. Kenney, M.R. Boyd, New colorimetric cytotoxicity assay for anticancer-drug screening, J. Natl. Cancer Inst. 82 (1990) 1107–1112.
[79] M.D. Hanwell, D.E. Curtis, D.C. Lonie, T. Vandermeersch, E. Zurek, G.R. Hutchison, Avogadro: an advanced semantic chemical editor, visualization, and analysis platform, J. Cheminform. 4 (2012) 17.
[80] E.F. Pettersen, T.D. Goddard, C.C. Huang, G.S. Couch, D.M. Greenblatt, E.C. Meng, T.E. Ferrin, UCSF chimera - a visualization system for exploratory research and analysis, J. Comput. Chem. 25 (2004) 1605–1612.